Collaborative study of bigeye and yellowfin tuna CPUE from multiple Indian Ocean longline fleets in 2019, with consideration of discarding.

Simon D. Hoyle[1], Shu-Ting Chang[2], Dan Fu[3], Doo Nam Kim[4], Sung Il Lee[4], Takayuki Matsumoto[5], Emmanuel Chassot[6], Yu-Min Yeh[7].

[1] IOTC consultant, New Zealand. Email: simon.hoyle@gmail.com.

[2]Overseas Fisheries Development Council, Invited Taiwanese expert.

[3] IOTC Stock Assessment Officer, Seychelles.

[4] National Institute of Fisheries Science, Republic of Korea.

[5] National Research Institute of Far Seas Fisheries, Japan.

[6] Seychelles Fishing Authority consultant, Seychelles.

[7] Nanhua University, invited Taiwanese expert.

Contents

Tables

Figures

Executive Summary

In April and May 2019 a collaborative study was conducted between national scientists with expertise in Japanese, Korean, Seychelles, and Taiwanese longline fleets, an independent scientist, and an IOTC scientist. The meetings addressed Terms of Reference covering several important issues related to yellowfin and albacore tuna CPUE indices in the Indian Ocean. The study was funded by the Indian Ocean Tuna Commission (IOTC) and the International Seafood Sustainability Foundation.

Terms of Reference

1. Validate and improve current methods for developing indices of abundance for bigeye tuna, using up-to-date fishery catch effort data
2. Provide indices of abundance for selected IOTC species to be presented at the IOTC Working Parties in 2019.
3. The analyses will consider data to be provided by key industrial fisheries operating in the Indian Ocean, including data from Japanese, Taiwanese, Korean, Seychelles longline fleets.
4. Analyses will be carried out in a meeting scheduled in April 2019. After the preliminary discussions between the consultant and participating data providers, the joint standardisation analysis will be carried out combining datasets from key fleets. The consultant is expected to undertake any analyses deemed relevant or necessary during the meeting.

Tasks will include the following, to the extent possible in the available time:

5. Load, prepare, and check each dataset, given that data formats and pre-processing often change between years and data extracts, and important changes to fleets and reporting sometimes occur in new data.
6. Apply cluster analyses or alternative methods for identifying targeting. Develop CPUE standardizations for bigeye tuna using reliable data from each CPC. Continue to explore residual patterns spatially and among clusters, fleets and vessels through time, and change models where necessary to address any problems identified
7. Develop maps showing the spatial coverage by the CPUE data used in the joint analysis over-time with emphasis on the most recent years, as requested by the IOTC Scientific Committee during its 21th session.
8. Document the analyses in accordance with the IOTC *Guidelines for the presentation of CPUE standardisations and stock assessment models*, adopted by the IOTC Scientific Committee in 2014; and provide draft reports to the IOTC Secretariat no later than 60 days prior to the relevant IOTC Working Party meeting.

All work is subject to the agreement of the respective fisheries agencies to make the data available.

In addition to bigeye tuna as described in the TOR, we also generated indices for yellowfin tuna.

This document covers only the joint indices of abundance, describing their development for bigeye and yellowfin tuna.

Other issues are covered in related papers that describe the data preparation, cluster analyses, and individual indices for each fleet.

Data for the four fleets were standardized for each region to estimate indices of abundance. Indices were estimated using two approaches, delta lognormal and lognormal + constant, but the main approach was the delta lognormal. All models included the explanatory variables year-quarter and 5° cell as categorical variables, and a cubic spline on hooks as a covariate. Models for tropical regions included a cubic spline fitted to hooks between floats, while models for temperate areas included a categorical variable for cluster. Some models included vessel identity as a categorical variable. Models were run for the period 1952-1979 without vessel identity, for the later period 1979-2018 with vessel identity (including the four quarters of 1979 in both analyses), and for the whole period 1952-2018 both with and without vessel identity. Two methods for addressing discarding were considered and their effects on the indices were explored.

Figures and tables are provided for each set of indices, including both quarterly and annual indices. Diagnostic plots are also presented.

Introduction

In April and May 2019 a collaborative study of longline data and CPUE standardization for albacore and yellowfin tunas was conducted between scientists with expertise in Japanese, Taiwanese, Korean, and Seychelles fleets, an independent scientist, and an IOTC scientist. The study was funded by the Indian Ocean Tuna Commission (IOTC). The study addressed the Terms of Reference outlined below, which cover the most important issues that had previously been highlighted by different working parties. In addition to the work for bigeye tuna specified in the Terms of Reference, indices were also generated for yellowfin tuna. Work was carried out, for those factors relevant to them, for the following:

- Area: Indian Ocean
- Fleets: Japanese longline; Taiwanese longline, Korean longline, Seychelles longline
- Stocks: bigeye tuna, yellowfin tuna.

This document covers only the joint indices of abundance, describing their development for bigeye and yellowfin tunas.

Terms of Reference

1. Validate and improve current methods for developing indices of abundance for bigeye tuna, using up-to-date fishery catch effort data
2. Provide indices of abundance for selected IOTC species to be presented at the IOTC Working Parties in 2019.
3. The analyses will consider data to be provided by key industrial fisheries operating in the Indian Ocean, including data from Japanese, Taiwanese, Korean, Seychelles longline fleets.
4. Analyses will be carried out in a meeting scheduled in April 2019. After the preliminary discussions between the consultant and participating data providers, the joint standardisation analysis will be carried out combining datasets from key fleets. The consultant is expected to undertake any analyses deemed relevant or necessary during the meeting.

Tasks will include the following, to the extent possible in the available time:

5. Load, prepare, and check each dataset, given that data formats and pre-processing often change between years and data extracts, and important changes to fleets and reporting sometimes occur in new data.
6. Apply cluster analyses or alternative methods for identifying targeting. Develop CPUE standardizations for bigeye tuna using reliable data from each CPC. Continue to explore residual patterns spatially and among clusters, fleets and vessels through time, and change models where necessary to address any problems identified
7. Develop maps showing the spatial coverage by the CPUE data used in the joint analysis over-time with emphasis on the most recent years, as requested by the IOTC Scientific Committee during its 21th session.
8. Document the analyses in accordance with the IOTC *Guidelines for the presentation of CPUE standardisations and stock assessment models*, adopted by the IOTC Scientific Committee in 2014; and provide draft reports to the IOTC Secretariat no later than 60 days prior to the relevant IOTC Working Party meeting.

All work is subject to the agreement of the respective fisheries agencies to make the data available.

Methods

Data cleaning and preparation

The four datasets had many similarities but also significant differences. The variables differed somewhat among datasets, as did other aspects such as the sample sizes, the data coverage and the natures of the fleets.

Data preparation and analyses were carried out by each participant, using a standard set of scripts developed for this purpose in R version 3.5.1 (R Core Team 2018). The approaches used are described by Hoyle et al. (2015b) and Hoyle et al. (2016). The datasets and the analyses are described in working papers by each participant and will not be further reported here. The Japanese data for 2018 are preliminary.

For more detail about the Japanese, Korean, and Taiwanese fleets, see the descriptive figures in the following WPTT information papers (Hoyle et al. 2015a, Hoyle and Okamoto 2015, Hoyle et al. 2015c). For detail about the Seychelles fleet, see the WPTT working paper provided by the Seychelles (ref).

Plotting and data selection

We pooled data from multiple fleets into a single dataset for years 1952-2018. The pooled dataset included all data from the Japanese (1952-2018) and Korean (1971-2018) fleets. For the Taiwanese fleet data from 2005-2018 were included. For the Seychelles fleet all data (2000-2018) were included, except in analyses that included hooks between floats.

During the analyses by national scientists, each set was allocated to bigeye and yellowfin regions according to several alternative regional definitions (Figures 1 and 2). Data outside these areas was ignored.

In recent CPUE analyses Taiwanese data prior to 2005 have been omitted due to concerns about data quality and bias. These concerns were based on coverage before 2001 that was below 50% and in 1992 as low as 4%; and a high level of systematic misreporting during the 2003-2004 period (Hoyle et al. 2015b). However in the current analysis we also explored a scenario in which Taiwanese data from 1995 to the present were included in the analysis dataset. Clustering of the Taiwanese data used for this analysis was done separately. It resulted in slightly different groupings of the sets, and different numbering for the four clusters.

Joint analyses included prepared and clustered data from each of the fleets. In some analyses clusters that caught very few of the species of interest were omitted, because they provide little relevant information and may cause analysis problems due to large numbers of zeroes, and memory problems due to large sample sizes. Cluster selection was based on review and discussion of the plots of covariates and species compositions by cluster.

For standardization of each regional structure and region, data were included in the analysis if they met a set of selection criteria (Table 6). Selection criteria were based on the minimum number of sets or substrata per stratum. Vessels needed to have fished for at least N1 quarters in the region. Vessels were included if they had made at least N2 sets. Each 5° cell was included if it contained at least N3 sets. A year-quarter was included if there were at least N4 sets. An option has been added to include each year-quarter by 5° cell stratum only if there were at least N5 sets, but the feature was not operational during these analyses.

For datasets with more than 60,000 sets the number of sets in each stratum (5° square * year-quarter) was limited by randomly selecting 15 sets without replacement from strata with more than this number of sets. Testing suggested that this approach did not cause bias, and the effects on random variation were reduced to relatively low levels at 15 sets per stratum (Hoyle and Okamoto 2011). The number of sets per stratum was set lower than in previous years (15 rather than 30) because many runs were required and there was limited time during the workshop.

Discards

For the first time, the effect of discards was considered in the standardization. Discards were considered to be potentially significant in the Taiwanese fleet. Discard rates of yellowfin and bigeye tuna for 2002 – 2018 were estimated from the Taiwanese longline commercial logbooks, which since 2002 have included fields for recording the number of fish discarded per set.

Two discard rate scenarios were calculated based on assuming either that all vessels recorded discards when they occurred, or that only a subset of vessels recorded discards and they were representative of the discard rates across all vessels. To represent these two hypotheses we calculated (i) total discards/total retained catch for all vessels and (ii) total discards / total retained catch for vessels that have reported discards at least in one year of the whole time series. The resulting discard rates for bigeye and yellowfin tuna respectively are reported in Tables 2 and 3 for method 1 and Tables 4 and 5 for method 2.

Analyses were carried out using scenarios without discards, with discard method 1, and with discard method 2. The three approaches to discards were combined in turn with each of the options used for other parameters, except that discard method 2 was not used with the dataset that included Taiwanese data since 1995.

CPUE standardization

CPUE standardization methods generally followed the approaches used by Hoyle and Okamoto (2011) with some modifications. The operational data were standardized using generalized linear models in R. Indices were prepared for each species and region using several approaches, summarised in Table 1 and further described below.

Table 1: Species, regions, distributions and variables used in CPUE analyses. The distributions used are lognC (lognormal constant), bin (binomial), and logn (lognormal).

Species	TW data	Discards	Regions	Target variable	Fleets (comb)	Vessel ID	Period	Dbn
YFT, BET	Since 2005	None, discard 1, discard 2	Temp	Cluster	All	N	1952-2018	lognC, bin, logn
						N	1952-1979	
						Y	1979-2018	
			Trop, Temp	HBF	Omit SY	N	1952-2018	
						N	1952-1979	
						Y	1979-2018	
		None	Trop, Temp	HBF & Cluster	Omit SY	N	1952-2018	lognC, bin, logn

						N	1952-1979	
						Y	1979-2018	
YFT, BET	Since 1995	None, discard 1	Temp	Cluster	All	N	1952-2018	lognC, bin, logn
						N	1952-1979	
						Y	1979-2018	
			Trop, Temp	HBF	Omit SY	N	1952-2018	
						N	1952-1979	
						Y	1979-2018	

Distributions

CPUE was defined at the set level as catch in number divided by hooks set. Two different approaches were used: lognormal constant and delta lognormal.

Lognormal constant analyses were carried out using generalized linear models that assumed a lognormal distribution. In this approach the response variable $\log(CPUE+k)$ was used, and a Normal distribution assumed. The constant *k*, added to allow for modelling sets with zero catches of the species of interest, was 10% of the mean CPUE across all sets.

ln($CPUE$+k)~ $yrqtr$+$vessid$+$latlong$5+*target*+ϕ($hooks$)+ϵ, or

The covariates were year-quarter (*yrqtr*), and 5° cell (*latlong5*) fitted as categorical variables, and a cubic spline function ϕ with 10 degrees of freedom applied to the continuous variable *hooks*. Analyses including the vessel identifier (*vessid*) fitted it as a categorical variable. The targeting variable (*target*) was either cluster (*cluster*), hooks between floats (*hbf*), or both *cluster* and *hbf*. Analyses including *hbf* fitted it as a continuous variable using a cubic spline φ with 3 degrees of freedom, while those including cluster (*cl*) fitted it as a categorical variable.

Delta lognormal analyses (Lo et al. 1992, Maunder and Punt 2004) used the same covariates as the lognormal constant model. They employed a binomial distribution for the probability *w* of catch rate being zero and a probability distribution *f(y)* , where y was log(catch/hooks set), for non-zero (positive) catch rates. The index estimated for each year-quarter was the product of the year effects for the two model components, $(1-w).E(y|y\neq 0)$.

$$\Pr(Y=y)=\begin{cases} w, & y=0 \\ (1-w)f(y) & otherwise \end{cases}$$

$g(w)=(CPUE=0)\sim covariates+\epsilon$, where *g* is the logistic function.

$f(y)=CPUE\sim covariates+\epsilon$, for nonzero sets

Data in all models except the binomial model were ‘area-weighted’, with the weights of the sets adjusted so that the total weight per year-quarter in each 5° square would sum to 1. This method was based on the approach identified using simulation by Punsly (1987) and Campbell (2004), that for set *j* in area *i* and year-quarter *t*, the weighting function that gave the least average bias was: $w_{ijt}=$

$\frac{log(h_{ijt}+1)}{\sum_{j=1}^{n}\log(h_{ijt}+1)}$. Given the relatively low variation in number of hooks between sets in a stratum, we simplified this to $w_{ijt} = \frac{h_{ijt}}{\sum_{j=1}^{n} h_{ijt}}$.

Data periods

Vessel identity information for Japan was only available from 1979, and most of the data before 1979 was Japanese. The Korean dataset started in 1971 and had vessel ids throughout, but covered a limited area with relatively low effort, so its influence was small in some analyses. The full Taiwanese dataset started in 1979, and in any case Taiwanese data before 2005 were omitted.

Overlap between vessels with the same id across years is required to avoid confounding between year effects and vessel ids. Thus we could not apply a consistent approach across all years when including vessel ids in the model.

The discontinuity in vessel 1979 could be addressed in several different ways. We therefore analysed the data in several ways so as to provide the assessment scientists with appropriate data.

First, we standardized the full dataset from 1952 to the present without including vessel effects.

Next we estimated two time series: 1952-1979 without vessel effects, and a second time series 1979-2018 with vessel effects (omitting all sets without vessel IDs). Subsequently the analyst may use the two time series as desired, either as separate indices in the assessment, or the recommended approach of concatenating them after adjusting the averages so that the estimates for 1979 are the same. This approach also has the advantage that it allows covariate estimates such as spatial effects to differ by time period.

In a change from recent approaches we did not standardize the full dataset with vessel effects. Using a dummy vessel effect introduces several problems, notably a discontinuity in 1979. These indices have not been used in stock assessments, and omitting them freed up time for other more useful analyses.

Covariate effects

The effects of covariates were examined by plotting the predicted effects, with 95% confidence limits, of each parameter at observed values of the explanatory variables. Spatial effects with 95% confidence intervals were plotted by latitude. The cumulative vessel effects through time were examined by plotting each vessel's effect at every time that vessel made a set. An average vessel effect over time was examined by calculating the mean of the vessel effects for all sets made by the fleet during each time period, and this was also plotted. There is insufficient space to include all plots in the report, but these are available on request.

Changes in catchability through time were investigated by fitting to the operational data both with and without a term for individual vessel. The two models were designated respectively the 'base model' and the 'vessel-effects model'. Abundance indices were calculated for each model, and normalized to average 1.

For all model comparisons, the indices estimated for each year-quarter were compared by dividing the base model by the vessel effects model, plotting the time series of ratios, and fitting a log-linear regression. The slope of the regression represented the average annual compounding rate of change in fishing power attributable to changes in the vessel identities; i.e. the introduction of new vessels and retirement of old vessels. Gradients are shown on the figures, together with confidence intervals.

Model diagnostics

Residual distributions and Q-Q plots were produced for all but the binomial analyses. For the lognormal positive analyses that included cluster in the model, median residuals were plotted by cluster. For all lognormal positive analyses, residuals by year-quarter were plotted by flag; median residuals by year-quarter were plotted by flag; and median residuals by 5° cell were mapped onto a contour plot for each flag.

The effects of covariates were examined using influence plots, using the R package influ (Bentley et al. 2011).

Indices of abundance

Indices of abundance were obtained by applying the R function predict.glm to model objects. The datasets used for prediction included all year-quarter values, with all other variables fixed at either the median for continuous variables, or the mode for categorical variables. Binomial time effects were obtained by a) generating logit time effects from the glm, and b) adding a constant to these logit time effects so that the mean of the back-transformed proportions was equal to the proportion of positive sets across the whole dataset. The main aim with this approach is to obtain a CPUE that varies appropriately, since variability for a binomial is greater when the mean is at 0.5 than at 0.02 or 0.98, and the multiplicative effect of the variability is greater when the mean is lower. The outcomes were normalised and reported as relative CPUE with mean of 1.

Uncertainty estimates were provided by applying the R function predict.glm with type = ”terms” and se.fit=TRUE, and taking the standard error of the year-quarter effect. For the delta lognormal models we used only the uncertainty in the positive component. Uncertainty estimates from standardizing commercial logbook data are in general biased low and often ignored by assessment scientists, since they assume independence and ignore autocorrelation associated with (for example) consecutive sets by the same vessels in the same areas. There may be a very large mismatch between the observation error in CPUE indices and the process error in the indices that is estimated in the assessment. This is particularly true for distant water longline CPUE, where very large sample sizes generate small observation errors.

Annualized indices were developed from the year-quarter indices. For each time series, the year-quarter estimates were modelled with a linear regression with normally distributed residuals, fitting year-quarter as a function of year + quarter. The year effects were then predicted in the second quarter of the year, and normalized to average 1. The second quarter was chosen because there were fewer missing values than other quarters.

Time-area interactions

We did not explicitly model time-area interactions, but explored the potential for them to occur in the 1979-2018 analyses for each region. We modelled the long term trends in median residuals for each 5° cell year-quarter stratum. We determined the median residual for each 5° cell year-quarter, and then fitted a regression of median residuals versus year-quarter for each 5° cell. We extracted the slope of each regression and plotted them on a map, with darker red representing decline and lighter yellow representing increase relative to the average model trend.

Results

We estimated a large number of indices for each region, and here present figures for the indices most likely to be used in assessments. In all cases we show results from the discards 1 analyses, which assume that all Taiwanese vessels have reported discards.

In temperate areas (bigeye and yellowfin regions 3 and 4, see Figures 1 and 2) we selected figures from the analysis that omits low-target clusters from the dataset, and conversely includes cluster but not HBF in the model. This is because in southern regions there are known differences in fishing behaviour among vessels targeting different species, and these differences are reflected in the species composition, making it appropriate to use cluster in the standardization model. For example, the Japanese southern bluefin tuna fishery takes largely SBT, with some catch of albacore. The Taiwanese oilfish fishery is also a clear example, with a very high representation of species 'other'.

In tropical areas (bigeye regions 1 and 2, yellowfin regions 2 and 5) we selected figures from the analysis that omits low-target clusters from the dataset, and includes HBF but not cluster in the model. Although there have been changes in targeting through time, vessels are believed to target bigeye and yellowfin at the same time and using similar methods, but to different extents by area and season, and with changes through time. In this complex situation clustering may be useful to remove data from clearly separate fisheries (such as the southern bluefin tuna fishery that occurred in eastern areas near Indonesia in the 1960s and 70s). However including cluster in the model may be problematic due to the confounding of clusters with abundance change. We have therefore used hooks between floats in the models for tropical areas, as was done in previous years' analyses. We excluded clusters with minimal catch of the species of interest for reasons described above.

We estimated delta lognormal indices for all regions of the bigeye regional structures B2 and B3 (Figures 3 to 8), which includes the split north-western bigeye region 1 (regional structure B3, Figures 5 and 6); and for all regions of the yellowfin regional structures Y and Y2, (Figures 9-14), which includes the split north-western yellowfin region 2 (regional structure Y2, Figures 11 and 12). We also estimated annualized indices for bigeye (Figures 15 to 20) and yellowfin (Figures 21-26). Diagnostics for the lognormal positive distribution indicated some negative skewness in the distributions of residuals (Figures 27- 30), with better fits for the indices that included vessel effects (comparison not shown).

Indices of abundance

In reporting results we focus on the two shorter sets of indices which cover the 1952 – 1979 period without vessel effects, and the 1979 – 2018 period with vessel effects.

For bigeye tuna the tropical indices in regions 1 (Figure 3) and 2 (Figure 4) show a moderate decline followed by a sharp spike upwards in the late 1970s. In the western area the declining trends subsequently resume and continue until the early 2000s, followed by a period of stable CPUE until about 2010 when a positive spike occurs. This is followed by a sharp decline so that CPUE is estimated to be currently at its lowest observed level. In the eastern tropical region 2 there is also a general decline in CPUE after 1980, with an increase in CPUE after 2010 that is much smaller than in the west. CPUE in the eastern tropical region 2 is currently also at or close to the lowest level observed.

The two split sections of western tropical bigeye region 1 show different patterns from one another and from the full region 1. In the period 1952 – 1979, the southern subregion 1s (Figure 5) shows slightly less decline until 1976 than the full region 1 while the northern subregion 1n declines more (Figure 6). All show similar spikes in the late 1970s. The decline from 1979 to the early 2000s is slightly less in the southern subregion than in the full region 1, but steeper in the northern subregion. The short-lived increase after 2010 is very large in the northern subregion, but smaller in the southern subregion.

For bigeye in western temperate region 3 (Figure 7), data are more sparse and less reliable than the tropical indices in the period before 1990, due to low sample sizes in the original data and omission of sets with very low bigeye species composition. Standardized CPUE increases during the 1960s to a peak in the early 1970s, then a few years of lower catch rates and sparse data. For the period since 1990 the indices are somewhat similar to the northern indices, with declining CPUE overall, and stability since 2010. In eastern temperate region 4 (Figure 8) the pattern is quite similar. Standardized CPUE increases during the 1960s to a peak in the early 1970s, after which it drops for a few years and then increases again. In the 1990s the CPUE drops, increases until 2000, then declines again and becomes sparse and variable.

For yellowfin tuna, indices in the tropical areas were characterized by very steep declines in standardized CPUE prior to 1965, after which declines continued at a slower rate until 1980. From 1980 the western tropical region 2 CPUE (Figure 9) increased until about 1986-87, then declined until around 1995, was stable until 2005, and then decreased again. Since about 2011 it has remained relatively stable, a little above the lowest level which was observed in the late 2000's, with recent increase but only in one quarter. The eastern tropical region 5 followed a similar pattern until 1990 but then declined steadily. Since 2017 there has been a small increase from what was the lowest level in the time series (Figure 10).

The western tropical region was split into two subregions in the regY2 structure. The south-western tropical region 2s (regY2_R2, Figure 11) and the north-western tropical region 2n (regY2_R7, Figure 12) followed similar trends before 1965, declining steeply. Estimated catch rates were highly variable, partly due to sparse data. After 1980 CPUE increased somewhat in both subregions and then declined with medium-term variability until 2010. Catch rates increased somewhat in both subregions after 2010. The most recent quarter shows a sharp increase particularly in the north, but a single data point may simply represent random variation in catchability.

Yellowfin in western temperate region 3 followed a similar but somewhat flatter pattern to the western tropical indices, with a decline until about 1965 followed by an increase from 1980 until the late 1980s, and subsequently a relatively stable pattern but with significant variability, both in the medium term and seasonally (Figure 13).

In eastern temperate region 4 the pattern was similar to the western temperate area before 1965 (Figure 14). After 1979 catch rates increased slightly overall until the mid-2000's, but then declined rapidly and reached their lowest observed levels by 2017. There was some increase in 2018.

Residuals for these analyses were reasonably normally distributed (Figures 27 to 30), with the residuals for the tropical indices tending to be more left skewed.

Discards and data periods

We compared trends between the standard approach used in previous CPUE analyses and the new approaches incorporating discards. Ratios between the standard approach used in previous CPUE analyses and the discard 1 and discard 2 methods show that both types of discard runs were similar to the standard runs, with relatively small effects due to consideration of discards by the Taiwanese fleet, for both bigeye (Figure 31) and yellowfin (Figure 32). Larger (but still small) changes in trend are observed for yellowfin than for bigeye. More variability between runs is observed for temperate than for tropical areas.

Including Taiwanese data from 1995-2018 instead of 2005-2018 also had a relatively small impact on the joint CPUE indices for yellowfin tuna (Figure 33).

Influence

The effects of the standardization process on the indices are shown in Figures 34 to 43. Most indices saw substantial reduction in variability, due to standardization of the effects of spatial movements of the fleets, and changes in targeting. The indices post-1979 showed larger changes in trend, particularly for yellowfin tuna. This is partly because the relatively large vessel effects could be only accounted for after 1979 when vessel ids were available. , but also due to large changes in both targeting and fleets.

The influence plots for bigeye tuna in western tropical areas before 1979 (Regions 1N and 1S, regB3_R1 and regB3_R5, and combined in regional structure regB2, region 1 (regB2_R1); Figures 46 - 48) show relatively little influence from most variables, with spatial patterns having the strongest effects. After 1979, vessel ids were available, and there were some larger changes in catch rates. In the south there was an increase in Japanese vessels and loss of Korean vessels with lower bigeye catch rates, followed by the 2005 introduction of data from Taiwanese vessels with relatively high bigeye catch rates. There was also an increase in hbf from 1979 to the mid-2000s which was linked to a small increase in catch rates.

In the eastern Indian Ocean we also found few influences on bigeye CPUE before 1979 (Figure 49). After 1979 there were increasing catch rates associated with increasing HBF, but some variability and decline in catch rates associated with vessel turnover. In this area the Taiwanese fleet had lower bigeye catch rates on average than the Japanese fleet, and similar to the Korean fleet.

In temperate regions 3 and 4 (regB2_R3 and regB2_R4, Figures 50 and 51) changes in spatial distribution of the effort had a strongly positive influence on the catch rates. In the east (Region 4) target change (represented by the cluster variable) also appeared to positively influence catch rates. After 1979 the western temperate area saw some decline in catch rate as the average number of hooks per set increased. There was also a change in catch rates after 2005 associated with changes in the fleet after 2005. The eastern temperate area Region 4 saw a change in targeting that increased catch rates for a time during the 1990s. Increases in the number of hooks per set were associated with long-term reductions in catch rates.

The influence plots for yellowfin in western tropical areas before 1979 (Regions 2N and 2S, regY2_R2 and regY2_R7, and combined in regional structure regY, region 2 (regY_R2); Figures 52, 53, and 54) show relatively little influence from most variables, with spatial patterns having the strongest effects. In the northern tropical area yellowfin catch rates declined due to changing spatial effects in the 1952-

1965 period. During the post-1979 period vessel ids were available, and there were some large changes in yellowfin catch rates 1995-2000 associated with changes in the fleet. Initially there was an increase in Japanese vessels with higher yellowfin catch rates than the Korean vessels they replaced. After 2005 there were fewer Japanese vessels and more Taiwanese vessels with lower yellowfin catch rates.

In the eastern tropical region 5 (regY_R5, Figure 55), there was a decline in catch rates after 1975 associated with a change in the numbers of hooks per set. After 1979 there appears to be a shift towards areas with higher yellowfin catch rates after 2005, possibly due to the introduction of the Taiwanese fleet. Hooks between floats and hooks per set have contrasting influence on CPUE, with HBF associated with a decline and hooks an increase in catch rates from 1995 to 2000. From 1979 to 1990 there is a shift to vessels with higher yellowfin catch rates. This declines again in the 1990s, but increases from about 2000 as the Seychelles and Taiwanese fleets arrive. These fleets may target yellowfin in region 5 more than the Japanese fleet does.

In the western temperate area (region 3, regY_R3, Figure 56) spatial effects were influential, showing the expected greater seasonality further south. Here there was no evidence of movement to areas with lower yellowfin catch rates in the period up to 1965. Cluster effects also showed seasonality, associated with seasonal targeting behaviour. Post-1979 clustering effects indicated a shift away from effort types associated with yellowfin targeting after 1990 , but an increase again from 2005 with the Taiwanese fleet. Vessel effects for the Japanese fleet were generally higher than the other fleets, and including vessel effects after 1979 was influential. There was an early increase in mean fishing power associated with vessel ids, but then a decline post-2005 with the introduction of the Taiwanese fleet to the analysis, and the reduced effort of the Japanese fleet.

In the eastern temperate region 4 (regY_R4, Figure 57) there was a substantial move of effort to areas with lower yellowfin catch rates 1952-1970. After 1979 catch rates varied with targeting clusters until about 1990, but after this time the Japanese cluster with higher yellowfin catch rates substantially reduced its effort. This change is also apparent in the spatial influence plot, with reduced variability after 1990, since the JP YFT cluster fished in the north of region 4.

Spatial effects

Spatial patterns of relative density are shown in figures 58 to 62. For bigeye tuna they show a trend towards higher catch rates in the east, while for yellowfin tuna the catch rates tend to be higher in the equatorial west, particularly near the African coast and in the Mozambique channel.

For bigeye tuna, trends through time in residuals from the 1979-2018 models in western equatorial region 1 were quite variable but showed more catch rate decline north of the equator than elsewhere (Figure 64). In the eastern tropics (region 2) and in temperate areas region 3 and 4 there was no clear pattern (Figure 65).

For yellowfin tuna, trends through time in residuals from the 1979-2018 models in equatorial regions 2 and 5 showed more catch rate decline between 5°N and 10°S than elsewhere in the tropical areas, corresponding to areas with more purse seine effort (Figure 64). In the temperate areas region 3 and 4 there was no clear pattern (Figure 65).

Discussion

The CPUE indices presented in this paper are derived from joint analysis of Japanese, Korean, Seychelles, and Taiwanese data. In 2015 and 2016 this joint paper included analyses of data from individual fleets, but since 2017 the methods and results for the individual fleets, including cluster analyses, have been provided in separate papers.

The general approach was to run separate models for different areas, so that parameter estimates and uncertainty distributions could differ among areas (Chang et al. 2011). The models used 5° cell area effects, as recommended by the 2013 IOTC CPUE workshop (Anon 2013) to account for changes in effort distribution, and adjusted statistical weights to allow for changing effort concentration (Punsly 1987, Campbell 2004). The models included vessel effects where available, to account for some effects of changing fishing power and targeting within the fleet (Hoyle and Okamoto 2011). They also used cluster analysis based on species composition in order to identify target change, and to separate out effort using different fishing strategies (He et al. 1997). Cluster was used as a variable in the standardization models in temperate areas, but not in tropical areas due to concerns about confounding with abundance changes in the species of interest.

Data from the Seychelles were first made available in 2017, and since that time have been included in the indices that used clustering. Most of the Seychelles time series does not report the hooks between floats variable, which is required for the tropical indices. This is unfortunate because most of the Seychelles effort is in the western tropical area. In future this dataset should be included in tropical indices, but we will need to find a way to address the lack of HBF, perhaps using a proxy variable based on understanding of how HBF and other setting methods are used for targeting.

Note that area weighting currently assumes that all cells are the same size, but in fact the ocean areas of cells vary due to both the presence of land and reduced cell areas further from the equator. Future work should adjust area weights based on ocean areas.

The western tropical area have been split into northern and southern sub-regions. The region was split in the 2016 bigeye stock assessment to improve tag mixing (Langley 2016). Trends appeared to differ between the sub-regions to some extent so we have also applied the approach to the yellowfin indices.

Temporal trends appear to vary within regions, with residual patterns indicating greater decline in CPUE in tropical areas close to the equator. Similar spatial patterns have been observed in Atlantic fisheries (Hoyle et al. 2018, Hoyle et al. 2019), with larger declines in catch rates in tropical areas. Tropical areas receive more purse seine effort, and this trend may be associated with greater depletion of areas subject to more purse seine fishing. There may be other explanations such as reduced efficiency or targeting ability in areas with more purse seine fishing. Further exploration is required to identify the timing of the changes, and whether other factors, such as target change, gear change, or fleet composition, are contributing to or causing these trends. If trends do vary spatially and non-randomly, then time-area interactions at appropriate scales should be included in future models.

Both adjusting for discards and changing the first year to include Taiwanese data from 2005 to 1995 had relatively small effects on trends. Differences are likely due to 4 sources:

1. Increases in recent catch rates due to higher catches by Taiwanese vessels where discards are substantial. Discards were very minor for bigeye, but reasonably large for yellowfin in regions 2, 3, and 5 in 2017 and 2018. In regions 3 and 5 there was considerable Japanese and (in region 3) Korean effort in 2017 and 2018 that did not change, reducing the impact of changes in the Taiwanese data.
2. Sets were randomly selected in order to reduce analysis time, which caused some variability between individual runs. The number of sets selected per stratum was lower than in previous years (15 rather than 30) because of the large numbers of runs required during limited workshop time. The smaller sample size would have increase the random variation between runs.
3. Changed estimates of covariate parameters, such as spatial, vessel, cluster and HBF effects, due to increased catch rates in areas fished by Taiwanese vessels, and random selection of different sets. Changes to covariates can spread to temporal effects across the whole time series.
4. For the change to the Taiwanese data, the larger dataset meant that clustering needed to be done again, which would have slightly changed the allocations and groupings of sets among clusters. In addition the clusters included in the analysis were changed in the south-eastern temperate region for bigeye tuna and in both temperate regions for yellowfin.

The joint data were only available for one week, and this time was also occupied by training, presentations, and discussions during the joint CPUE workshop. This limited data access was a constraint on testing and development.

The analyses presented here used an R package 'cpue.rfmo', which the first author of this report is developing for the standardization of pelagic longline data used by tuna RFMOs.

CPUE indices are very influential components of stock assessment models, and further work to improve and validate indices is a high priority. We suggest the following priorities for further work:

1) Explore options for extending the Japanese time series of vessel effects into the pre-1979 period.
2) Increase understanding of the fisheries that provide the CPUE by a) further exploring the size data associated with each fleet, if possible with size data at the vessel set level; and b) exploring vessel movement patterns through time.
3) Explore alternative subarea-time interactions to the standardization models, to address differences in trends among areas. Continue to explore residual patterns spatially and among clusters, fleets and vessels through time, and change models where necessary to address any problems identified. Develop additional residual and exploratory plots to explore possible confounding effects, such as maps of residuals by season to explore seasonal catchability changes.
4) Test alternative methods for identifying and accounting for targeting.
5) Adjust area weighting to employ ocean area rather than giving equal weighting to every spatial cell.

Acknowledgments

We thank the Japanese, Korean, Seychelles, and Taiwanese fishing industries and governments for collecting these data and giving us access for scientific analysis. Thanks to the Indian Ocean Tuna Commission (IOTC) for funding this work. We are grateful to the IOTC Secretariat for their support, particularly Paul De Bruyn and James Geehan. Thanks to the Korean National Institute of Fisheries Science, Taiwanese Overseas Fisheries Development Council, the Japanese Institute for Far Seas Fisheries, and the Seychelles Fishing Authority for providing their support. Thanks to AZTI Tecnalia for the use of their facilities for the joint meeting. Thank you to Gorka Merino for chairing the joint meeting, and to Hilario Murua and Miguel Herrera for their contributions.

References

Anon. 2013. Report of the IOTC CPUE Workshop, San Sebastian, Spain, 21–22 October, 2013. IOTC–2013–SC16–12[E], Indian Ocean Tuna Commission.

Bentley, N., T. H. Kendrick, P. J. Starr, and P. A. Breen. 2011. Influence plots and metrics: tools for better understanding fisheries catch-per-unit-effort standardizations. Ices Journal of Marine Science **69**:84-88.

Campbell, R. A. 2004. CPUE standardisation and the construction of indices of stock abundance in a spatially varying fishery using general linear models. Fisheries Research **70**:209-227.

Chang, S.-K., S. Hoyle, and H.-I. Liu. 2011. Catch rate standardization for yellowfin tuna (Thunnus albacares) in Taiwan's distant-water longline fishery in the Western and Central Pacific Ocean, with consideration of target change. Fisheries Research **107**:210-220.

He, X., K. A. Bigelow, and C. H. Boggs. 1997. Cluster analysis of longline sets and fishing strategies within the Hawaii-based fishery. Fisheries Research **31**:147-158.

Hoyle, S., D. Kim, S. Lee, T. Matsumoto, K. Satoh, and Y. Yeh. 2016. Collaborative study of tropical tuna CPUE from multiple Indian Ocean longline fleets in 2016. IOTC–2016–WPTT18–14.

Hoyle, S. D., J. H.-w. Huang, D. N. Kim, M. K. Lee, T. Matsumoto, and J. Walter III. 2018. Collaborative study of bigeye tuna CPUE from multiple Atlantic Ocean longline fleets in 2018.

Hoyle, S. D., M. Lauretta, M. K. Lee, T. Matsumoto, R. Sant'Ana, H. Yokoi, and N.-J. Su. 2019. Collaborative study of yellowfin tuna CPUE from multiple Atlantic Ocean longline fleets in 2019.

Hoyle, S. D., S. I. Lee, and Z. G. Kim. 2015a. Descriptive analyses of the Korean Indian Ocean longline fishery, focusing on tropical areas. Indian Ocean Tuna Commission Working Party on Tropical Tunas.

Hoyle, S. D., and H. Okamoto. 2011. Analyses of Japanese longline operational catch and effort for bigeye and yellowfin tuna in the WCPO, WCPFC-SC7-SA-IP-01. Western and Central Pacific Fisheries Commission, 9th Scientific Committee, Pohnpei, Federated States of Micronesia.

Hoyle, S. D., and H. Okamoto. 2015. Descriptive analyses of the Japanese Indian Ocean longline fishery, focusing on tropical areas. Indian Ocean Tuna Commission Working Party on Tropical Tunas.

Hoyle, S. D., H. Okamoto, Y.-m. Yeh, Z. G. Kim, S. I. Lee, and R. Sharma. 2015b. IOTC–CPUEWS02 2015: Report of the 2nd CPUE Workshop on Longline Fisheries, 30 April – 2 May 2015. Indian Ocean Tuna Commission.

Hoyle, S. D., Y.-M. Yeh, S.-T. Chang, and R.-F. Wu. 2015c. Descriptive analyses of the Taiwanese Indian Ocean longline fishery, focusing on tropical areas. Indian Ocean Tuna Commission Working Party on Tropical Tunas.

Langley, A. 2016. Stock assessment of bigeye tuna in the Indian Ocean for 2016-model development and evaluation. IOTC Proceedings, volume IOTC-2016-WPTT18-20, page 98p, Victoria, Seychelles:11-13.

Lo, N. C. H., L. D. Jacobson, and J. L. Squire. 1992. Indices of relative abundance from fish spotter data based on delta-lognormal models. Canadian Journal of Fisheries and Aquatic Sciences **49**:2515-2526.

Maunder, M. N., and A. E. Punt. 2004. Standardizing catch and effort data: a review of recent approaches. Fisheries Research **70**:141-159.

Punsly, R. 1987. Estimation of the relative annual abundance of yellowfin tuna, *Thunnus albacares*, in the eastern Pacific Ocean during 1970-1985. Inter-American Tropical Tuna Commission, La Jolla, CA.

R Core Team. 2018. R: A language and environment for statistical computing. R Foundation for Statistical Computing, Vienna, Austria.

Tables

Table 2: Bigeye tuna discards by the Taiwanese longline fleet since 2002, calculated using method 1.

	R1S			R1N			R1 all		
Year	Retained	Discarded	Rate	Retained	Discarded	Rate	Retained	Discarded	Rate
2002	363305	15	0.004%	389248	0	0.000%	752553	15	0.002%
2003	537354	97	0.018%	392400	37	0.009%	929754	134	0.014%
2004	578325	162	0.028%	506950	310	0.061%	1085275	472	0.043%
2005	391520	879	0.224%	302505	3246	1.062%	694025	4125	0.594%
2006	176137	546	0.309%	192659	565	0.292%	368796	1111	0.301%
2007	277826	251	0.090%	186075	34	0.018%	463901	285	0.061%
2008	129029	30	0.023%	161144	147	0.091%	290173	177	0.061%
2009	171773	21	0.012%	98861	32	0.032%	270634	53	0.020%
2010	173134	45	0.026%	25625	0	0.000%	198759	45	0.023%
2011	177743	45	0.025%	16445	0	0.000%	194188	45	0.023%
2012	260891	12	0.005%	291807	11	0.004%	552698	23	0.004%
2013	165954	0	0.000%	84742	0	0.000%	250696	0	0.000%
2014	103945	304	0.292%	44840	0	0.000%	148785	304	0.204%
2015	126816	285	0.224%	40971	21	0.051%	167787	306	0.182%
2016	158163	298	0.188%	34254	113	0.329%	192417	411	0.214%
2017	134742	257	0.190%	18186	3	0.016%	152928	260	0.170%
2018	137352	63	0.046%	18061	0	0.000%	155413	63	0.041%
	R2			R3			R4		
Year	Retained	Discarded	Rate	Retained	Discarded	Rate	Retained	Discarded	Rate
2002	118092	7	0.006%	86210	21	0.024%	65562	0	0.000%
2003	176529	247	0.140%	50090	36	0.072%	69907	2	0.003%
2004	185170	711	0.383%	50599	0	0.000%	49013	5	0.010%
2005	43349	140	0.322%	32273	177	0.545%	11796	80	0.674%
2006	34668	93	0.268%	13343	30	0.224%	6347	0	0.000%
2007	118306	69	0.058%	4010	47	1.158%	6673	7	0.105%
2008	69902	10	0.014%	4074	2	0.049%	7530	0	0.000%
2009	186550	17	0.009%	7184	0	0.000%	4362	0	0.000%
2010	82052	13	0.016%	3549	0	0.000%	11949	0	0.000%
2011	127521	5	0.004%	1904	0	0.000%	7552	0	0.000%
2012	20671	0	0.000%	1818	2	0.110%	1418	1	0.070%
2013	20787	0	0.000%	11428	21	0.183%	6583	0	0.000%
2014	13443	0	0.000%	7341	0	0.000%	12008	0	0.000%
2015	13461	0	0.000%	8612	27	0.313%	6973	0	0.000%
2016	13402	0	0.000%	12314	15	0.122%	5427	0	0.000%
2017	9701	0	0.000%	20560	83	0.402%	9280	0	0.000%
2018	8989	0	0.000%	18877	3	0.016%	4032	0	0.000%

Table 3: Yellowfin tuna discards by the Taiwanese longline fleet since 2002, calculated using method 1.

	R2S			R2N			R2 all		
Year	Retained	Discarded	Rate	Retained	Discarded	Rate	Retained	Discarded	Rate
2002	133775	0	0.000%	165032	0	0.000%	298807	0	0.000%
2003	298590	109	0.036%	187267	49	0.026%	485857	158	0.033%
2004	294098	146	0.050%	285722	217	0.076%	579820	363	0.063%
2005	337613	446	0.132%	387947	99	0.026%	725560	545	0.075%
2006	84463	85	0.101%	151049	38	0.025%	235512	123	0.052%
2007	58470	19	0.032%	54107	2	0.004%	112577	21	0.019%
2008	20582	2	0.010%	17569	13	0.074%	38151	15	0.039%
2009	21766	0	0.000%	8715	4	0.046%	30481	4	0.013%
2010	29190	12	0.041%	1566	0	0.000%	30756	12	0.039%
2011	68864	11	0.016%	232	0	0.000%	69096	11	0.016%
2012	63942	4	0.006%	54137	2	0.004%	118079	6	0.005%
2013	37336	0	0.000%	32385	0	0.000%	69721	0	0.000%
2014	48277	0	0.000%	37443	0	0.000%	85720	0	0.000%
2015	74579	50	0.067%	27576	0	0.000%	102155	50	0.049%
2016	121067	131	0.108%	35920	91	0.253%	156987	222	0.141%
2017	69138	3077	4.261%	23520	188	0.793%	92658	3265	3.524%
2018	83373	6701	7.439%	26602	938	3.406%	109975	7639	6.946%
	R3			R4			R5		
Year	Retained	Discarded	Rate	Retained	Discarded	Rate	Retained	Discarded	Rate
2002	35677	12	0.034%	35313	0	0.000%	30104	1	0.003%
2003	37619	15	0.040%	29234	37	0.126%	38459	95	0.246%
2004	42079	0	0.000%	45575	1	0.002%	58682	357	0.605%
2005	54641	34	0.062%	17701	79	0.444%	24134	81	0.335%
2006	8754	5	0.057%	7033	7	0.099%	14986	31	0.206%
2007	9378	111	1.170%	5615	1	0.018%	31478	12	0.038%
2008	7560	8	0.106%	3271	0	0.000%	18339	0	0.000%
2009	9965	0	0.000%	2826	0	0.000%	28334	6	0.021%
2010	16712	0	0.000%	8885	4	0.045%	16616	0	0.000%
2011	7528	0	0.000%	1394	0	0.000%	27846	2	0.007%
2012	8354	0	0.000%	941	0	0.000%	7432	0	0.000%
2013	14142	1	0.007%	4697	1	0.021%	2740	0	0.000%
2014	7168	0	0.000%	1103	0	0.000%	2512	0	0.000%
2015	16169	24	0.148%	6160	0	0.000%	2635	0	0.000%
2016	28055	0	0.000%	5428	0	0.000%	2578	0	0.000%
2017	17193	1795	9.453%	1338	12	0.889%	2459	0	0.000%
2018	28093	2428	7.955%	6478	108	1.640%	4786	230	4.585%

Table 4: Bigeye tuna discards by the Taiwanese longline fleet since 2002, calculated using method 2.

	R1S			R1N			R1 all		
Year	Retained	Discarded	Rate	Retained	Discarded	Rate	Retained	Discarded	Rate
2002	189493	15	0.008%	150123	0	0.000%	339616	15	0.004%
2003	285093	97	0.034%	179188	37	0.021%	464281	134	0.029%
2004	298071	162	0.054%	236946	310	0.131%	535017	472	0.088%
2005	196083	879	0.446%	143173	3246	2.217%	339256	4125	1.216%
2006	95290	546	0.570%	100238	565	0.560%	195528	1111	0.568%
2007	155603	251	0.161%	93045	34	0.037%	248648	285	0.115%
2008	69393	30	0.043%	74212	147	0.198%	143605	177	0.123%
2009	86904	21	0.024%	40657	32	0.079%	127561	53	0.042%
2010	113635	45	0.040%	10954	0	0.000%	124589	45	0.036%
2011	123687	45	0.036%	15772	0	0.000%	139459	45	0.032%
2012	176944	12	0.007%	192284	11	0.006%	369228	23	0.006%
2013	108481	0	0.000%	65886	0	0.000%	174367	0	0.000%
2014	69451	304	0.436%	26960	0	0.000%	96411	304	0.315%
2015	92370	285	0.308%	27291	21	0.077%	119661	306	0.256%
2016	116974	298	0.254%	23386	113	0.481%	140360	411	0.293%
2017	99164	257	0.258%	12055	3	0.025%	111219	260	0.234%
2018	91669	63	0.069%	10734	0	0.000%	102403	63	0.062%
	R2			R3			R4		
Year	Retained	Discarded	Rate	Retained	Discarded	Rate	Retained	Discarded	Rate
2002	73633	7	0.010%	52758	21	0.040%	21990	0	0.000%
2003	108896	247	0.226%	30108	36	0.119%	34567	2	0.006%
2004	116891	711	0.605%	38030	0	0.000%	27483	5	0.018%
2005	26566	140	0.524%	23640	177	0.743%	6954	80	1.137%
2006	19441	93	0.476%	10870	30	0.275%	5280	0	0.000%
2007	84701	69	0.081%	3390	47	1.367%	5918	7	0.118%
2008	46415	10	0.022%	3345	2	0.060%	6155	0	0.000%
2009	116830	17	0.015%	4844	0	0.000%	3636	0	0.000%
2010	53601	13	0.024%	2812	0	0.000%	7438	0	0.000%
2011	88283	5	0.006%	1580	0	0.000%	6160	0	0.000%
2012	13797	0	0.000%	1818	2	0.110%	1418	1	0.070%
2013	14330	0	0.000%	10103	21	0.207%	5034	0	0.000%
2014	10626	0	0.000%	5910	0	0.000%	10056	0	0.000%
2015	11036	0	0.000%	7400	27	0.364%	4449	0	0.000%
2016	9404	0	0.000%	9739	15	0.154%	3935	0	0.000%
2017	6508	0	0.000%	17569	83	0.470%	7478	0	0.000%
2018	4720	0	0.000%	14528	3	0.021%	2902	0	0.000%

Table 5: Yellowfin tuna discards by the Taiwanese longline fleet since 2002, calculated using method 2.

	R2S			R2N			R2 all		
Year	Retained	Discarded	Rate	Retained	Discarded	Rate	Retained	Discarded	Rate
2002	73434	0	0.000%	64940	0	0.000%	138374	0	0.000%
2003	154935	109	0.070%	97125	49	0.050%	252060	158	0.063%
2004	154926	146	0.094%	132304	217	0.164%	287230	363	0.126%
2005	150847	446	0.295%	150271	99	0.066%	301118	545	0.181%
2006	41403	85	0.205%	66820	38	0.057%	108223	123	0.114%
2007	30606	19	0.062%	23955	2	0.008%	54561	21	0.038%
2008	9309	2	0.021%	7318	13	0.177%	16627	15	0.090%
2009	10324	0	0.000%	4031	4	0.099%	14355	4	0.028%
2010	19348	12	0.062%	898	0	0.000%	20246	12	0.059%
2011	45758	11	0.024%	232	0	0.000%	45990	11	0.024%
2012	43471	4	0.009%	35876	2	0.006%	79347	6	0.008%
2013	24027	0	0.000%	24253	0	0.000%	48280	0	0.000%
2014	32688	0	0.000%	21780	0	0.000%	54468	0	0.000%
2015	52199	50	0.096%	20220	0	0.000%	72419	50	0.069%
2016	85479	131	0.153%	25015	91	0.362%	110494	222	0.201%
2017	51152	3077	5.674%	16485	188	1.128%	67637	3265	4.827%
2018	62587	6701	9.671%	17398	938	5.116%	79985	7639	9.551%
	R3			R4			R5		
Year	Retained	Discarded	Rate	Retained	Discarded	Rate	Retained	Discarded	Rate
2002	20638	12	0.058%	13015	0	0.000%	16865	1	0.006%
2003	18521	15	0.081%	12857	37	0.287%	21887	95	0.432%
2004	26179	0	0.000%	28015	1	0.004%	30798	357	1.146%
2005	31879	34	0.107%	12736	79	0.616%	10011	81	0.803%
2006	5652	5	0.088%	6099	7	0.115%	6984	31	0.442%
2007	6155	111	1.771%	5350	1	0.019%	16556	12	0.072%
2008	4410	8	0.181%	2993	0	0.000%	8407	0	0.000%
2009	6396	0	0.000%	1656	0	0.000%	14958	6	0.040%
2010	12510	0	0.000%	6143	4	0.065%	9246	0	0.000%
2011	5164	0	0.000%	1235	0	0.000%	18387	2	0.011%
2012	7540	0	0.000%	941	0	0.000%	6126	0	0.000%
2013	11117	1	0.009%	4394	1	0.023%	2014	0	0.000%
2014	5649	0	0.000%	883	0	0.000%	1846	0	0.000%
2015	12858	24	0.186%	4417	0	0.000%	1922	0	0.000%
2016	23337	0	0.000%	4423	0	0.000%	1831	0	0.000%
2017	13670	1795	11.607%	1151	12	1.032%	1934	0	0.000%
2018	22910	2428	9.582%	5169	108	2.047%	3117	230	6.872%

Table 6: Criteria defining the minimum numbers of strata by region and regional structure, for 5 different types of strata.

Regional structure	Num of regions	Min vessel qtrs (N1)	Min sets vessel (N2)	Min sets latlong (N3)	Min sets yq (N4)	Min sets yq latlong (N5)
Y	6	2, 5, 5, 2, 5, 2	40, 100, 100, 40, 100, 40	20, 50, 50, 20, 50, 20	20, 50, 50, 20, 50, 20	3, 5, 5, 3, 5, 3
Y2	7	2, 5, 5, 2, 5, 2, 5	40, 100, 100, 40, 100, 40, 100	20, 50, 50, 20, 50, 20, 50	20, 50, 50, 20, 50, 20, 50	3, 5, 5, 3, 5, 3, 5
B2	4	5, 5, 5, 3	100, 100, 100, 60	50, 50, 50, 30	50, 50, 50, 30	5, 5, 5, 3
B3	5	5, 5, 5, 3, 5	100, 100, 100, 60, 100	50, 50, 50, 30, 50	50, 50, 50, 30, 50	5, 5, 5, 3, 5

Figures

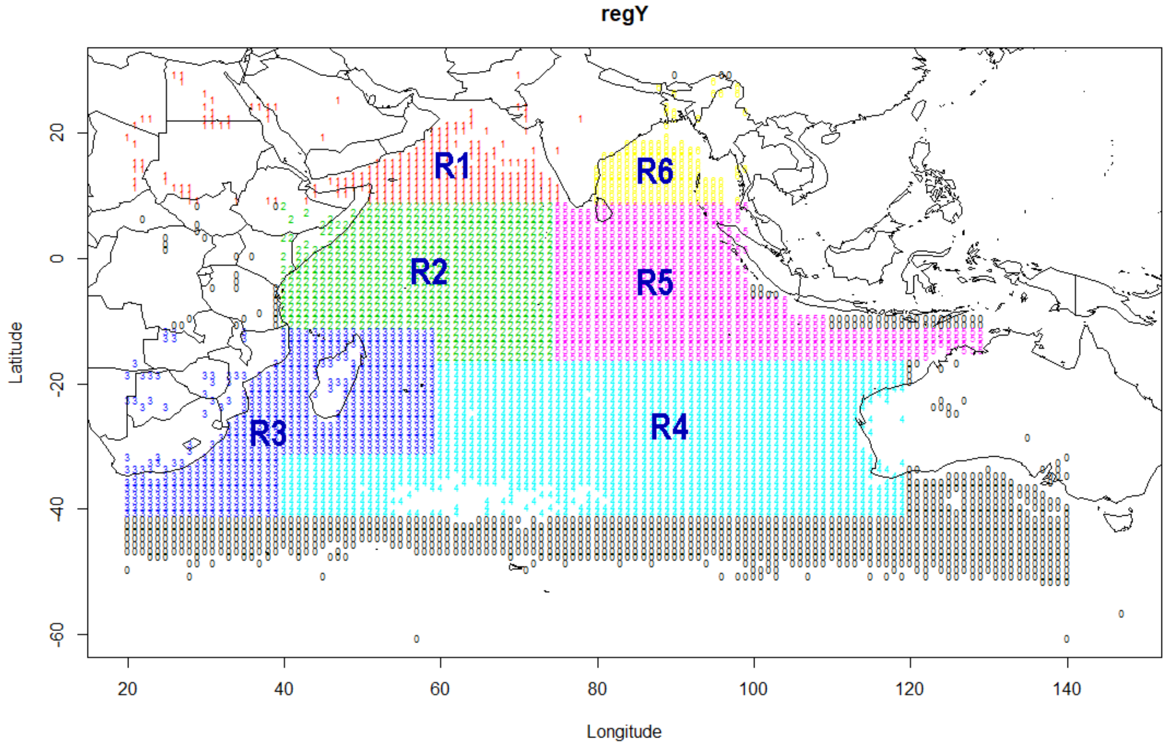

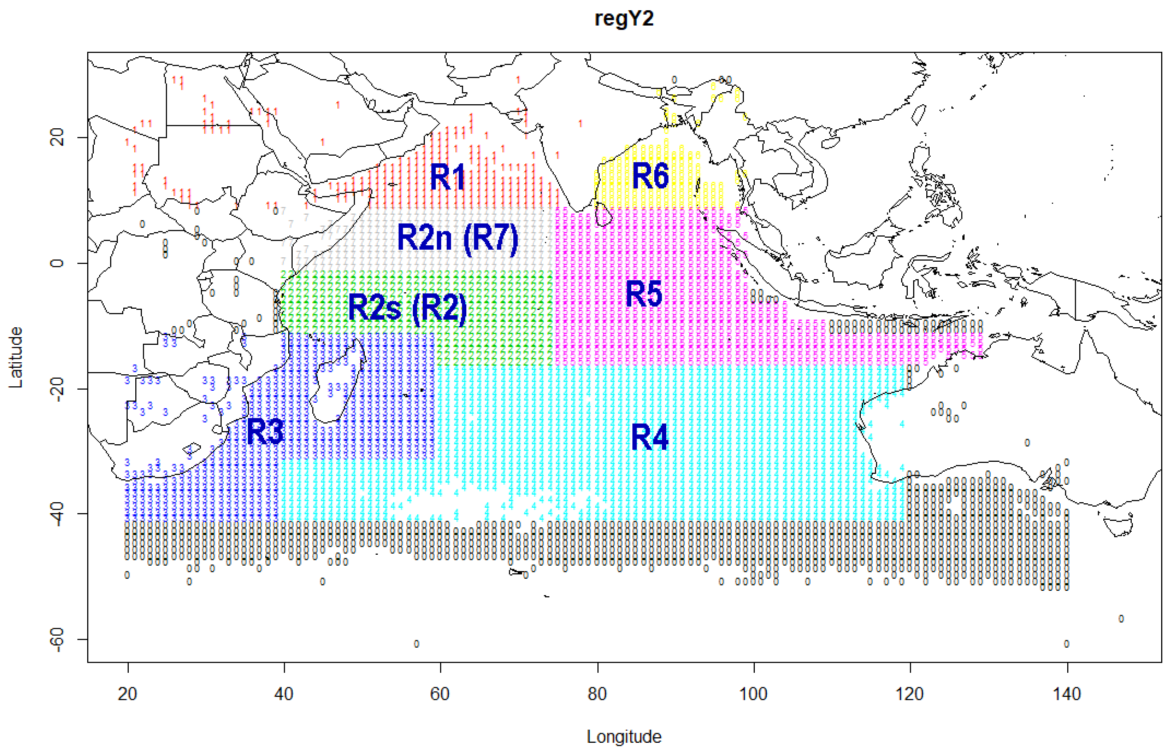

Figure 1: Maps of the regional structures used to estimate yellowfin CPUE indices for the versions in which the western tropical region is contiguous (Y, above) and split (Y2, below).

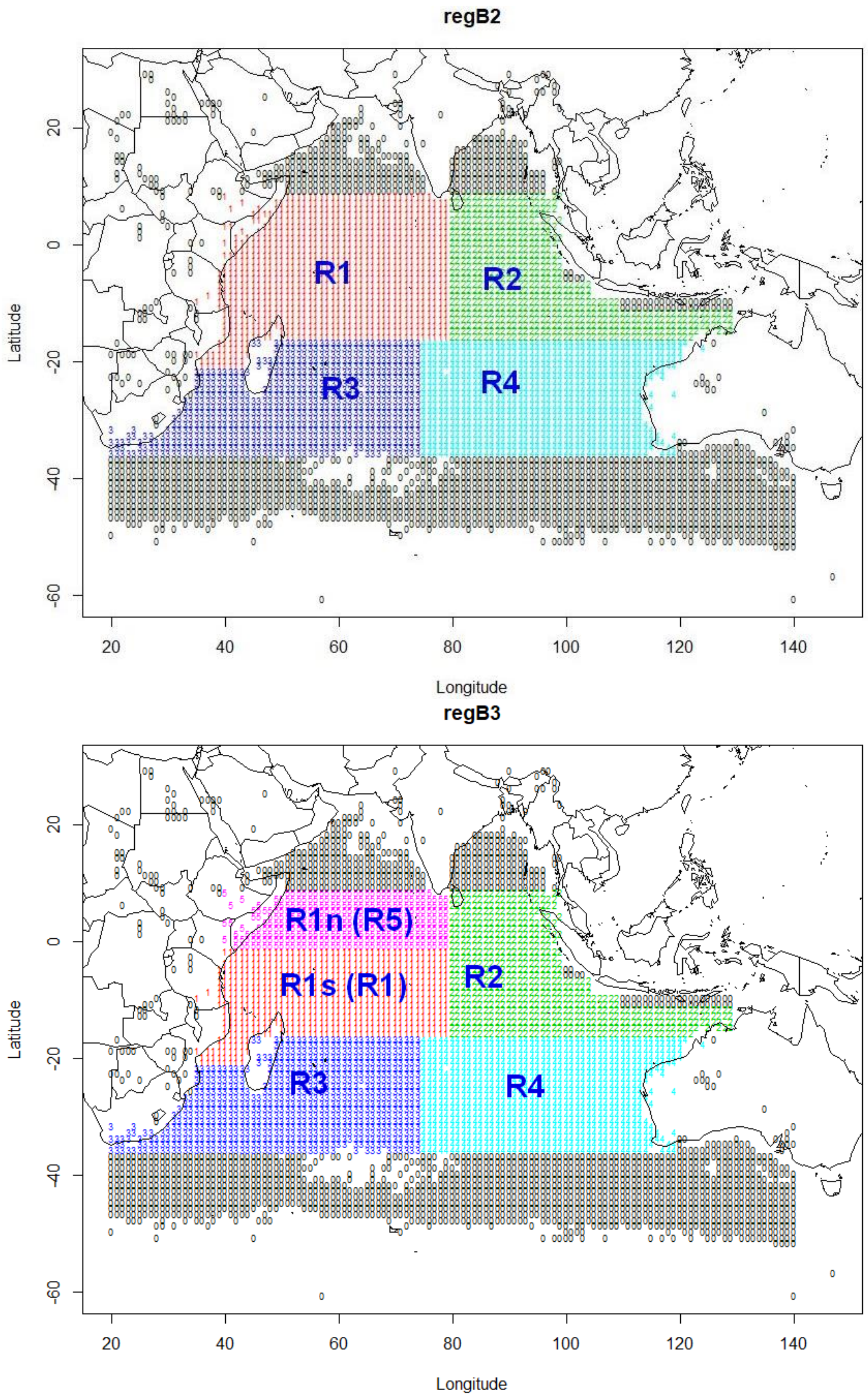

Figure 2: Maps of the regional structures used to estimate bigeye tuna CPUE indices for the versions in which the western tropical region is contiguous (B2, above) and split (B3, below).

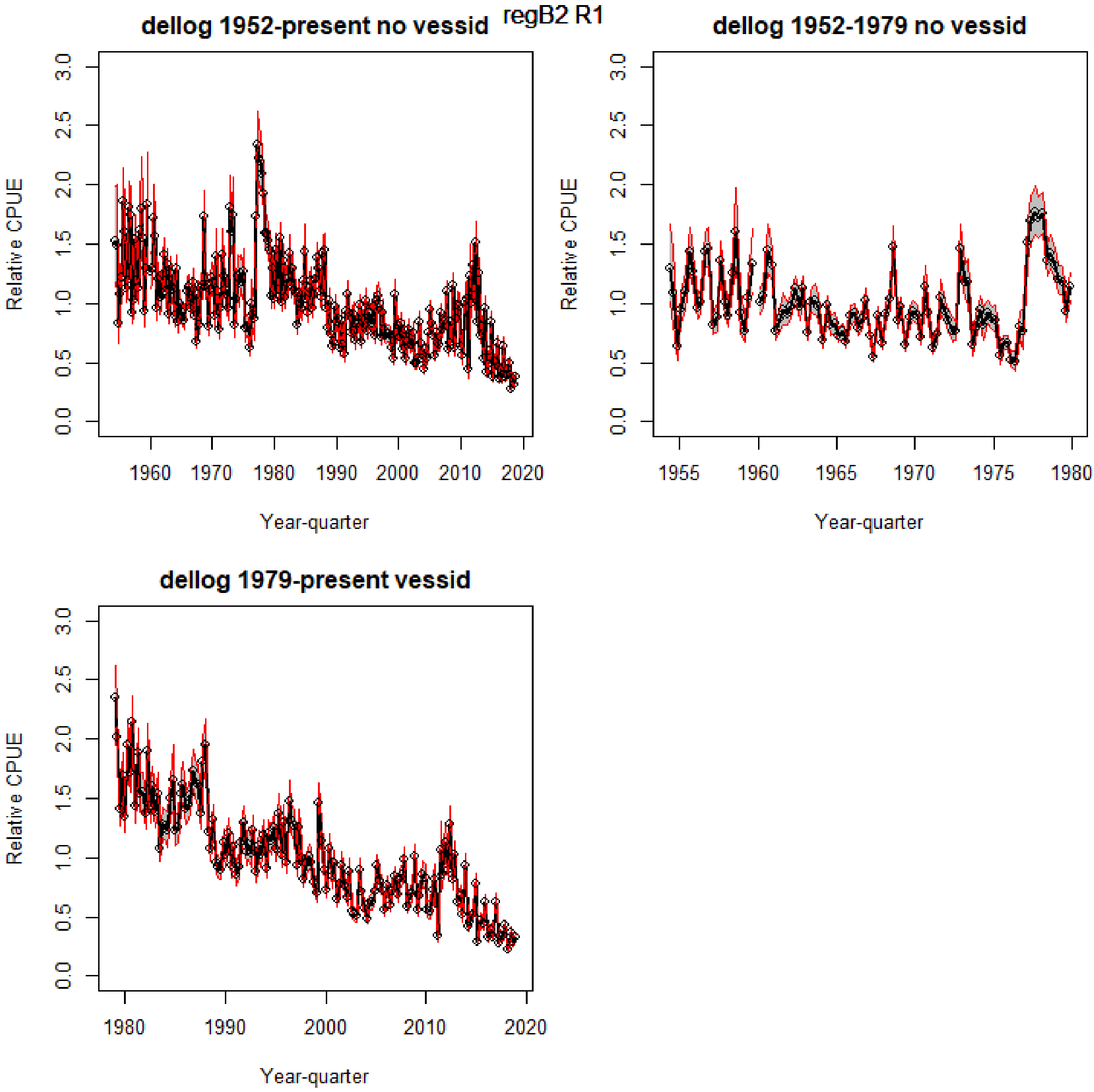

Figure 3: Quarterly CPUE series for bigeye region 1 (western tropical, regB2_R1), including time series for all years without vessel effects (top left), and time series for 1952-79 without vessel effects (top right), and 1979-2018 with vessel effects (bottom left).

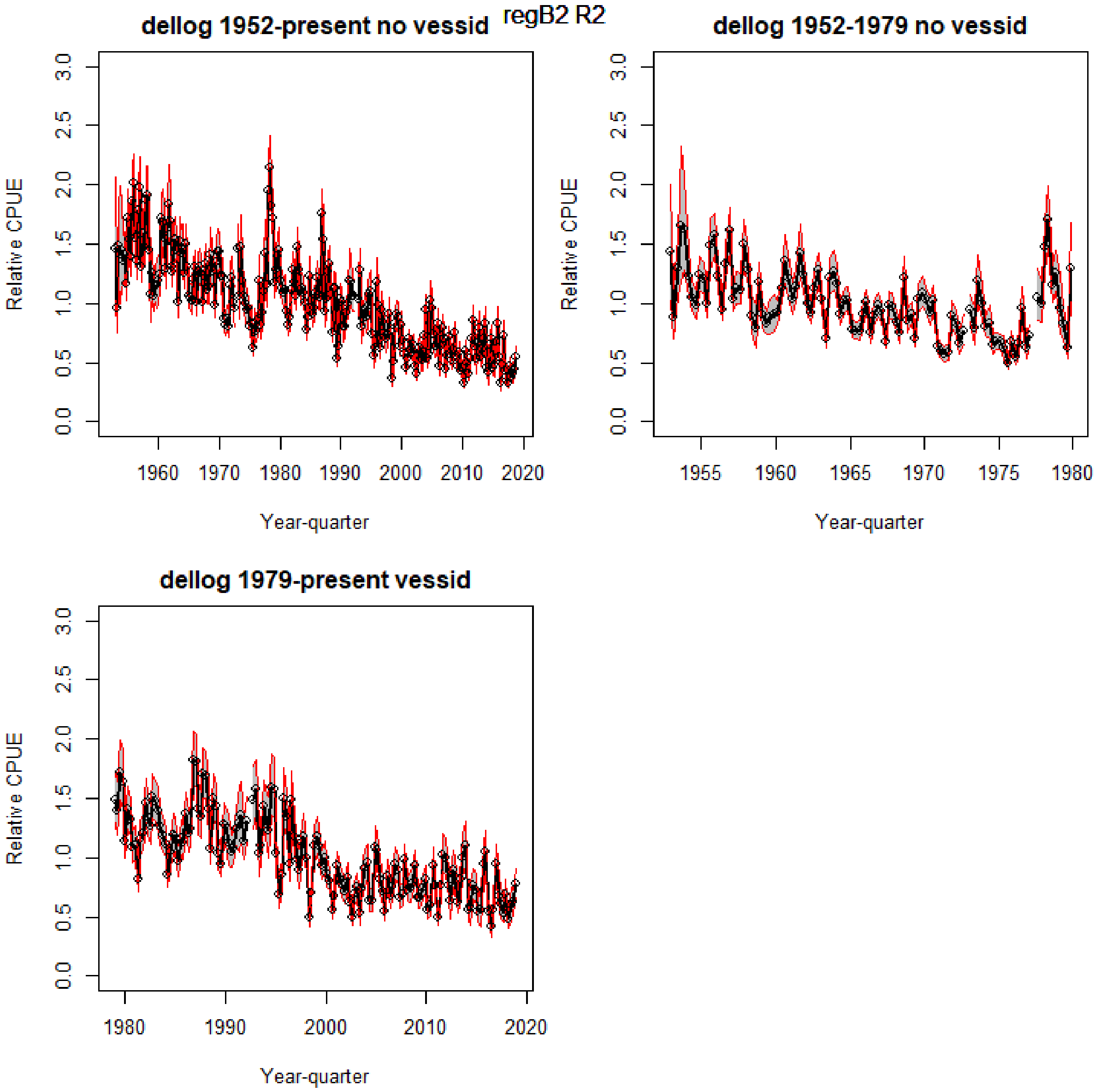

Figure 4: Quarterly CPUE series for bigeye region 2 (eastern tropical, regB2_R2), including time series for all years without vessel effects (top left), and time series for 1952-79 without vessel effects (top right), and 1979-2018 with vessel effects (bottom left).

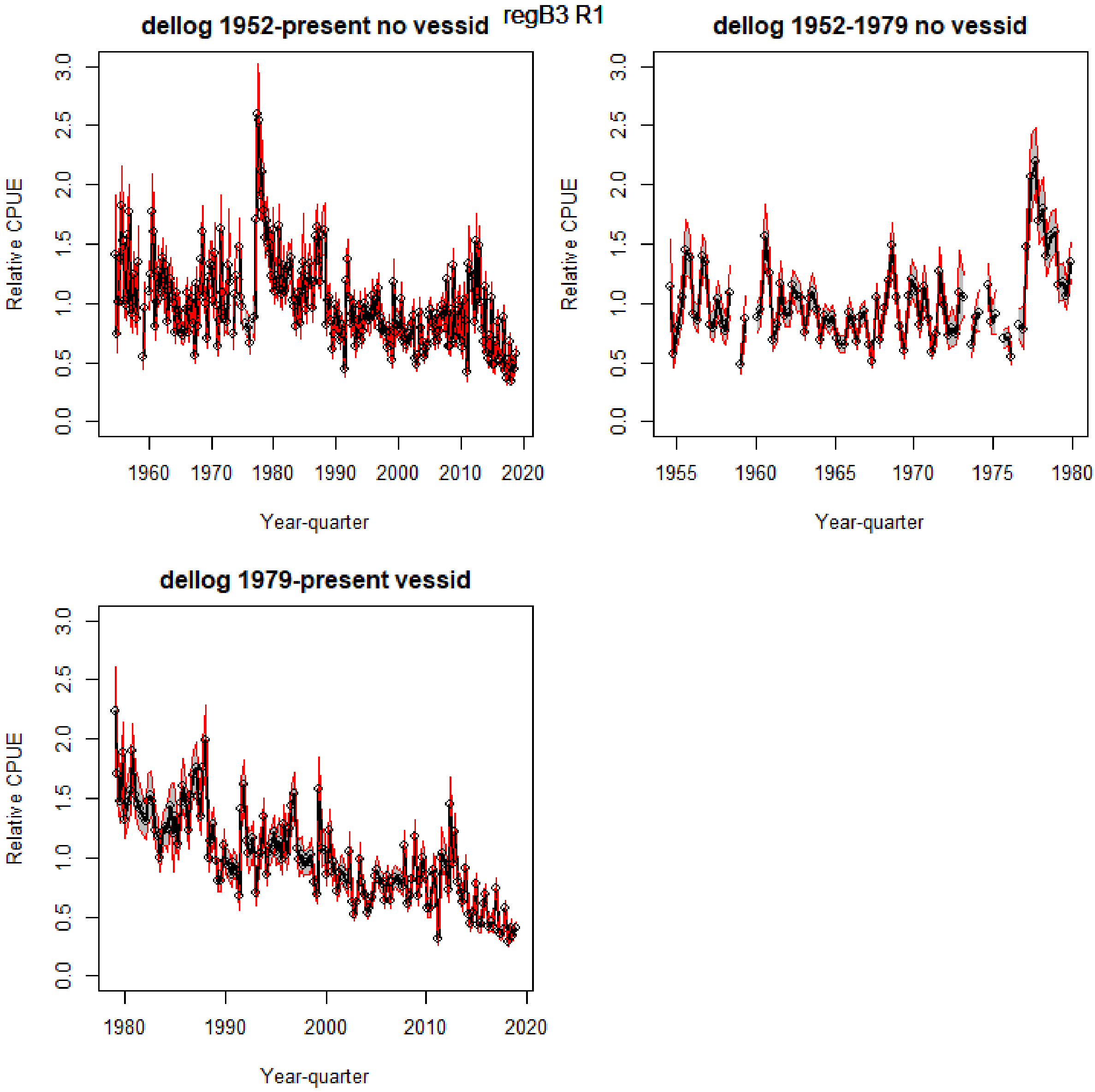

Figure 5: Quarterly CPUE series for bigeye region 1s (south-western tropical, regB3_R1) in regional structure B3, which is the southern part of the western tropical region. The plots include time series for all years (top) both with (right) and without (left) vessel effects, and time series for 1952-79 without vessel effects, and 1979-2018 with vessel effects.

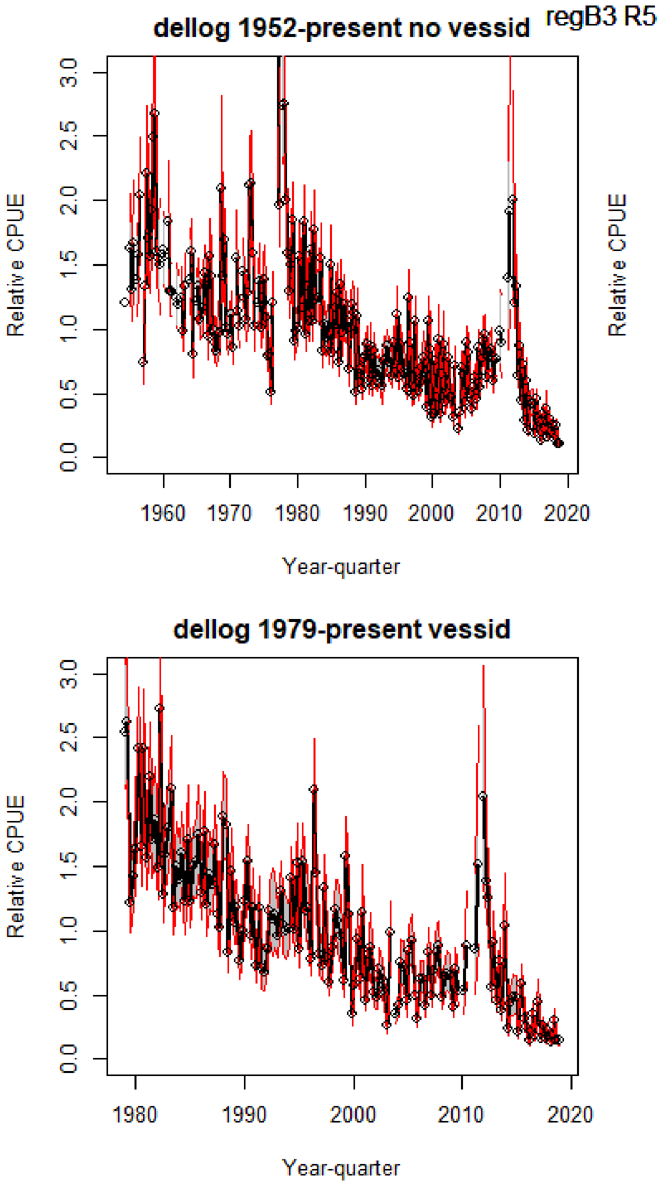

Figure 6: Quarterly CPUE series for bigeye region 1n (north-western tropical, regB3_R5) in regional structure B3, which is the northern part of the western tropical region. The plots include time series for all years (top) both with (right) and without (left) vessel effects, and time series for 1952-79 without vessel effects, and 1979-2018 with vessel effects.

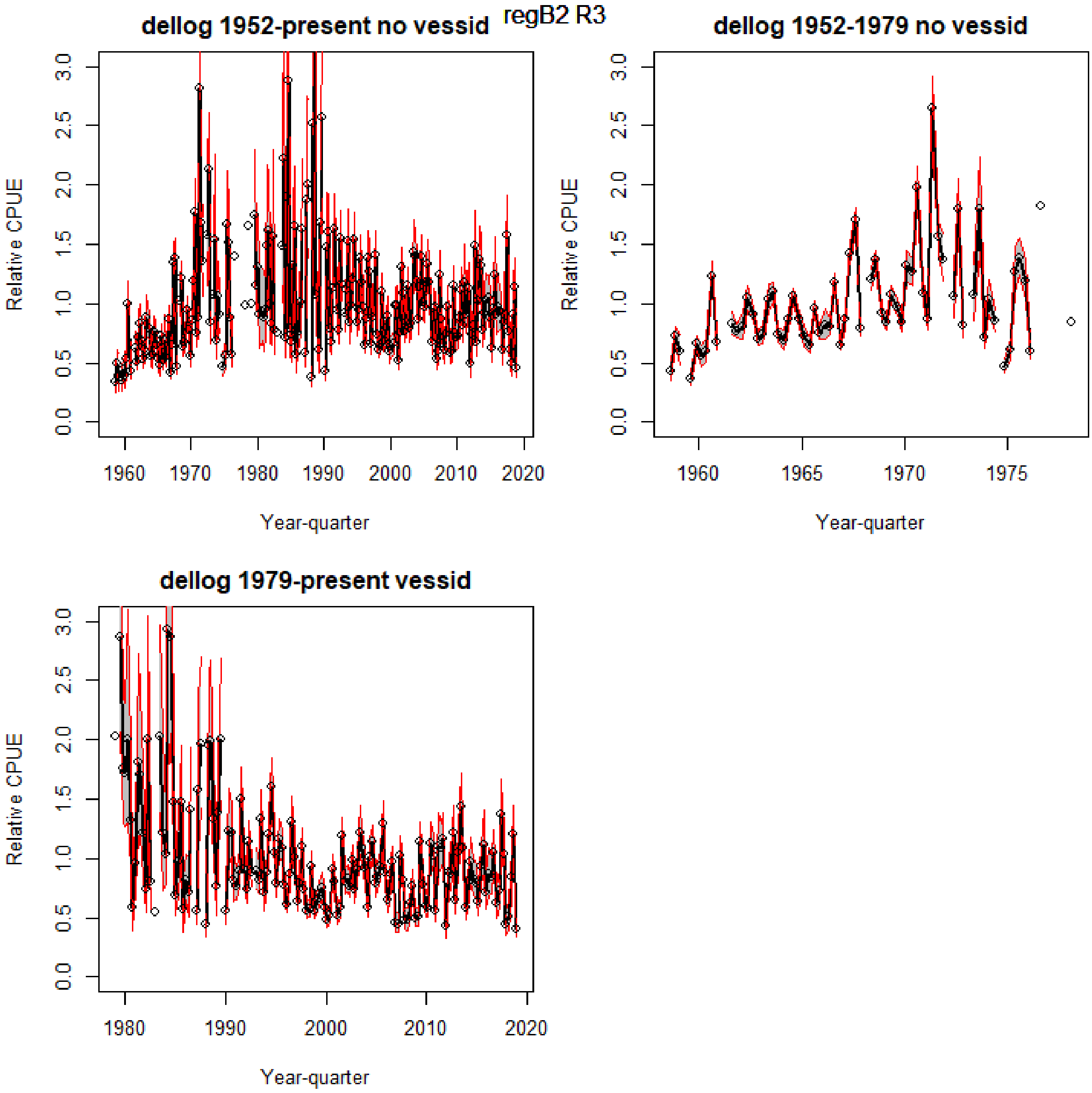

Figure 7: Quarterly CPUE series for bigeye region 3 (western temperate, regB2_R3), including time series for all years without vessel effects (top left), and time series for 1952-79 without vessel effects (top right), and 1979-2018 with vessel effects (bottom left).

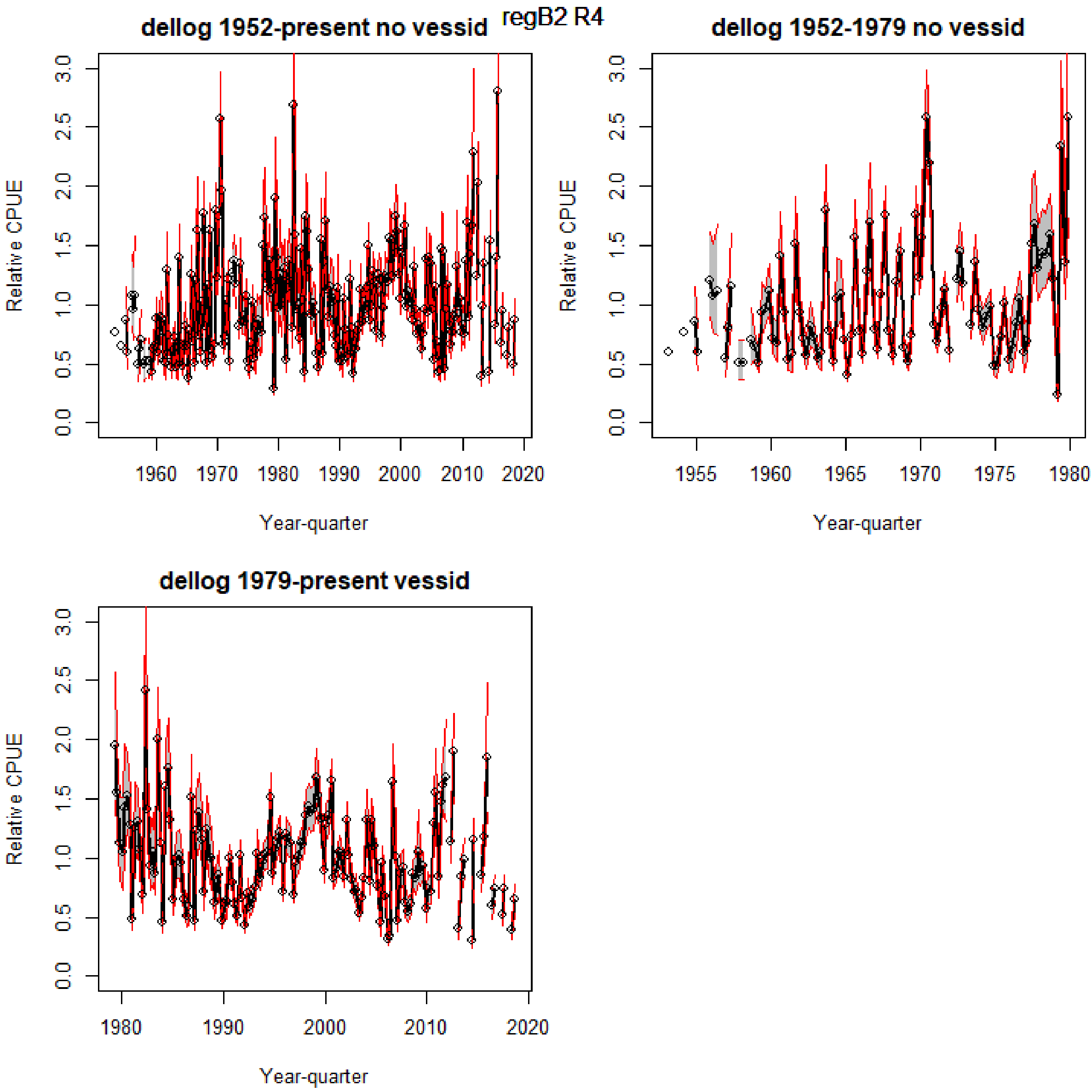

Figure 8: Quarterly CPUE series for bigeye region 4 (eastern temperate, regB2_R4), including time series for all years without vessel effects (top left), and time series for 1952-79 without vessel effects (top right), and 1979-2018 with vessel effects (bottom left).

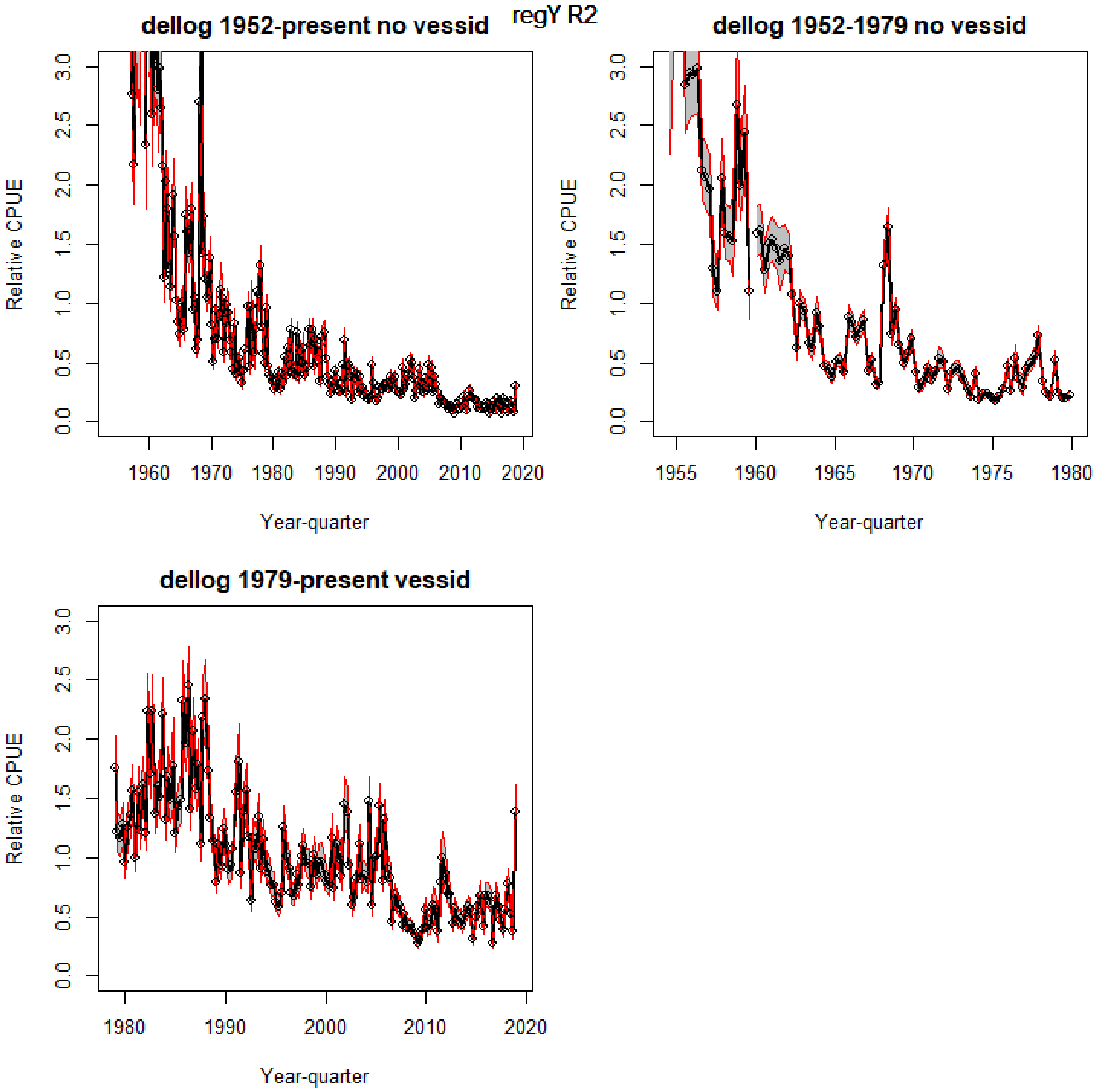

Figure 9: Quarterly CPUE series for yellowfin region 2 (western tropical, regY_R2), including time series for all years without vessel effects (top left), and time series for 1952-79 without vessel effects (top right), and 1979-2018 with vessel effects (bottom left).

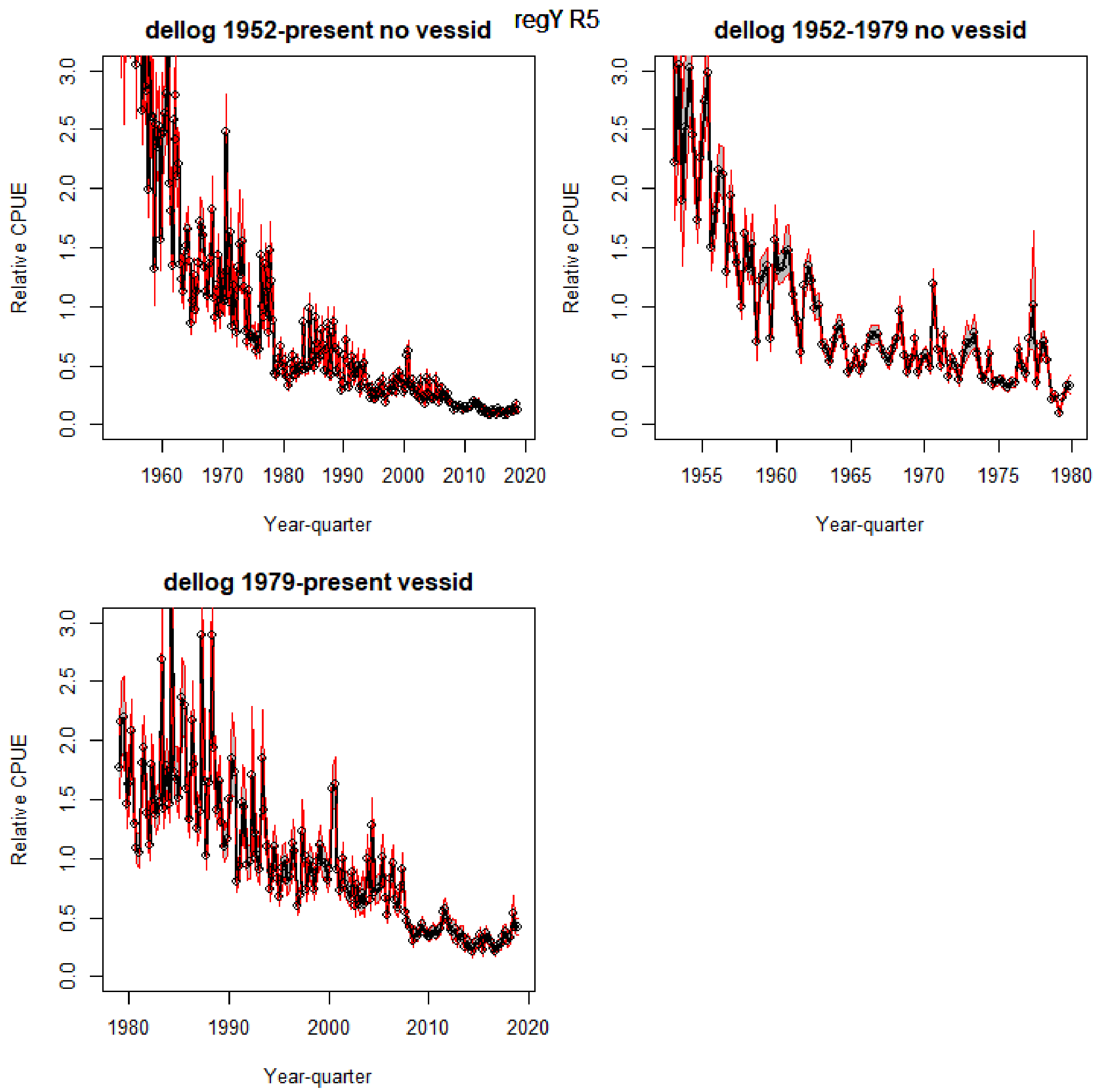

Figure 10: Quarterly CPUE series for yellowfin region 5 (eastern tropical, regY_R5), including time series for all years without vessel effects (top left), and time series for 1952-79 without vessel effects (top right), and 1979-2018 with vessel effects (bottom left).

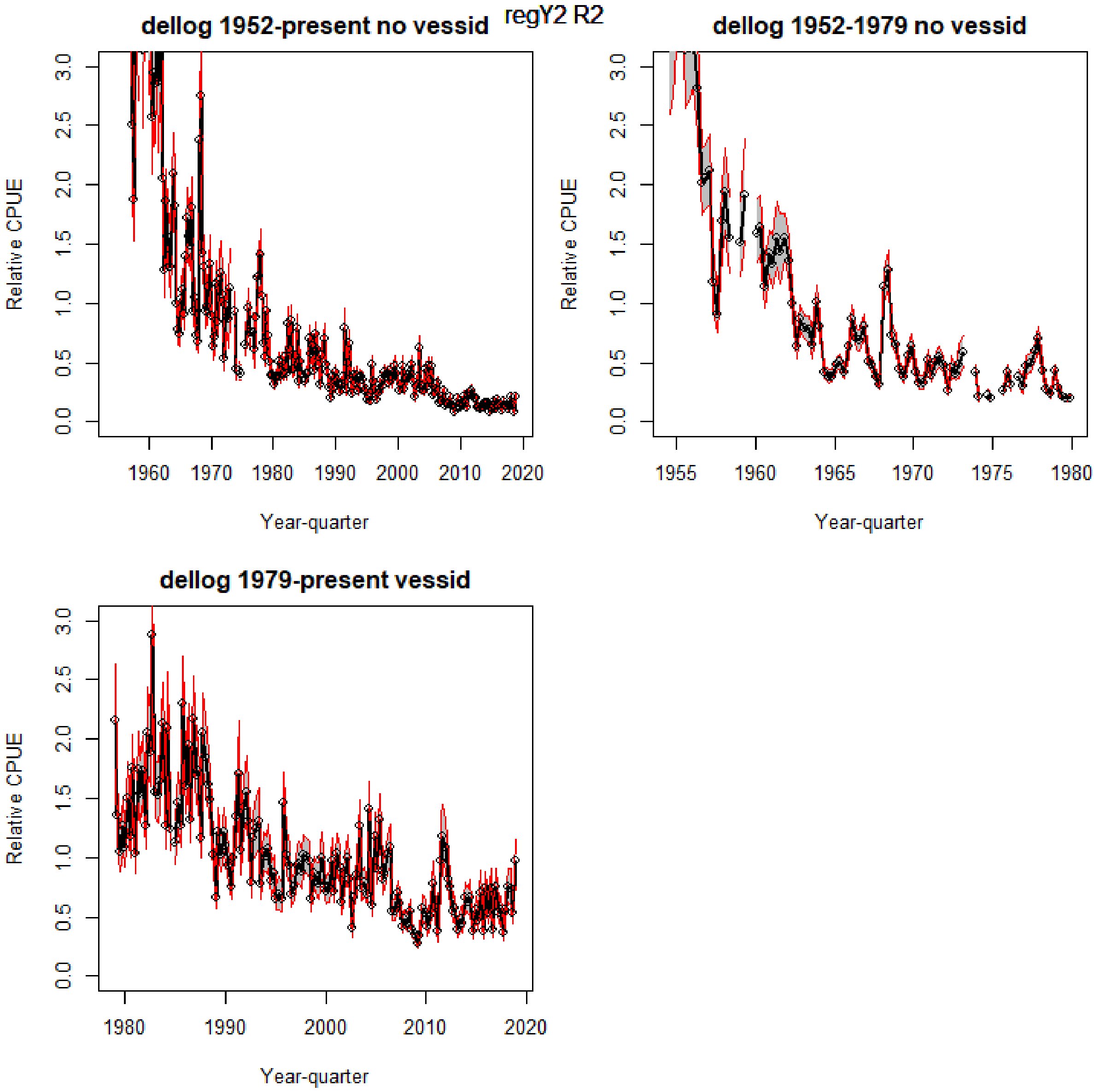

Figure 11: Quarterly CPUE series for yellowfin region 2s (south-western tropical, regY2_R2) in regional structure Y2, which is the southern part of the western tropical region. The plots include time series for all years (top) both with (right) and without (left) vessel effects, and time series for 1952-79 without vessel effects, and 1979-2018 with vessel effects.

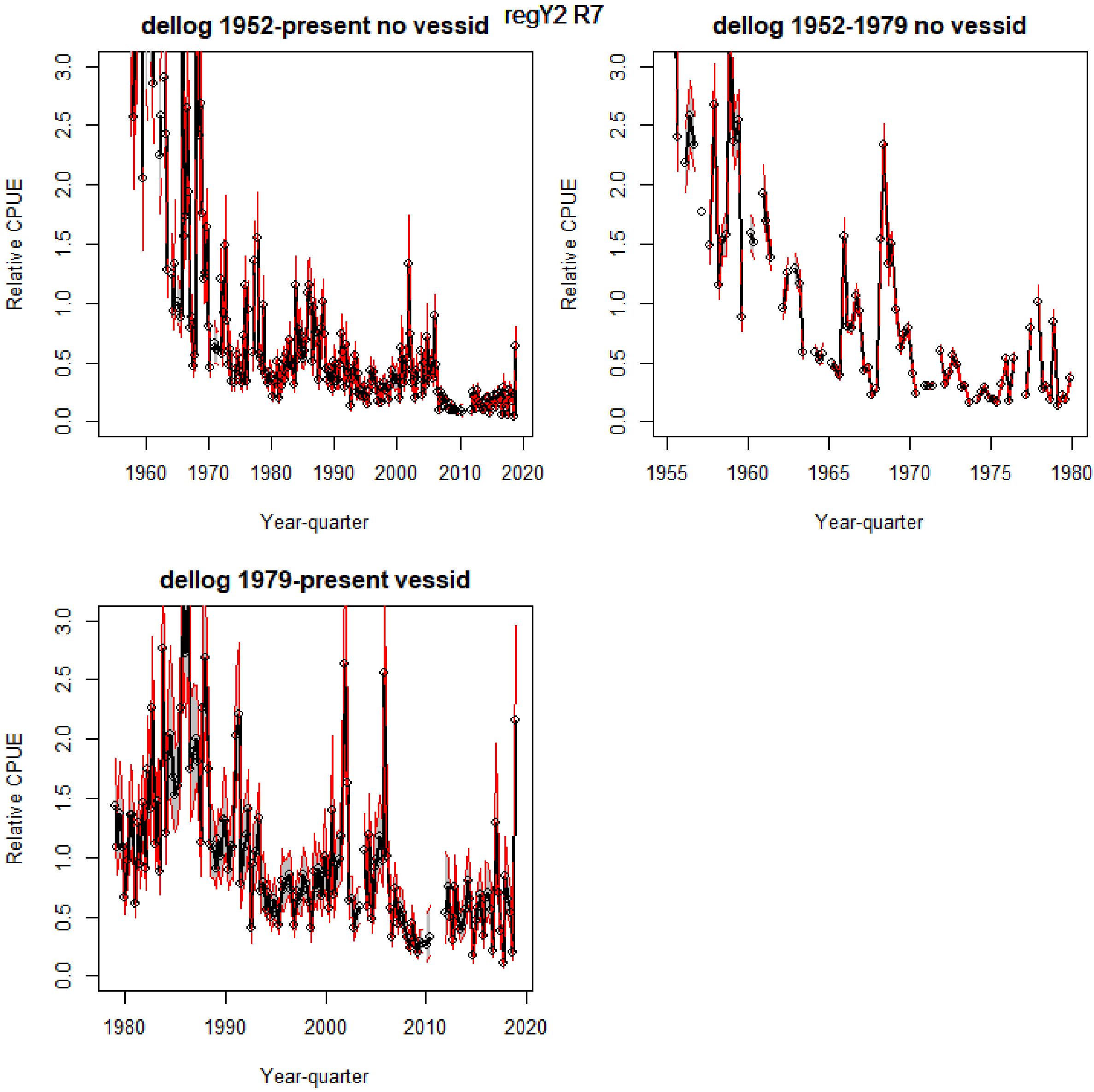

Figure 12: Quarterly CPUE series for yellowfin region 2n (north-western tropical, regY2_R7) in regional structure Y2, which is the northern part of the western tropical region. The plots include time series for all years (top) both with (right) and without (left) vessel effects, and time series for 1952-79 without vessel effects, and 1979-2018 with vessel effects.

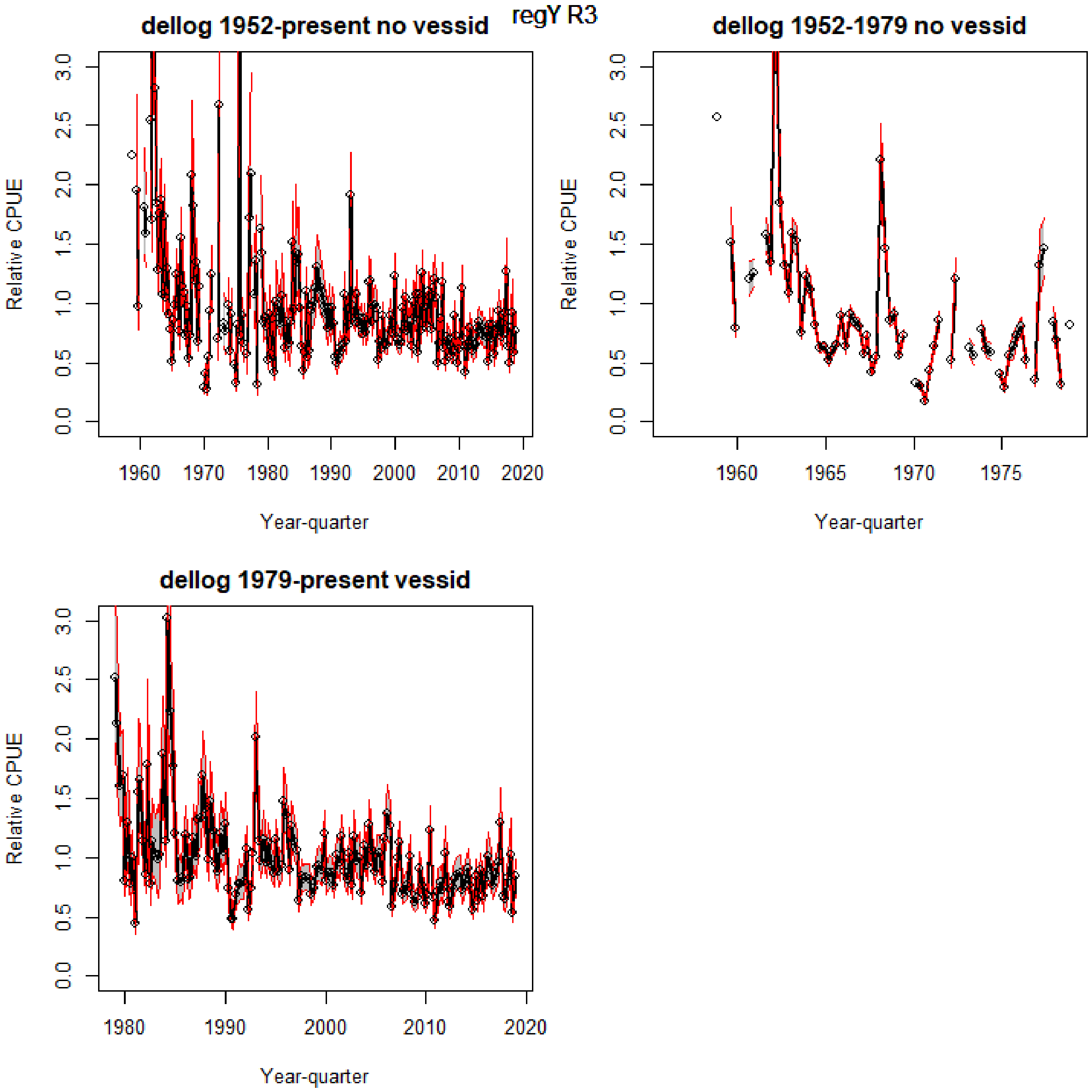

Figure 13: Quarterly CPUE series for yellowfin region 3 (western temperate, regY_R3), including time series for all years without vessel effects (top left), and time series for 1952-79 without vessel effects (top right), and 1979-2018 with vessel effects (bottom left).

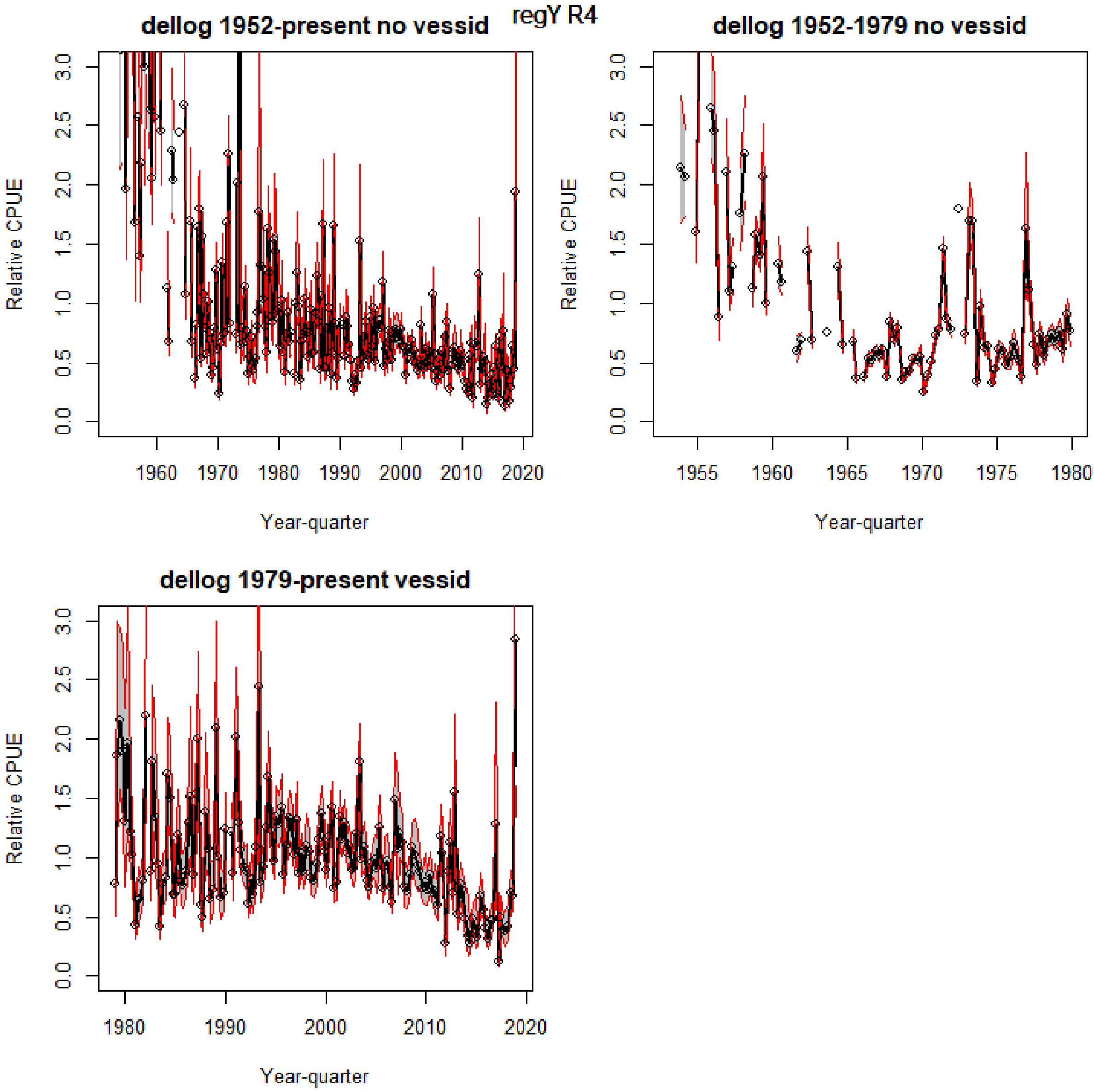

Figure 14: Quarterly CPUE series for yellowfin region 4 (eastern temperate, regY_R4), including time series for all years without vessel effects (top left), and time series for 1952-79 without vessel effects (top right), and 1979-2018 with vessel effects (bottom left).

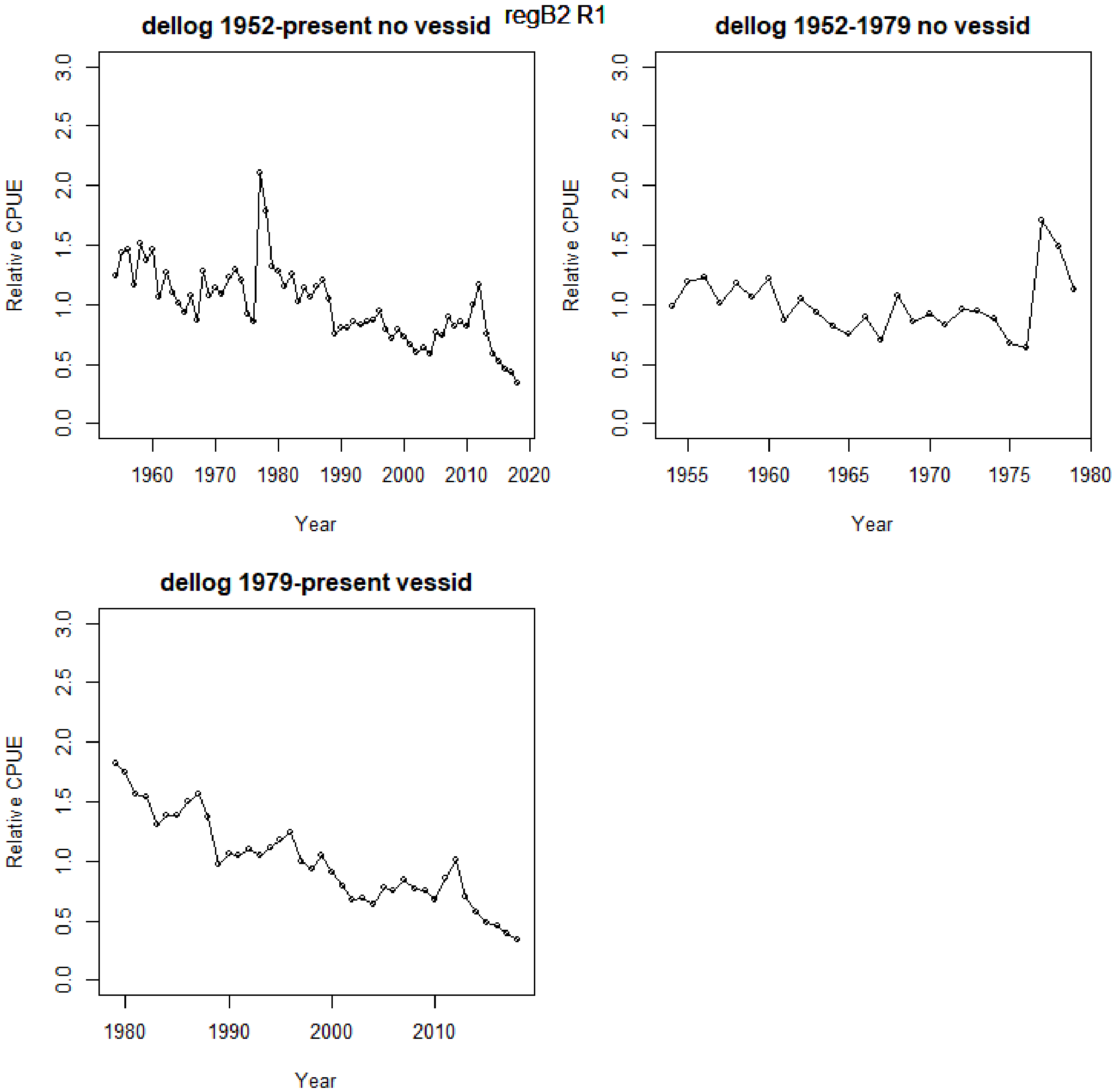

Figure 15: Annual CPUE series for bigeye region 1 (western tropical, regB2_R1), including time series for all years without vessel effects (top left), and time series for 1952-79 without vessel effects (top right), and 1979-2018 with vessel effects (bottom left).

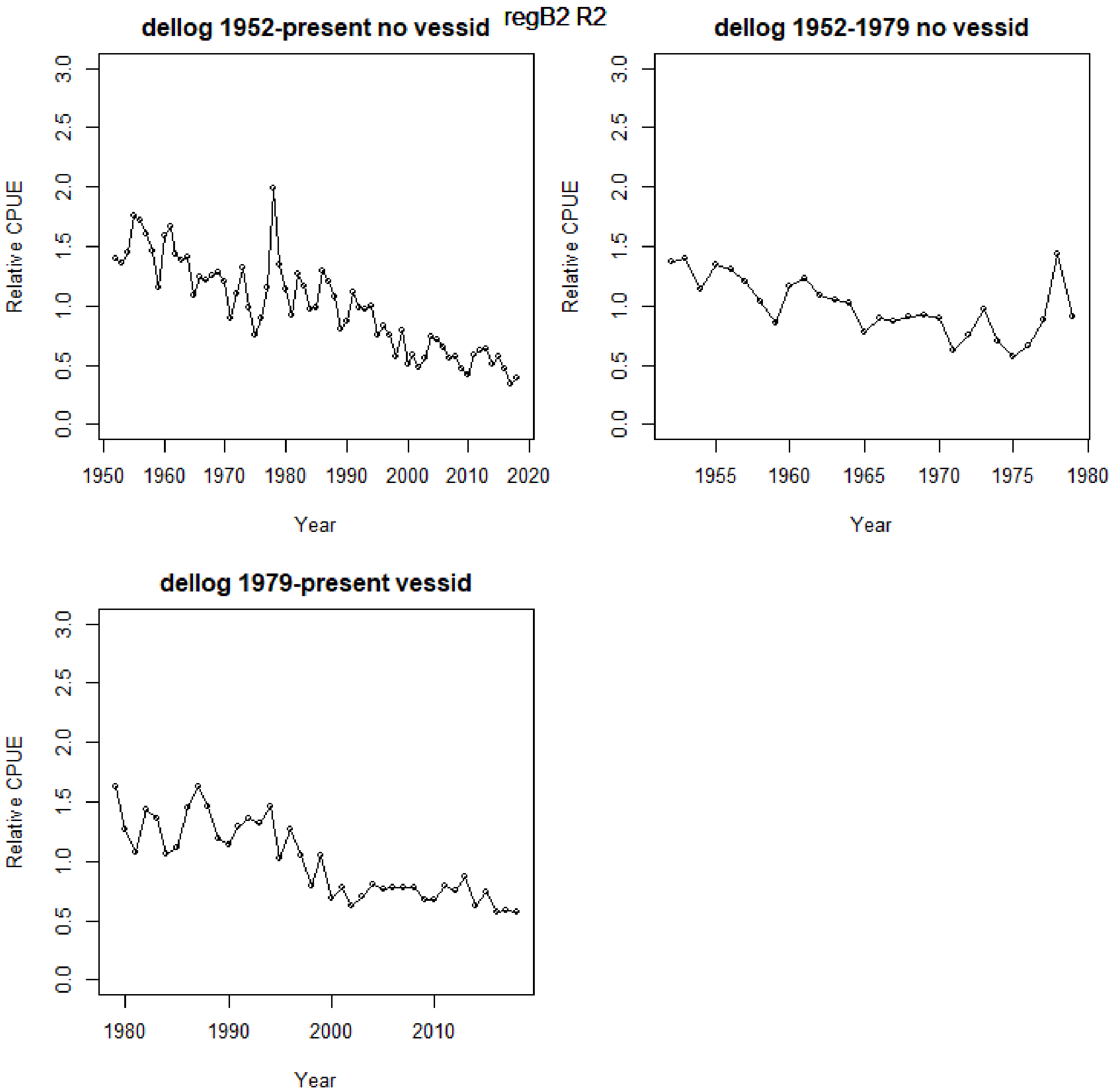

Figure 16: Annual CPUE series for bigeye region 2 (eastern tropical, regB2_R2), including time series for all years without vessel effects (top left), and time series for 1952-79 without vessel effects (top right), and 1979-2018 with vessel effects (bottom left).

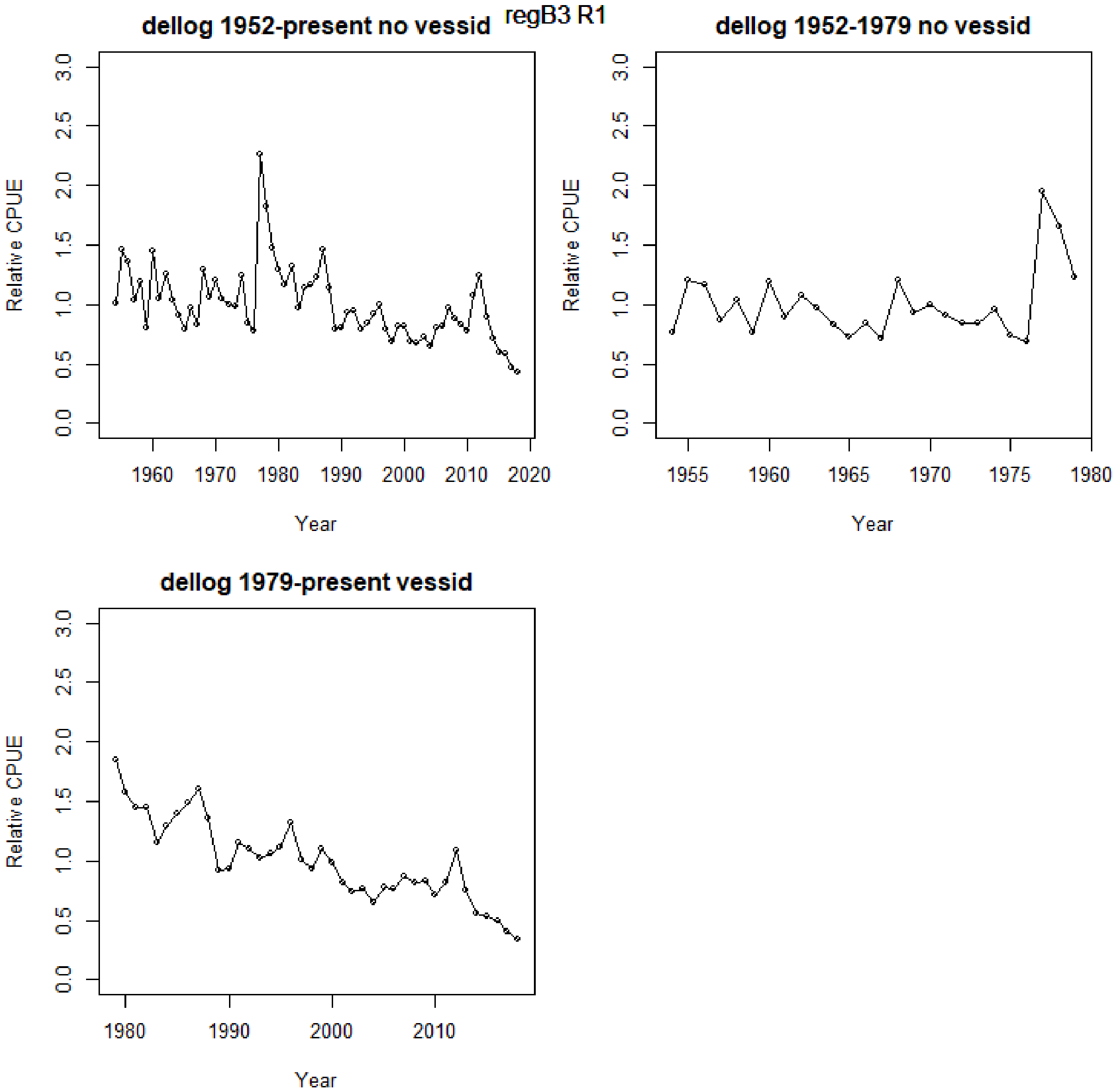

Figure 17: Annual CPUE series for bigeye region 1S (south-western tropical, regB3_R1 including time series for all years without vessel effects (top left), and time series for 1952-79 without vessel effects (top right), and 1979-2018 with vessel effects (bottom left).

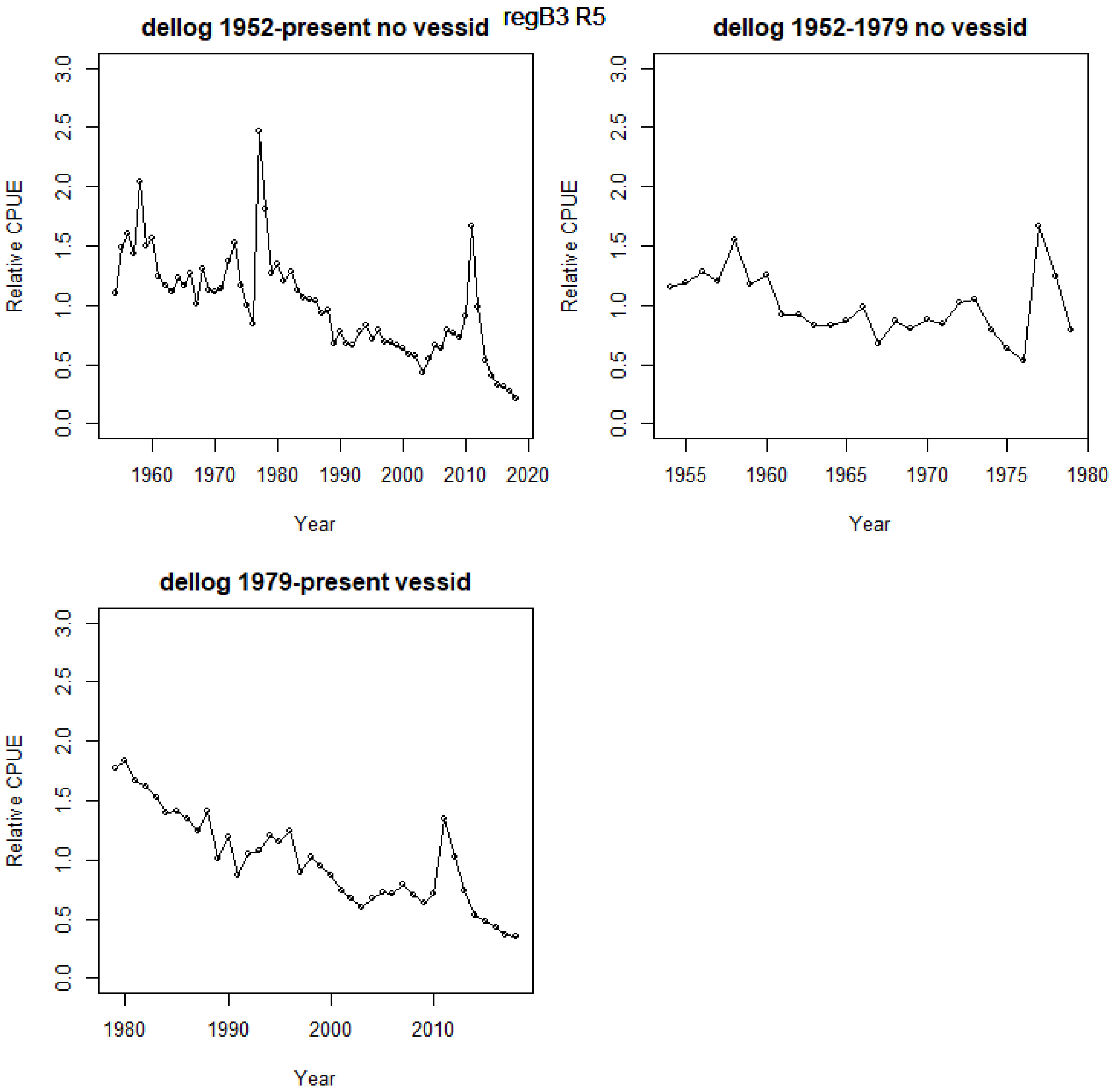

Figure 18: Annual CPUE series for bigeye region 1N (north-western tropical, regB3_R5), including time series for all years without vessel effects (top left), and time series for 1952-79 without vessel effects (top right), and 1979-2018 with vessel effects (bottom left).

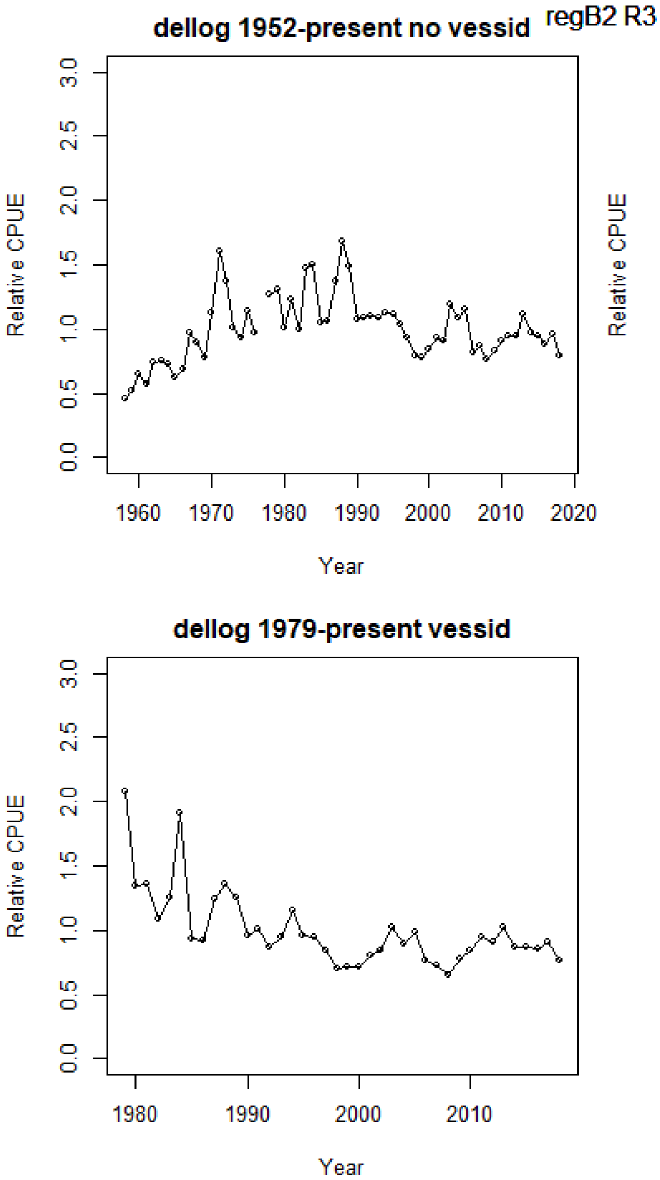

Figure 19: Annual CPUE series for bigeye region 3 (western temperate, regB2_R3), including time series for all years without vessel effects (top left), and time series for 1952-79 without vessel effects (top right), and 1979-2018 with vessel effects (bottom left).

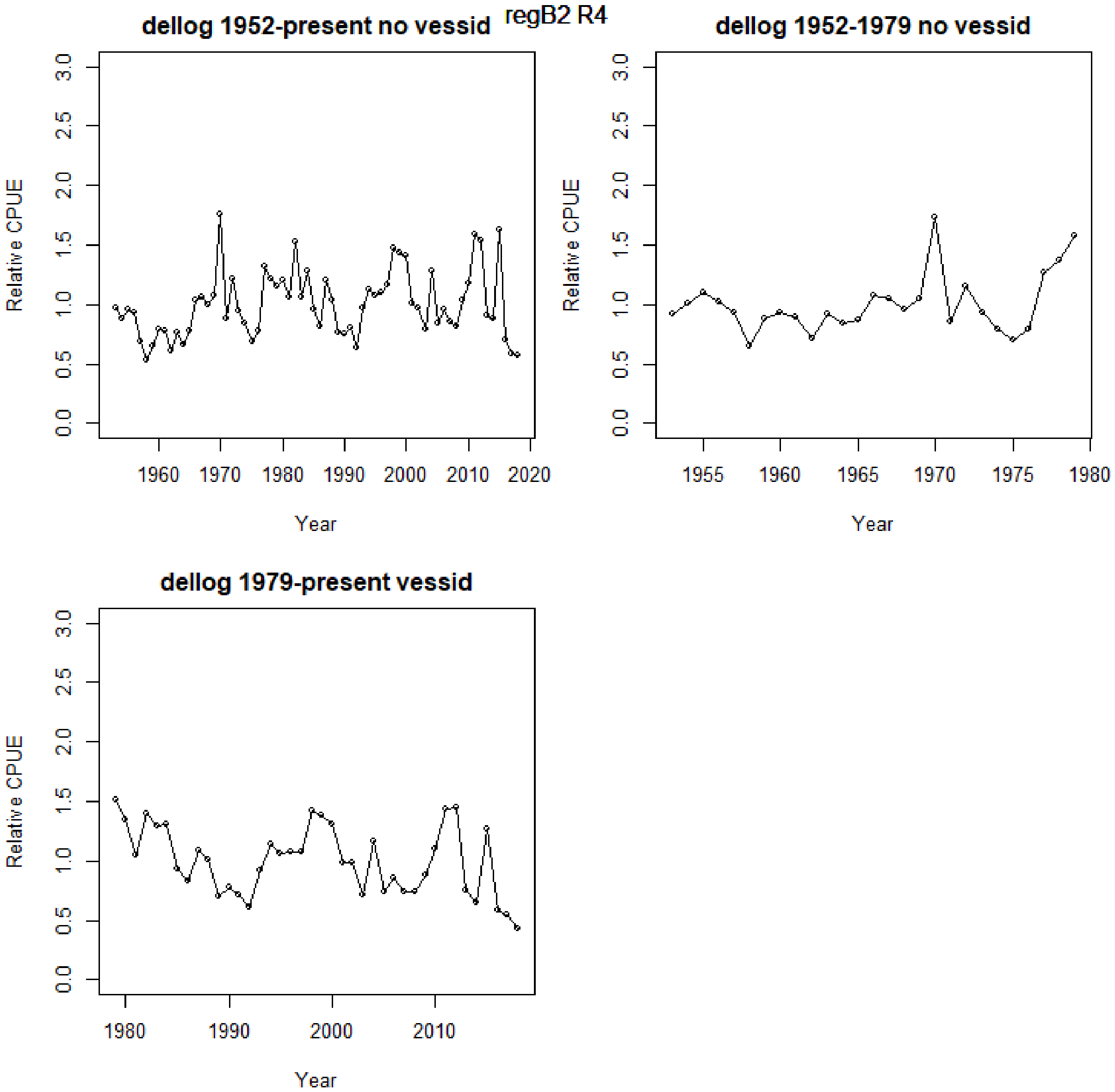

Figure 20: Annual CPUE series for bigeye region 4 (eastern temperate, regB2_R4), including time series for all years without vessel effects (top left), and time series for 1952-79 without vessel effects (top right), and 1979-2018 with vessel effects (bottom left).

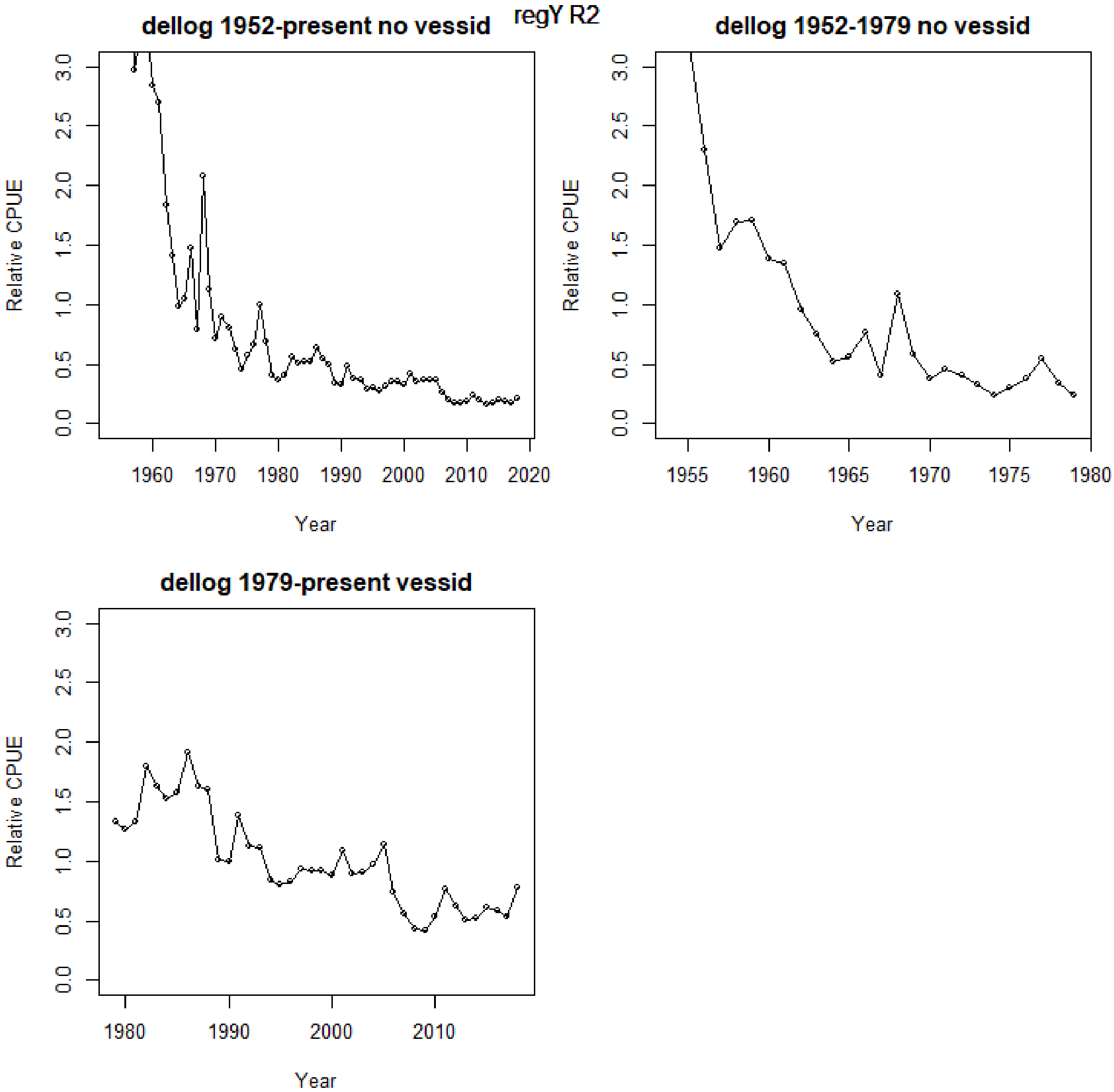

Figure 21: Annual CPUE series for yellowfin region 2 (western tropical, regY_R2), including time series for all years without vessel effects (top left), and time series for 1952-79 without vessel effects (top right), and 1979-2018 with vessel effects (bottom left).

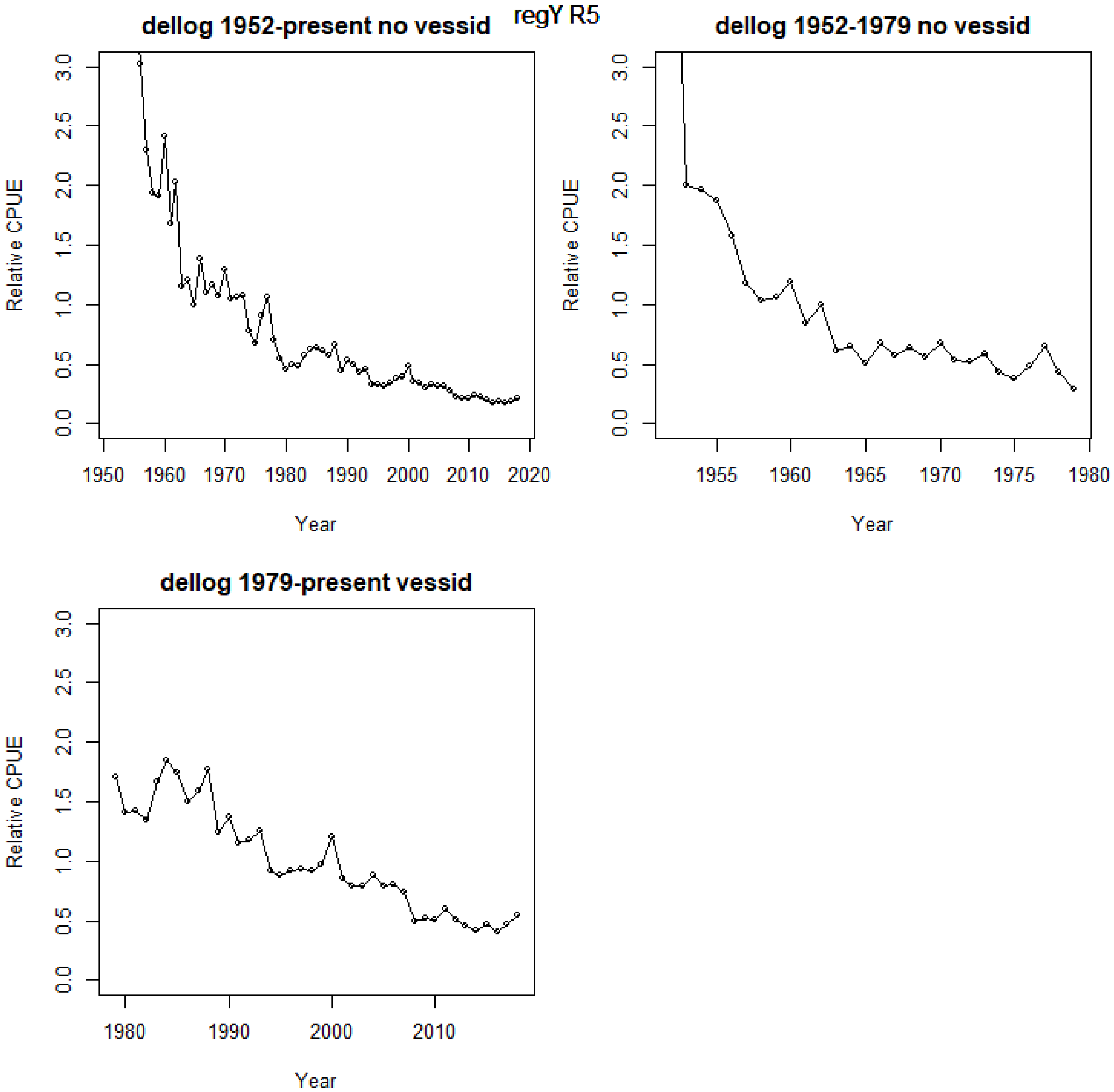

Figure 22: Annual CPUE series for yellowfin region 5 (eastern tropical, regY_R5), including time series for all years without vessel effects (top left), and time series for 1952-79 without vessel effects (top right), and 1979-2018 with vessel effects (bottom left).

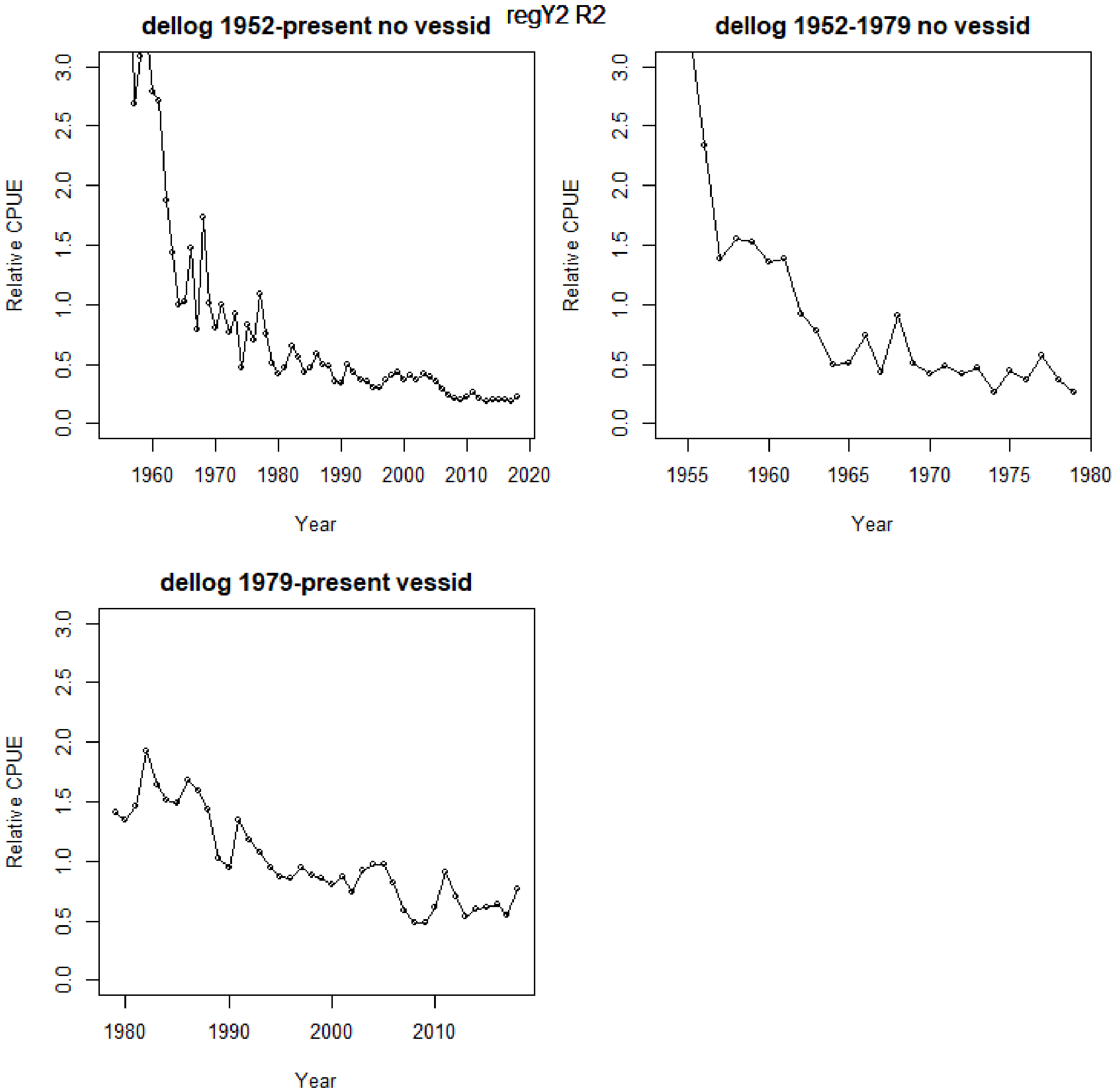

Figure 23: Annual CPUE series for yellowfin region 2S (south-western tropical, regY2_R2), including time series for all years without vessel effects (top left), and time series for 1952-79 without vessel effects (top right), and 1979-2018 with vessel effects (bottom left).

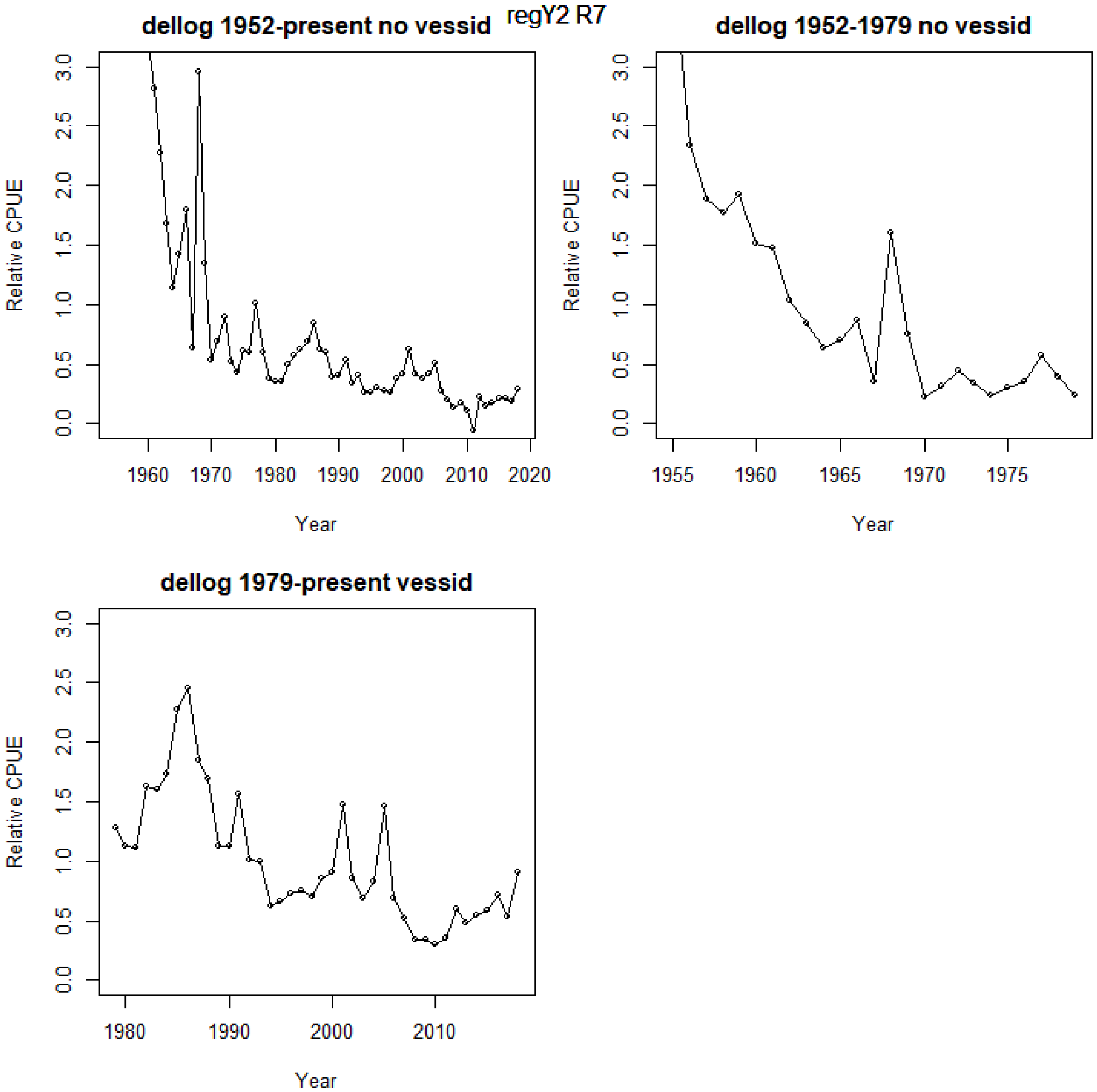

Figure 24: Annual CPUE series for yellowfin region 2N (north-western tropical, regY2_R7), including time series for all years without vessel effects (top left), and time series for 1952-79 without vessel effects (top right), and 1979-2018 with vessel effects (bottom left).

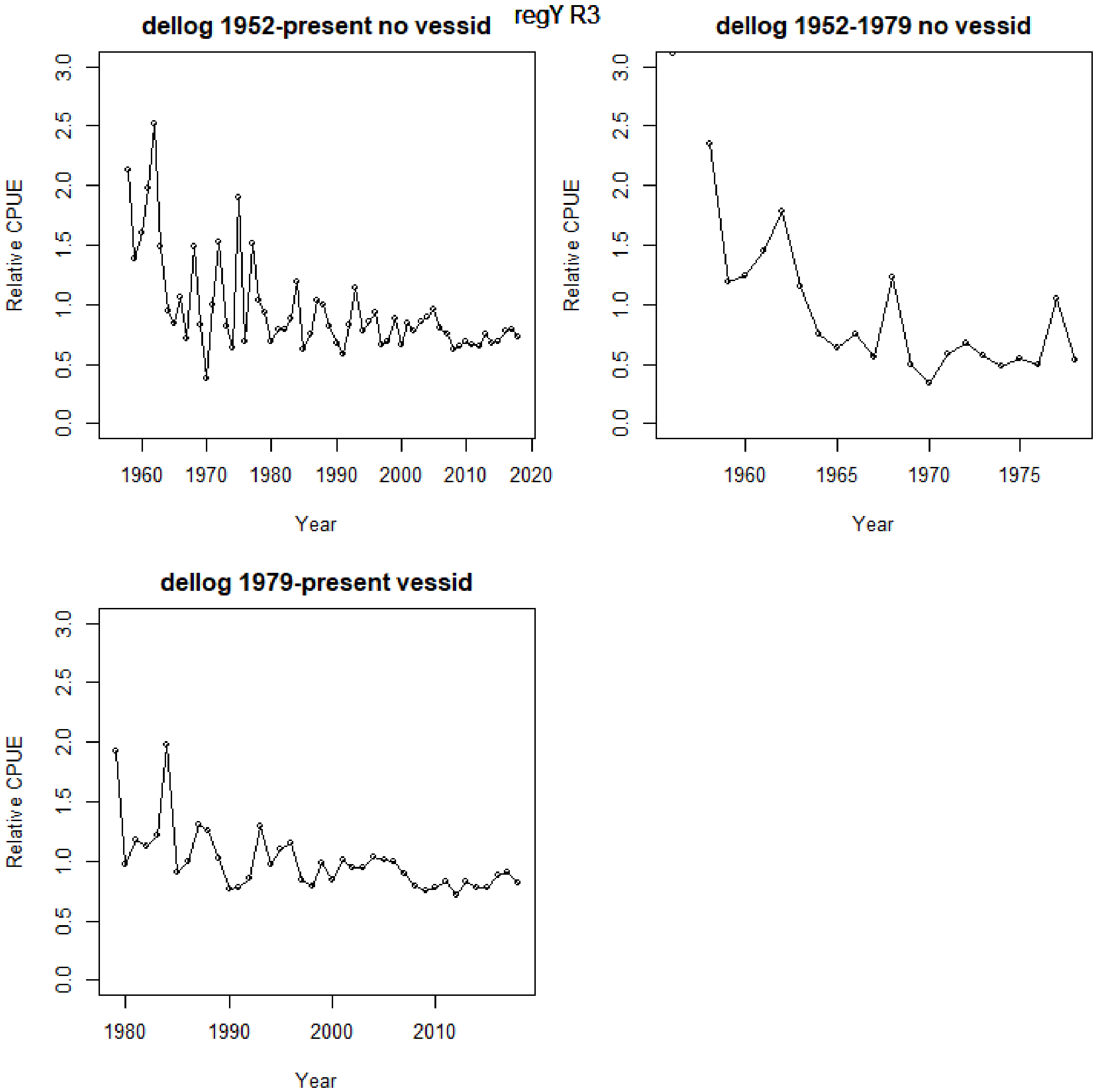

Figure 25: Annual CPUE series for yellowfin region 3 (western temperate, regY_R3), including time series for all years without vessel effects (top left), and time series for 1952-79 without vessel effects (top right), and 1979-2018 with vessel effects (bottom left).

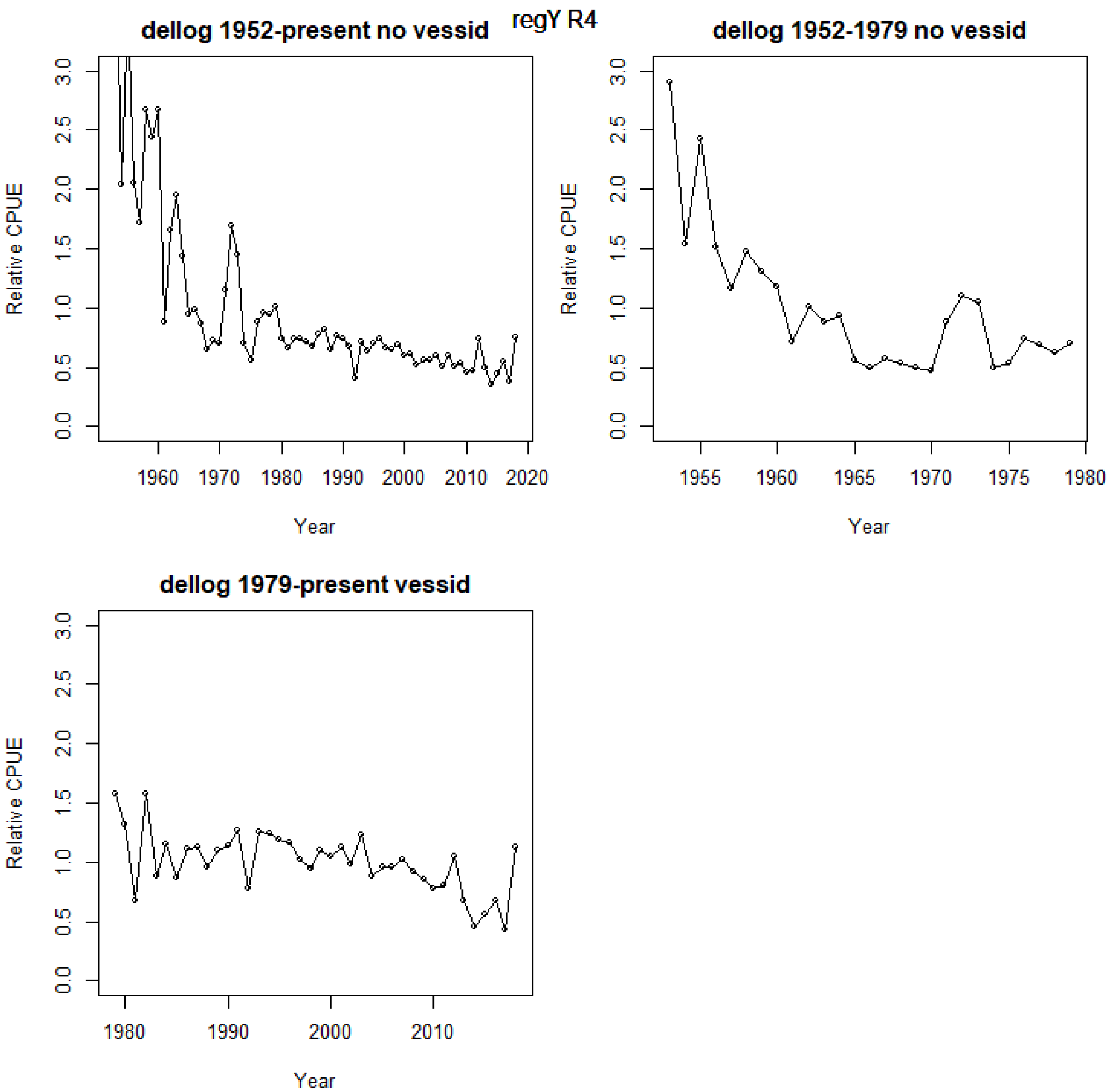

Figure 26: Annual CPUE series for yellowfin region 4 (eastern temperate, regY_R4), including time series for all years without vessel effects (top left), and time series for 1952-79 without vessel effects (top right), and 1979-2018 with vessel effects (bottom left).

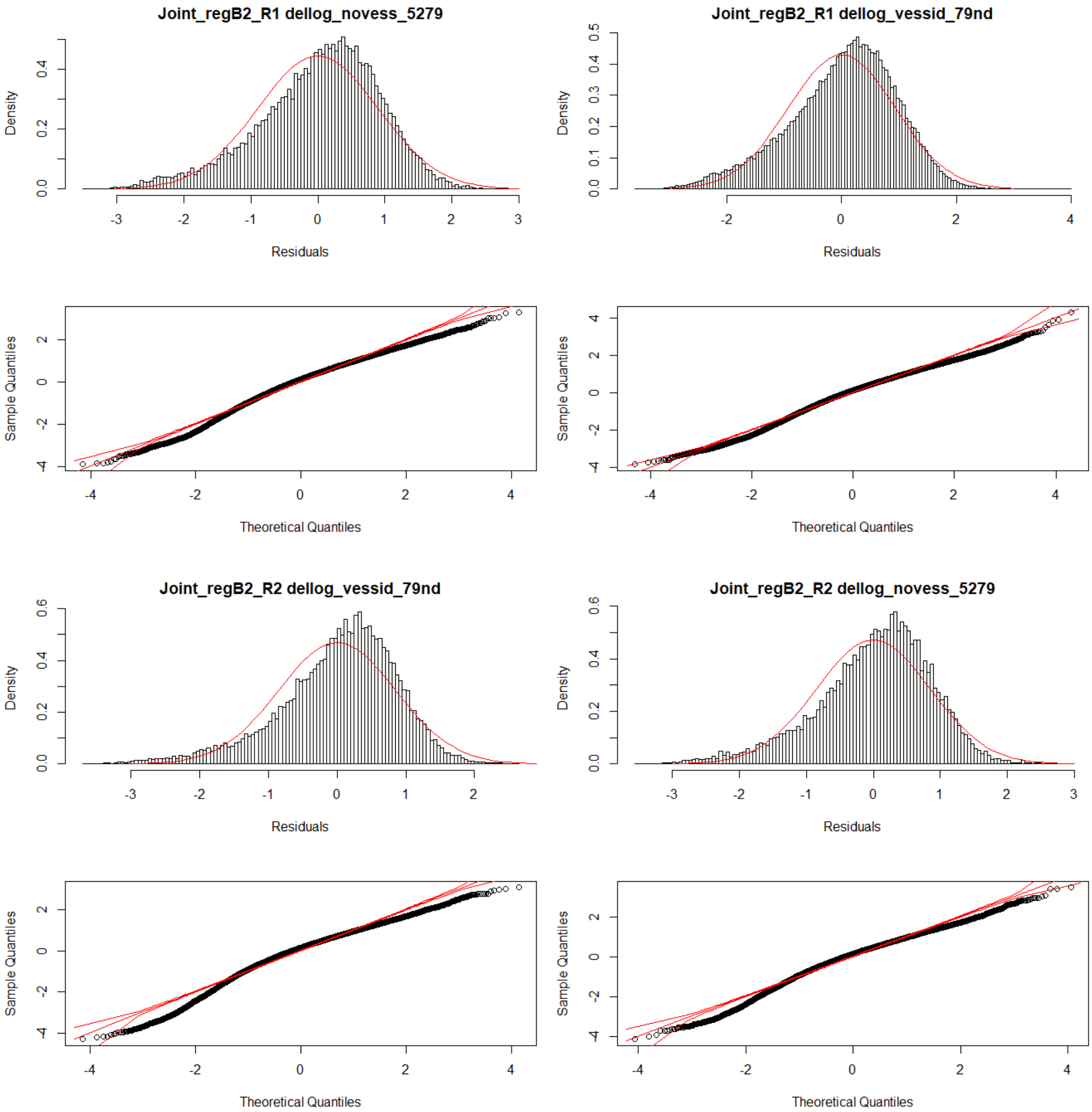

Figure 27: Diagnostic plots for bigeye lognormal positive models in tropical regions 1 and 2 (regB2_R1 and regB2_R2), for 1952-79 without vessel effects (left) and for 1979-2018 with vessel effects (right).

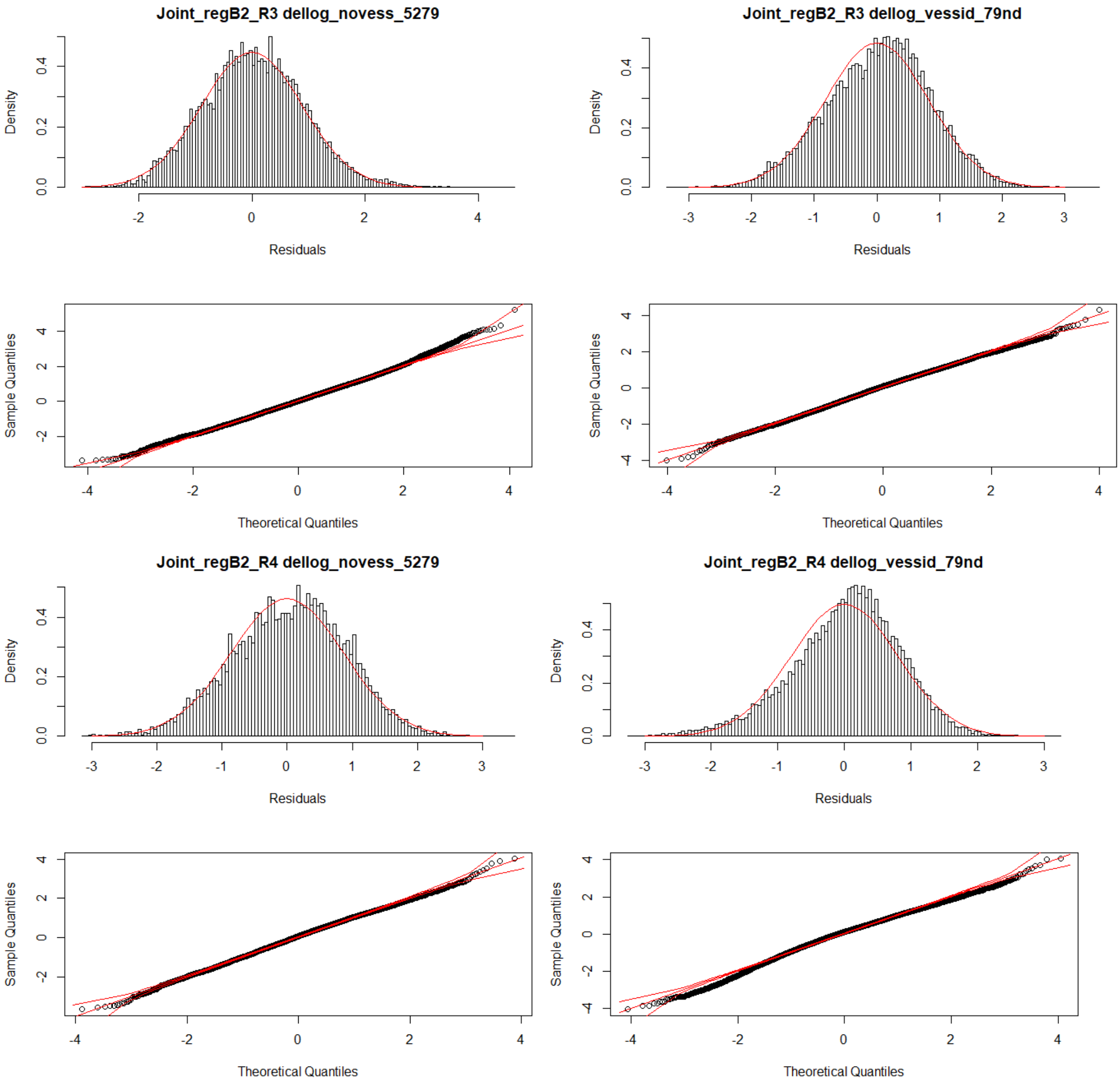

Figure 28: Diagnostic plots for bigeye lognormal positive models in temperate regions 3 and 4 (regB2_R3 and regB2_R4), for1952-79 without vessel effects (left) and for 1979-2018 with vessel effects (right).

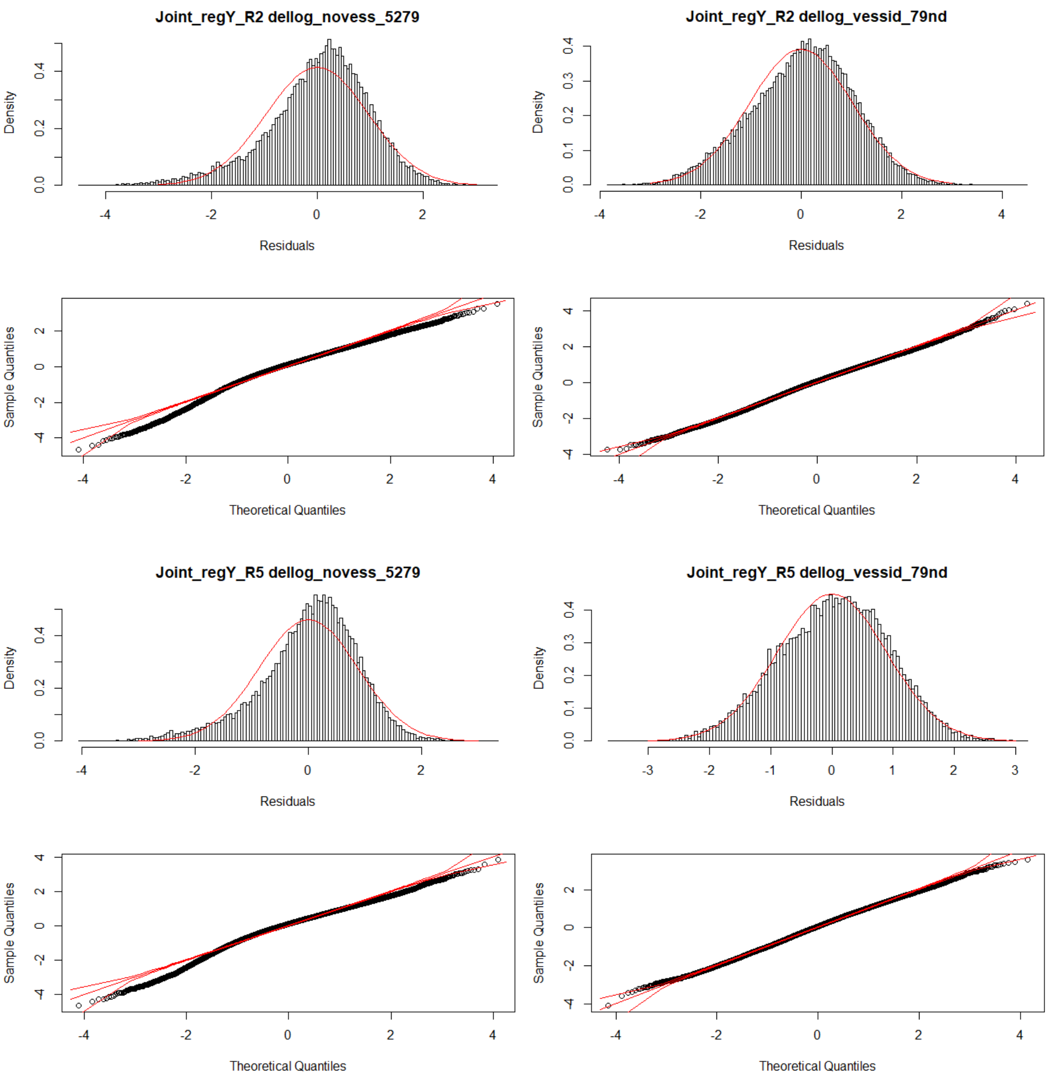

Figure 29: Diagnostic plots for yellowfin lognormal positive models in tropical regions 2 and 5 (regY_R2 and regY_R5), for 1952-79 without vessel effects (left) and for 1979-2018 with vessel effects (right).

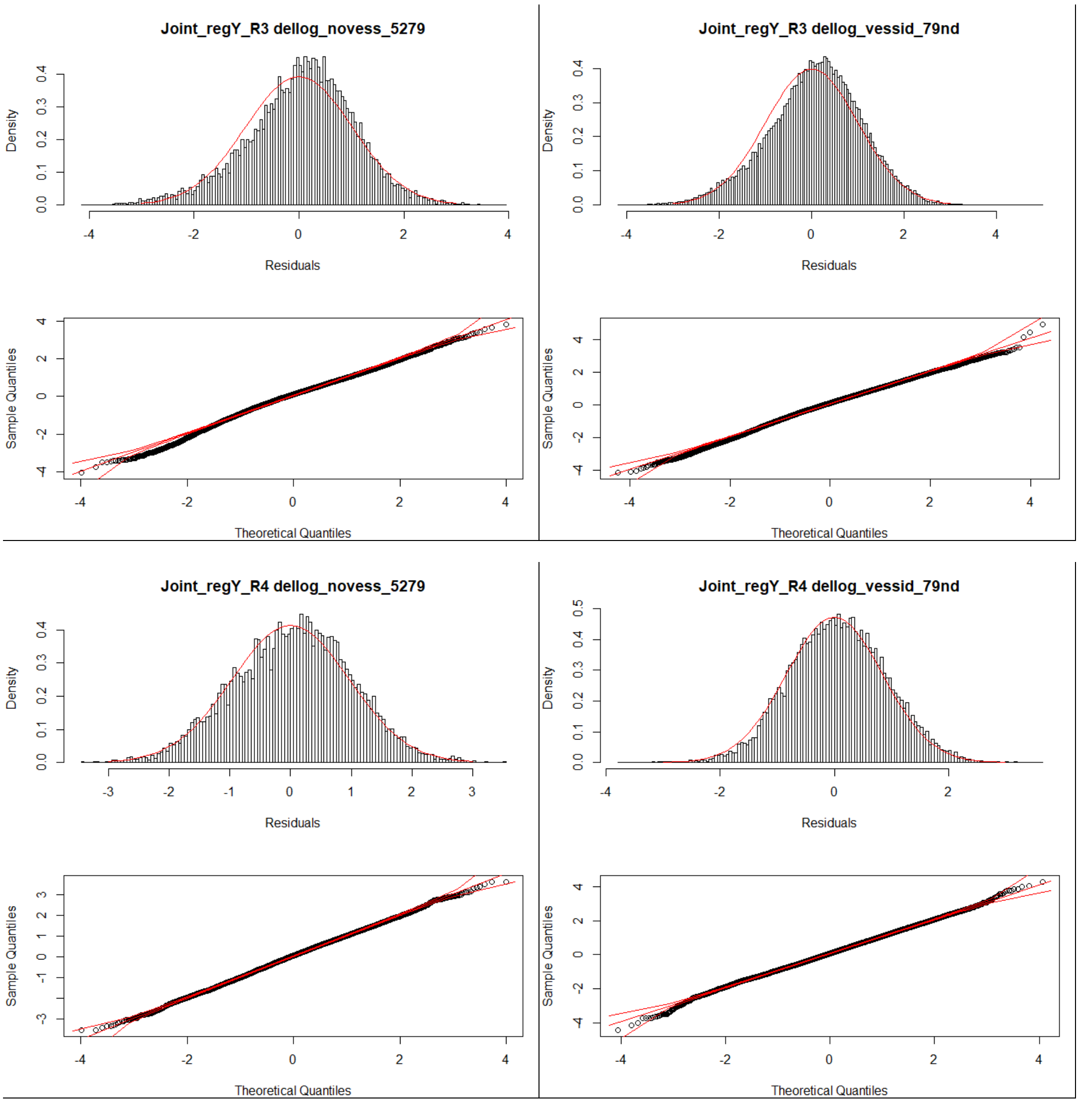

Figure 30: Diagnostic plots for yellowfin lognormal positive models in temperate regions 3 and 4 (regY_R3 and regY_R4), for1952-79 without vessel effects (left) and for 1979-2018 with vessel effects (right).

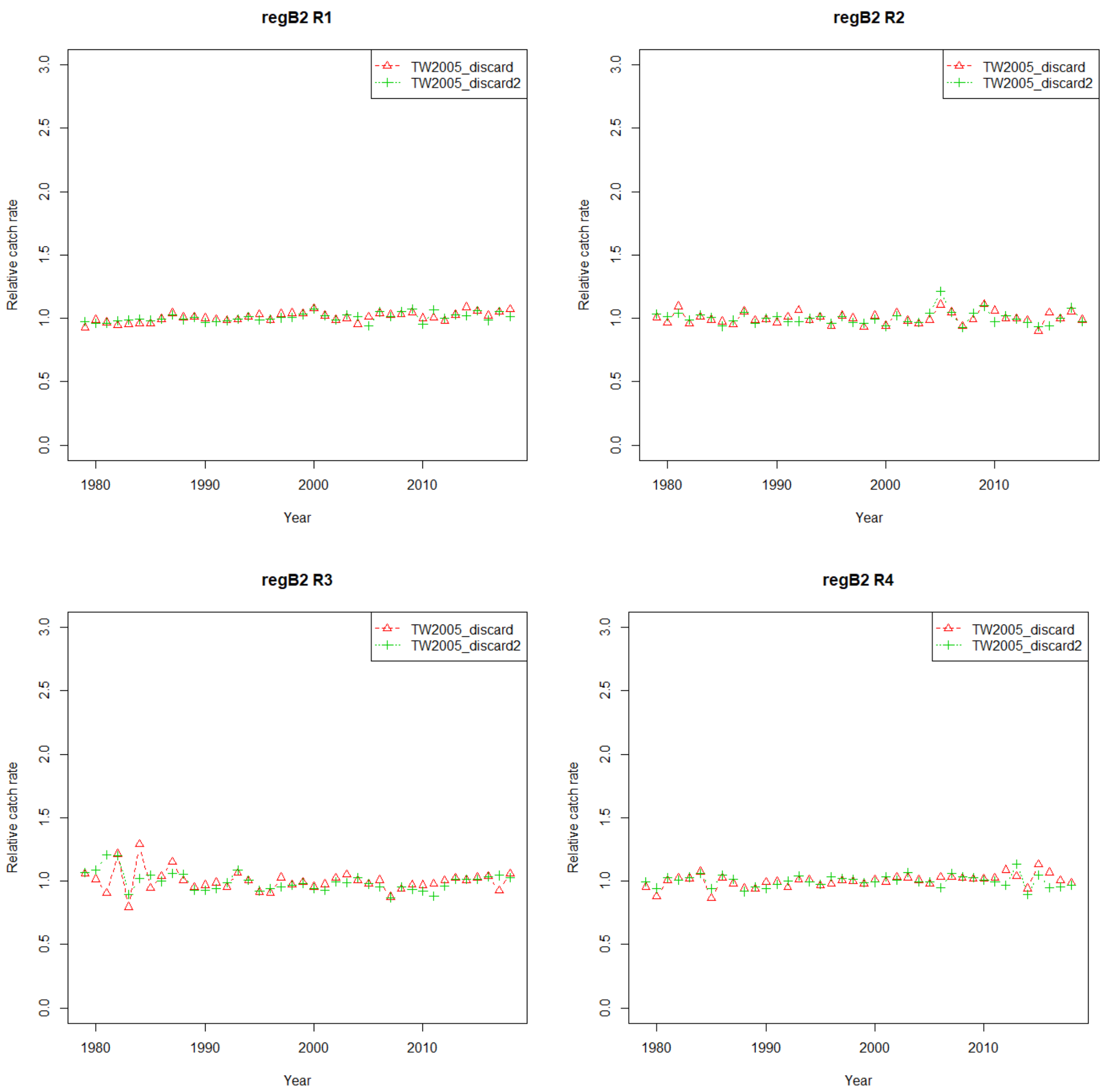

Figure 31: Ratios of the annual bigeye tuna CPUE series that incorporate discards to the annual CPUE of the unadjusted data. CPUE series that include HBF are used for regions 1 and 2, and series that include clusters are used for regions 3 and 4.

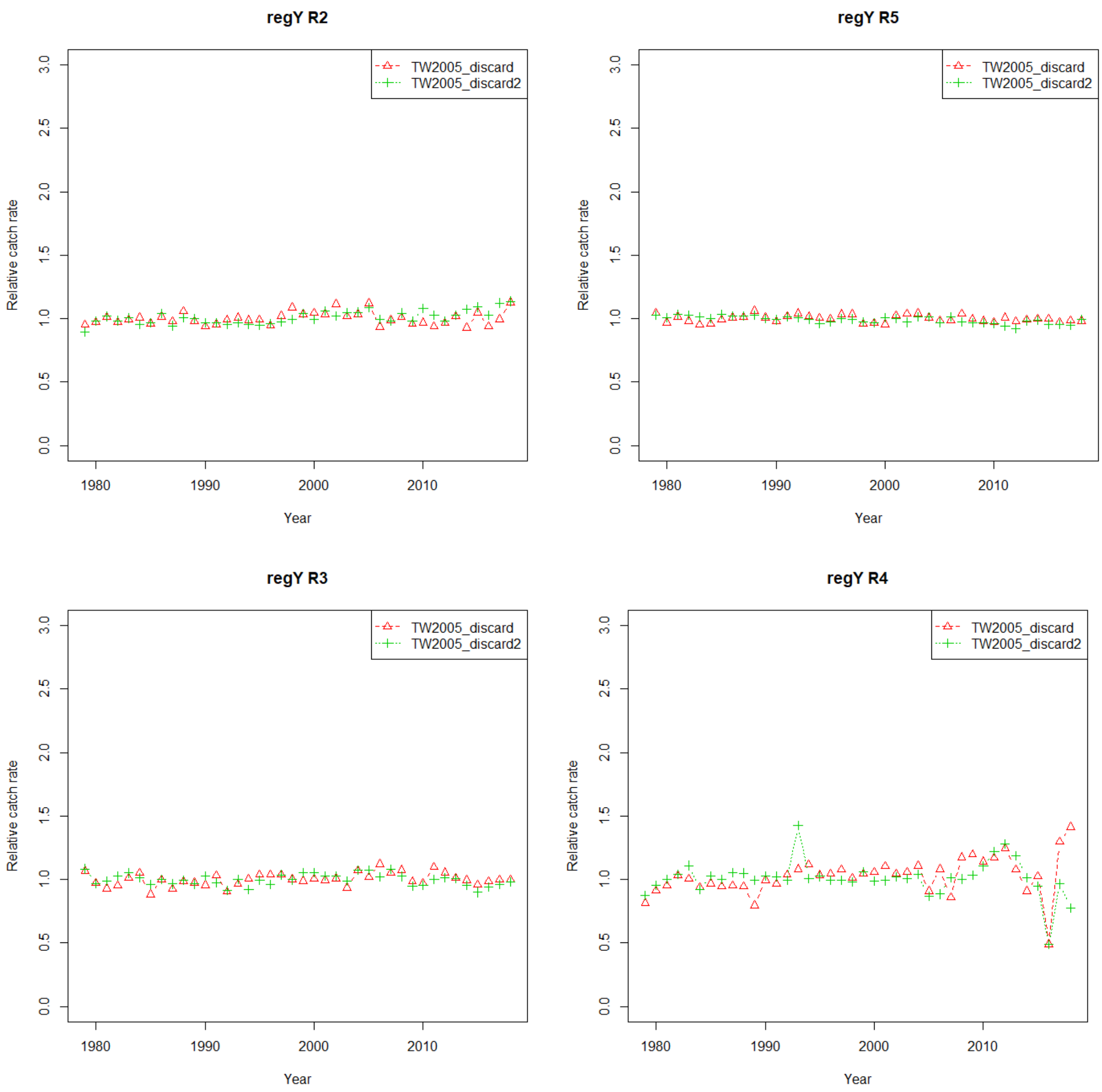

Figure 32: Ratios of the annual yellowfin tuna CPUE series that incorporate discards to the annual CPUE of the unadjusted data. CPUE series that include HBF are used for regions 2 and 5, and series that include clusters are used for regions 3 and 4.

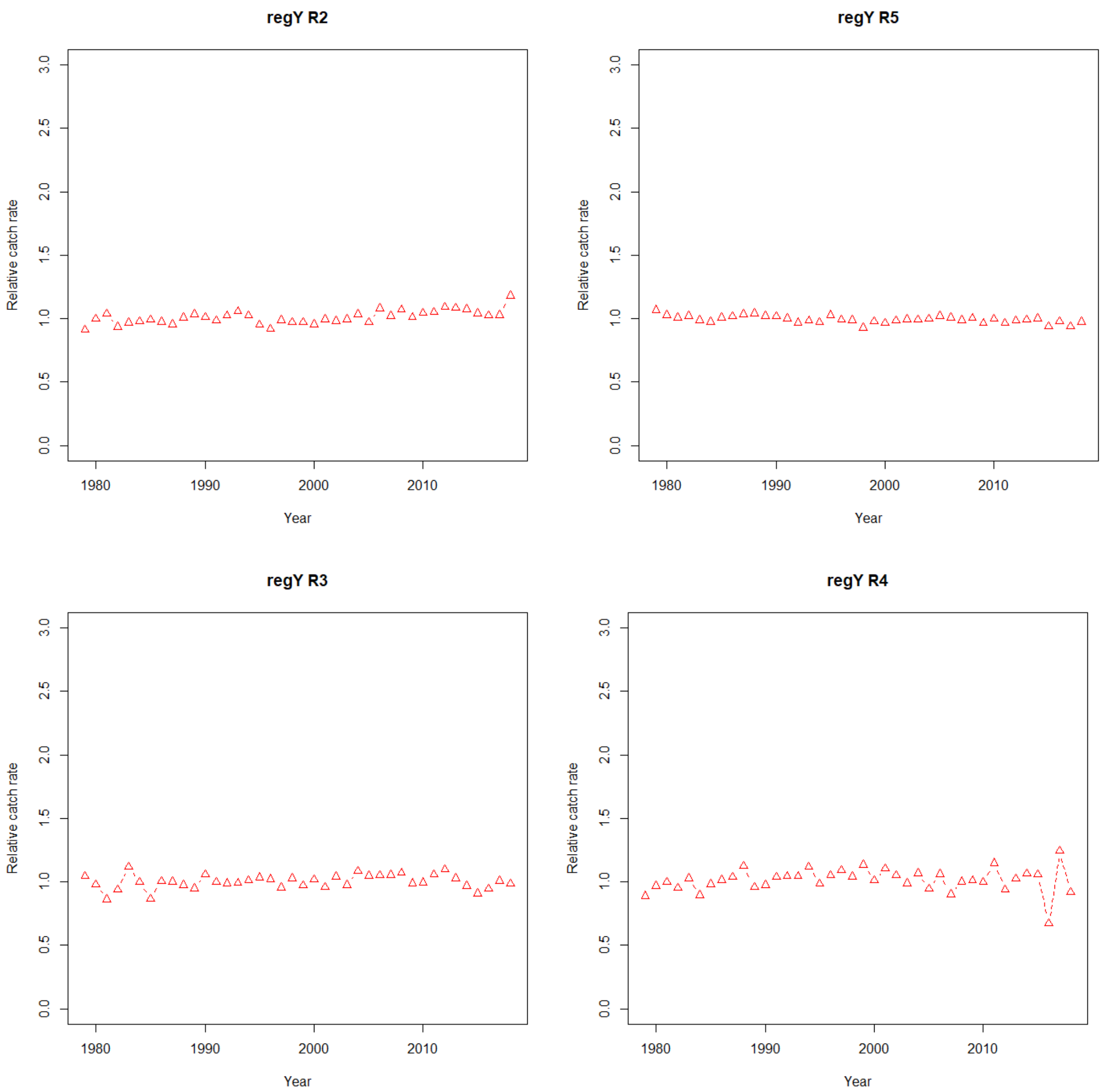

Figure 33: Ratios of the annual yellowfin tuna CPUE series that incorporate Taiwanese data starting in 1995 to the annual CPUE using the standard approach of using Taiwanese data since 2005. CPUE series that include HBF are used for regions 2 and 5, and series that include clusters are used for regions 3 and 4.

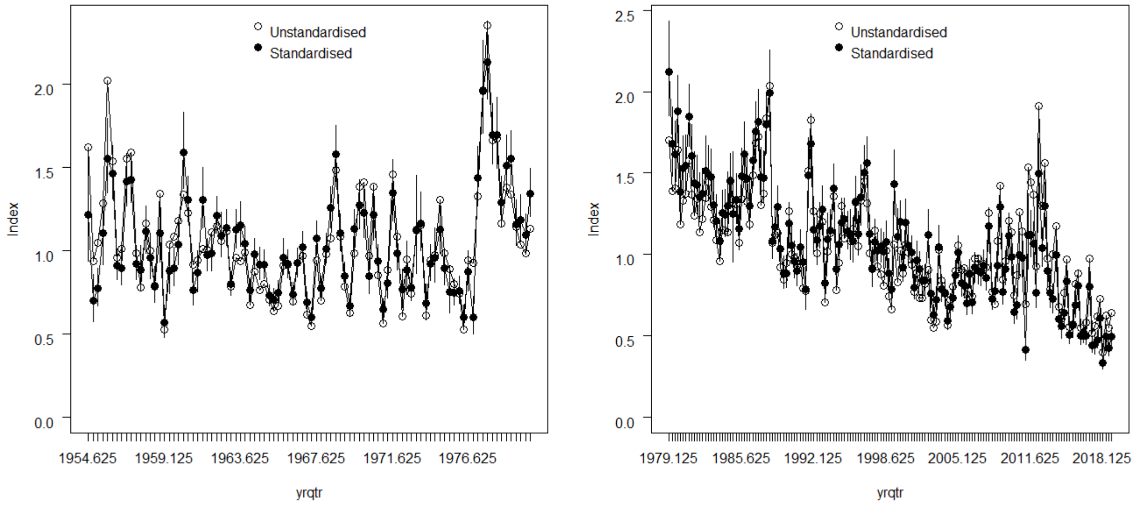

Figure 34: Comparison plot of unstandardised and standardised indices for bigeye tuna in region 1S (south-western tropical, regB3_R1) in the periods 1952-1979 (left) and 1979-2018 (right).

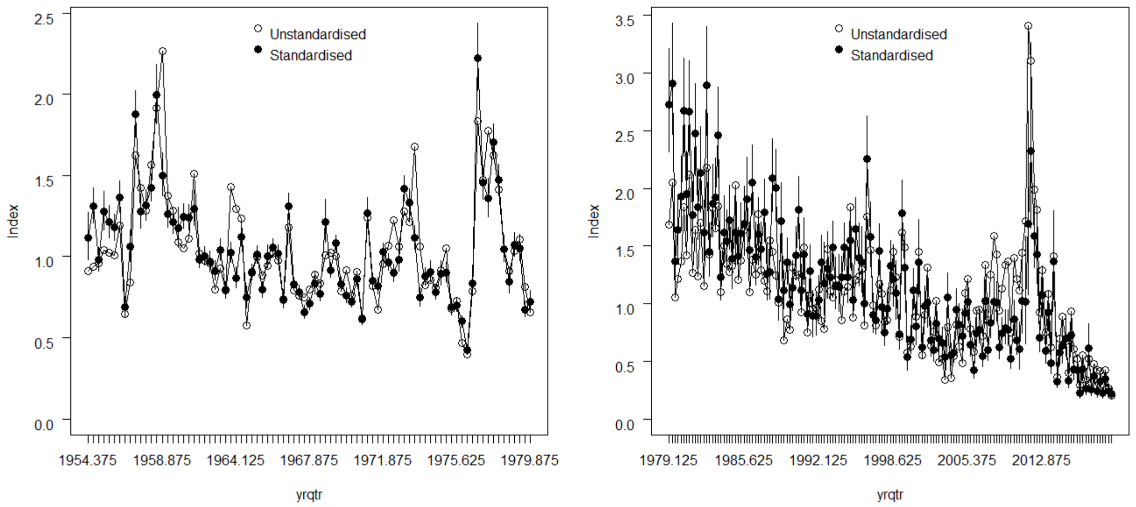

Figure 35: Comparison plot of unstandardised and standardised indices for bigeye tuna in region 1N (north-western tropical, regB3_R5) in the periods 1952-1979 (left) and 1979-2018 (right).

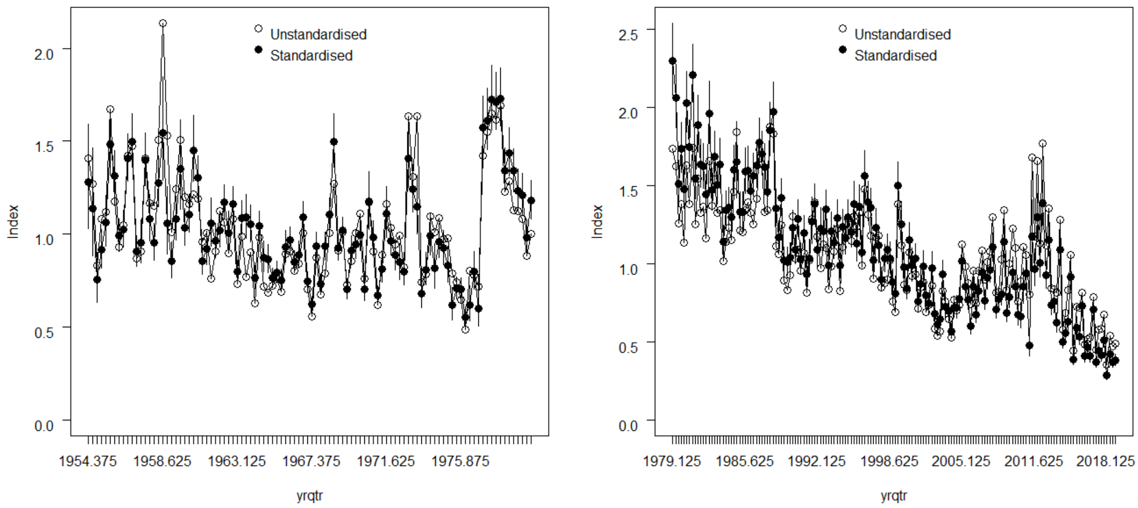

Figure 36: Comparison plot of unstandardised and standardised indices for bigeye tuna in region 1 (western tropical, regB2_R1) in the periods 1952-1979 (left) and 1979-2018 (right).

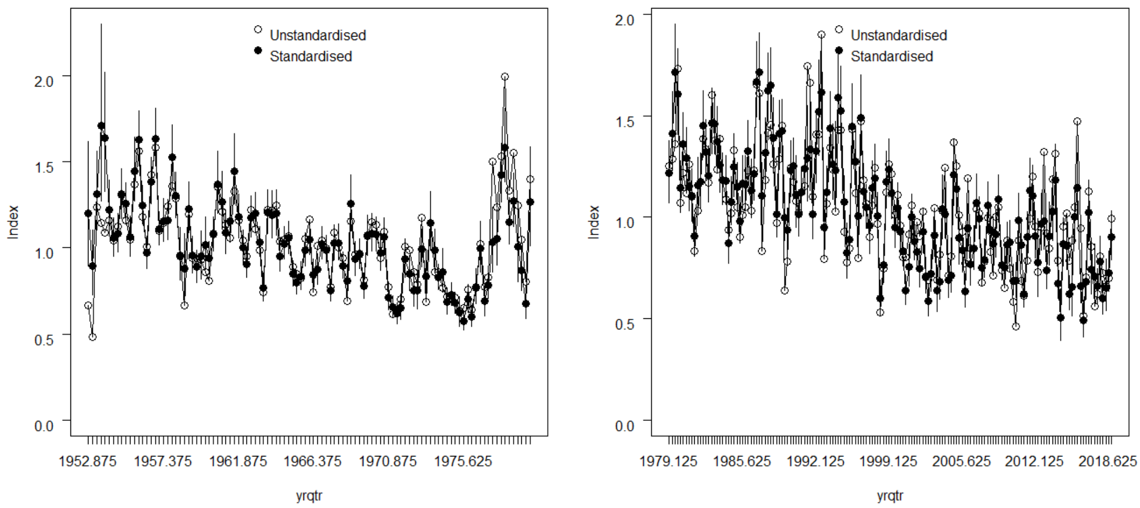

Figure 37: Comparison plot of unstandardised and standardised indices for bigeye tuna in region 2 (eastern tropical, regB2_R2) in the periods 1952-1979 (left) and 1979-2018 (right).

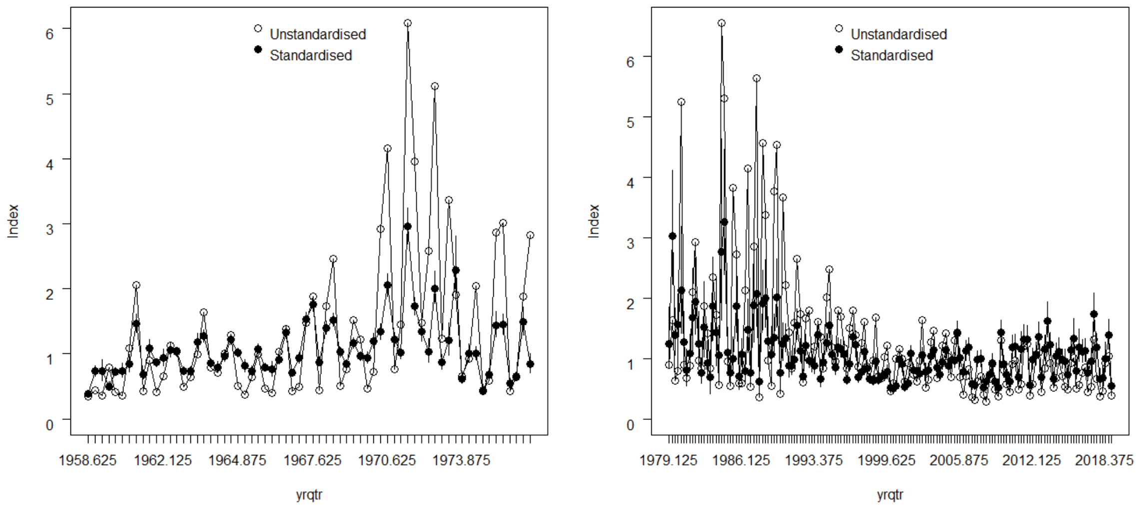

Figure 38: Comparison plot of unstandardised and standardised indices for bigeye tuna in region 3 (western temperate, regB2_R3) in the periods 1952-1979 (left) and 1979-2018 (right).

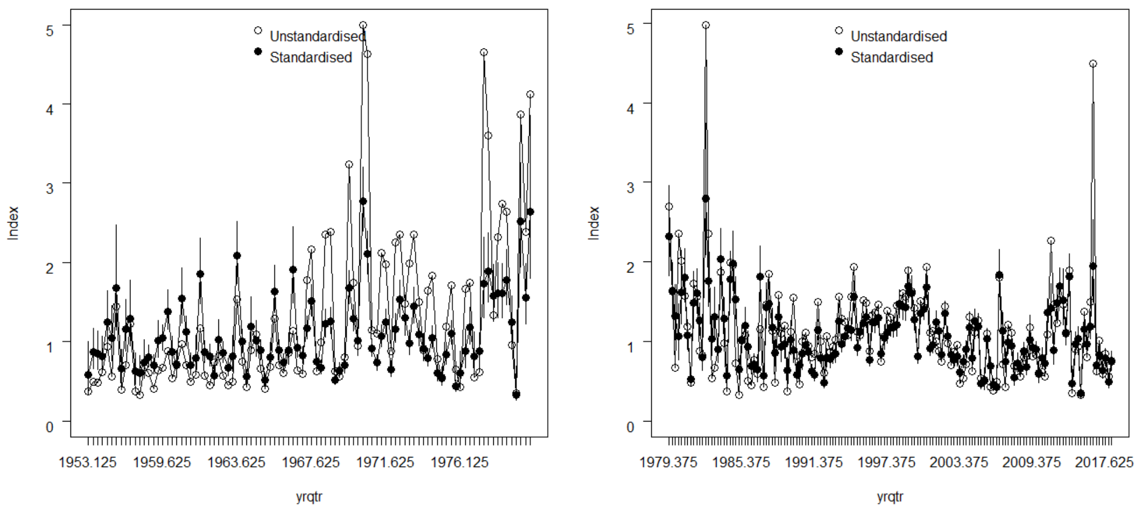

Figure 39: Comparison plot of unstandardised and standardised indices for bigeye tuna in region 4 (eastern temperate, regB2_R4) in the periods 1952-1979 (left) and 1979-2018 (right).

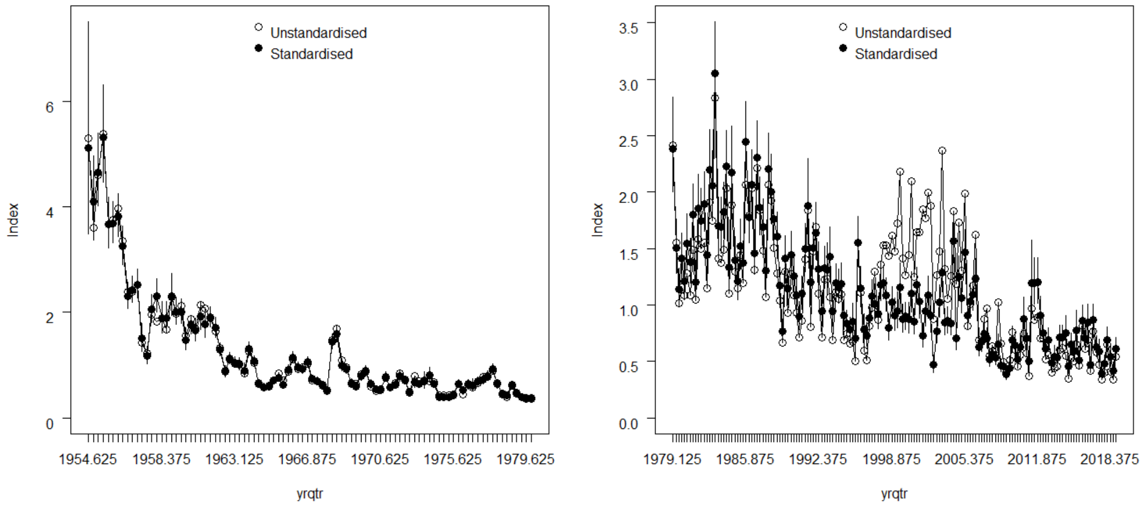

Figure 40: Comparison plot of unstandardised and standardised indices for yellowfin tuna in region 2S (south-western tropical, regY2_R2) in the periods 1952-1979 (left) and 1979-2018 (right).

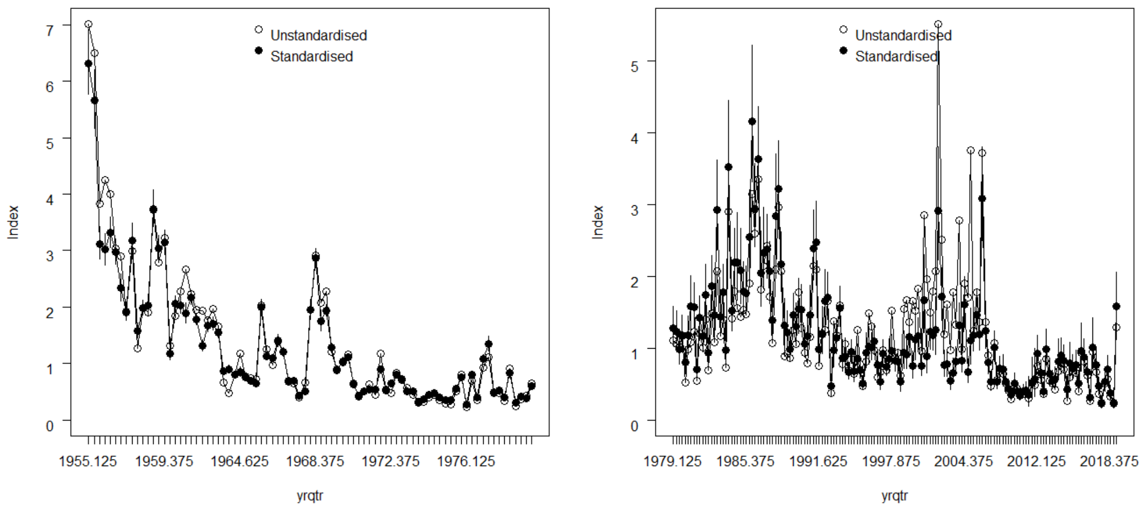

Figure 41: Comparison plot of unstandardised and standardised indices for yellowfin tuna in region 2N (north-western tropical, regY2_R7) in the periods 1952-1979 (left) and 1979-2018 (right).

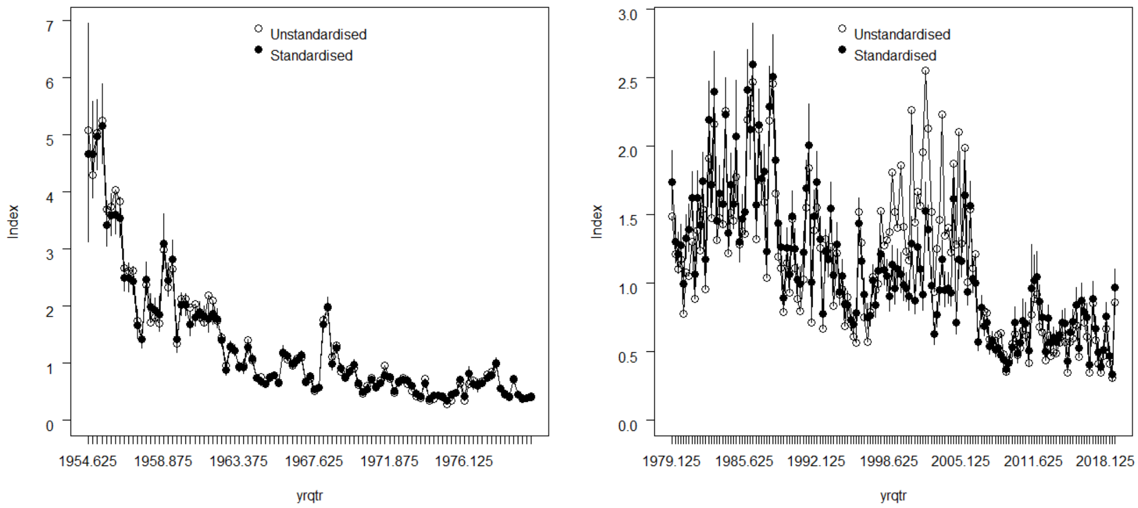

Figure 42: Comparison plot of unstandardised and standardised indices for yellowfin tuna in region 2 (western tropical, regY_R2) in the periods 1952-1979 (left) and 1979-2018 (right).

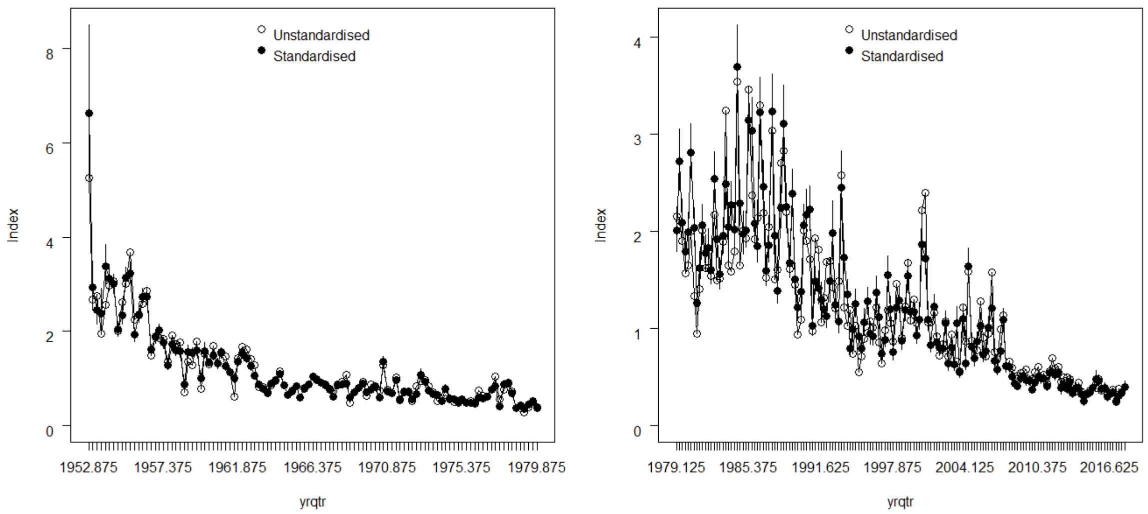

Figure 43: Comparison plot of unstandardised and standardised indices for yellowfin tuna in region 5 (eastern tropical, regY_R5) in the periods 1952-1979 (left) and 1979-2018 (right).

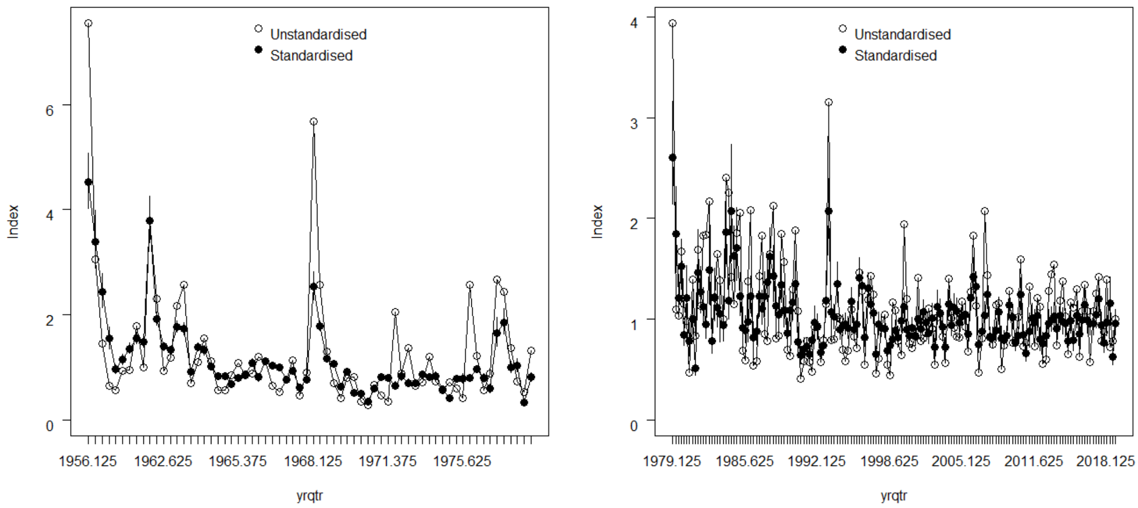

Figure 44: Comparison plot of unstandardised and standardised indices for yellowfin tuna in region 3 (western temperate, regY_R3) in the periods 1952-1979 (left) and 1979-2018 (right).

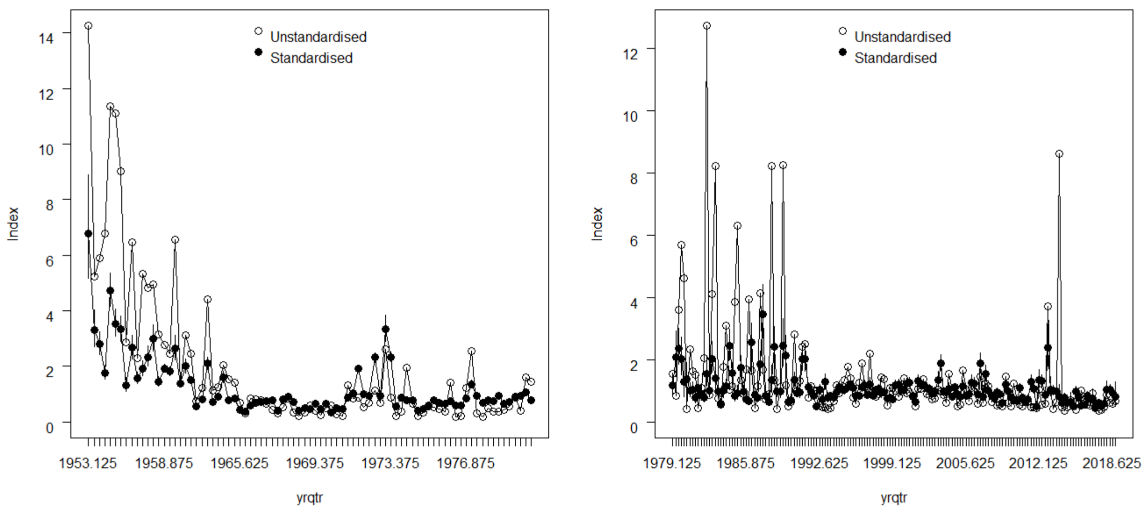

Figure 45: Comparison plot of unstandardised and standardised indices for yellowfin tuna in region 4 (eastern temperate, regY_R4) in the periods 1952-1979 (left) and 1979-2018 (right).

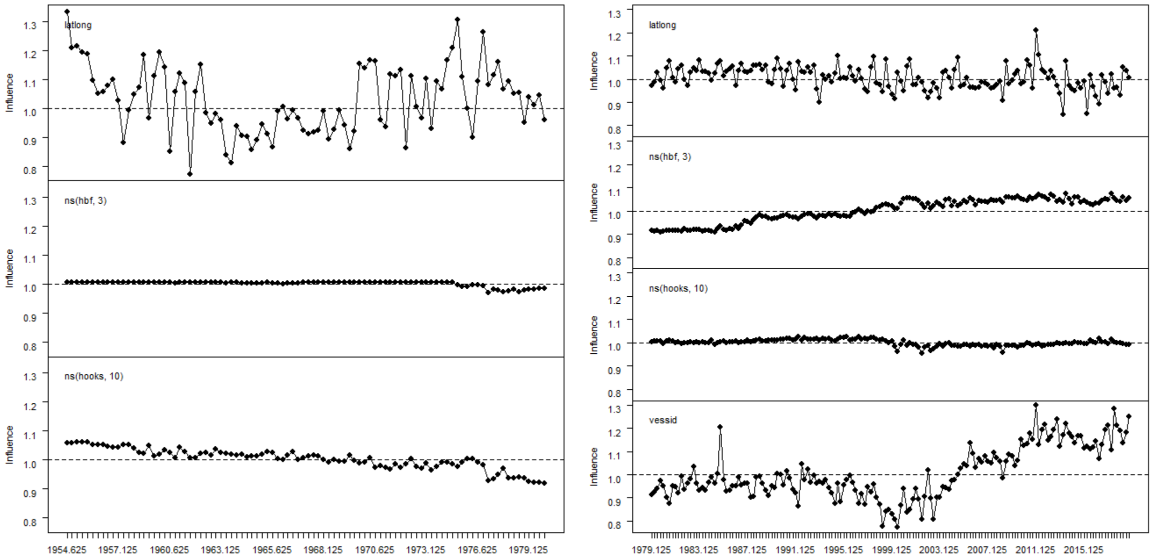

Figure 46: Influence plot for bigeye tuna in region 1S (south-western tropical, regB3_R1) in the periods 1952-1979 (left) and 1979-2018 (right), showing the multiplicative effect (y axis) of each variable on the standardized index.

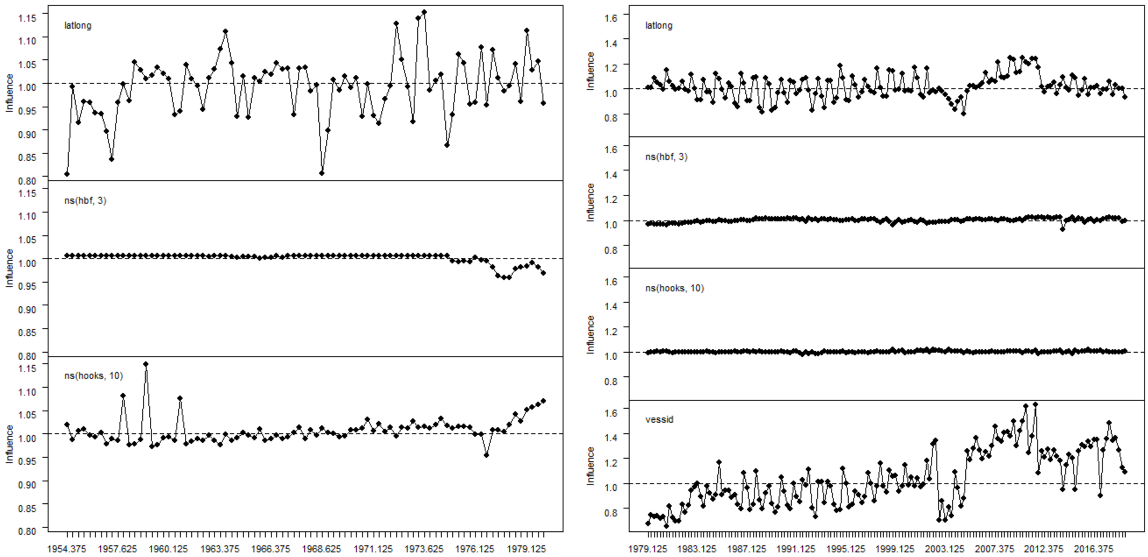

Figure 47: Influence plot for bigeye tuna in region 1N (north-western tropical, regB3_R5) in the periods 1952-1979 (left) and 1979-2018 (right), showing the multiplicative effect (y axis) of each variable on the standardized index.

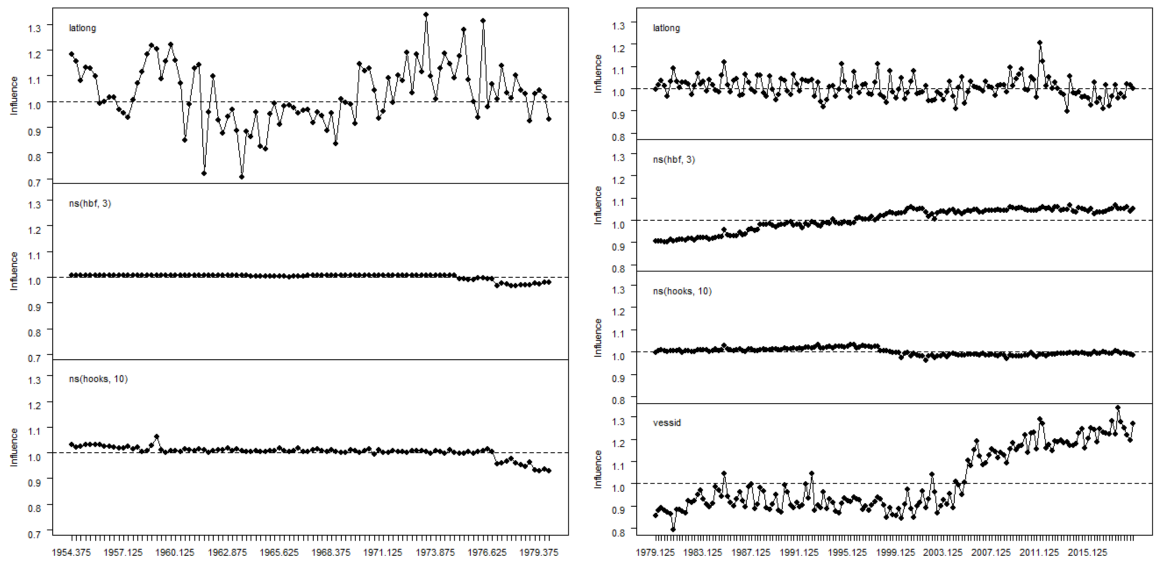

Figure 48: Influence plot for bigeye tuna in region 1 (western tropical, regB2_R1) in the periods 1952-1979 (left) and 1979-2018 (right), showing the multiplicative effect (y axis) of each variable on the standardized index.

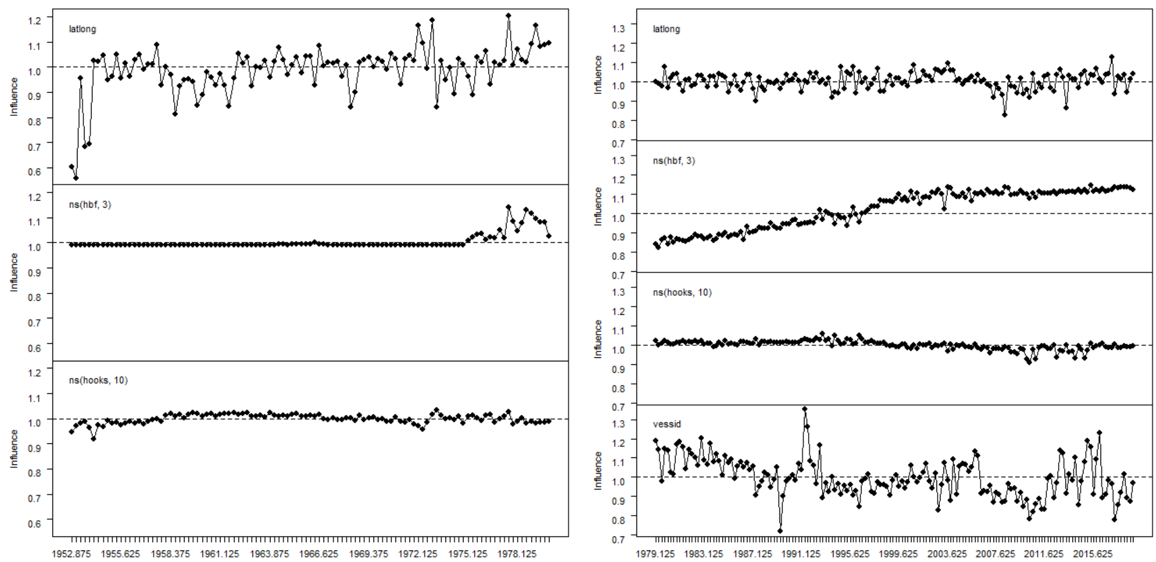

Figure 49: Influence plot for bigeye tuna in region 2 (eastern tropical, regB2_R2) in the periods 1952-1979 (left) and 1979-2018 (right), showing the multiplicative effect (y axis) of each variable on the standardized index.

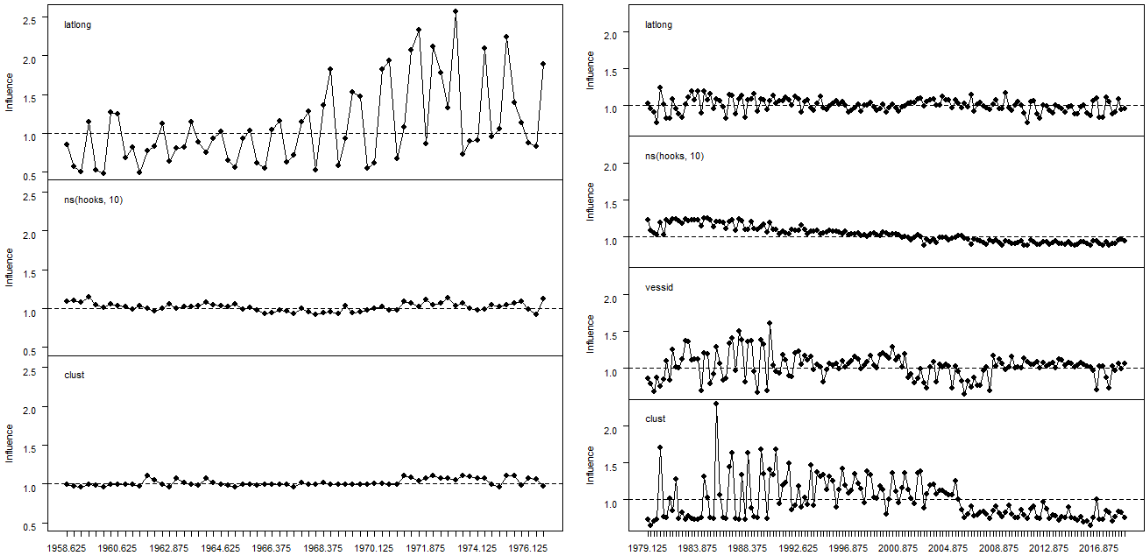

Figure 50: Influence plot for bigeye tuna in region 3 (western temperate, regB2_R3) in the periods 1952-1979 (left) and 1979-2018 (right), showing the multiplicative effect (y axis) of each variable on the standardized index.

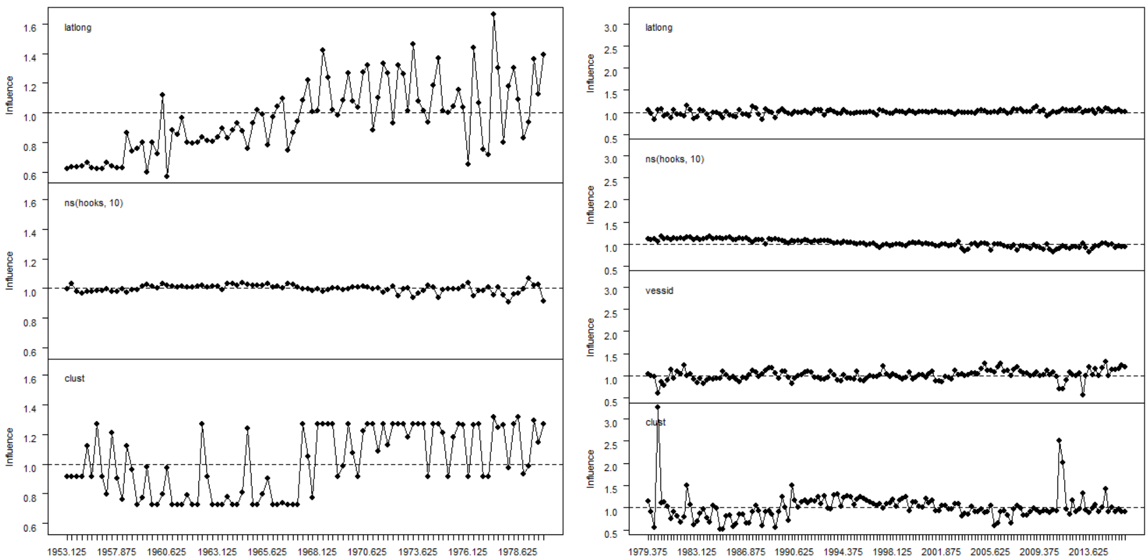

Figure 51: Influence plot for bigeye tuna in region 4 (western temperate, regB2_R4) in the periods 1952-1979 (left) and 1979-2018 (right), showing the multiplicative effect (y axis) of each variable on the standardized index.

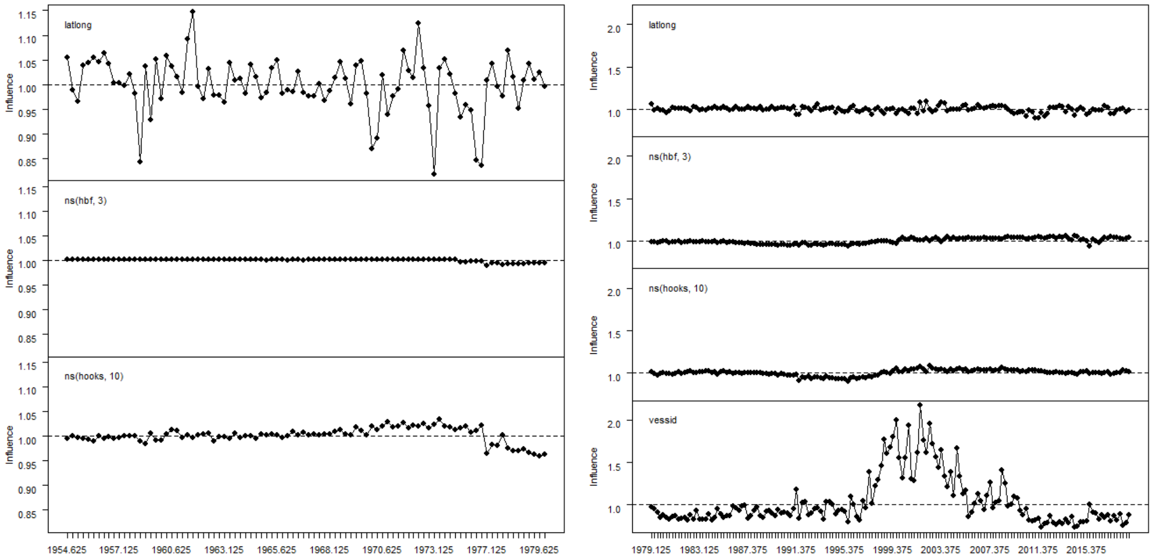

Figure 52: Influence plot for yellowfin region 2S (south-western tropical, regY2_R2) in the periods 1952-1979 (left) and 1979-2018 (right), showing the multiplicative effect (y axis) of each variable on the standardized index.

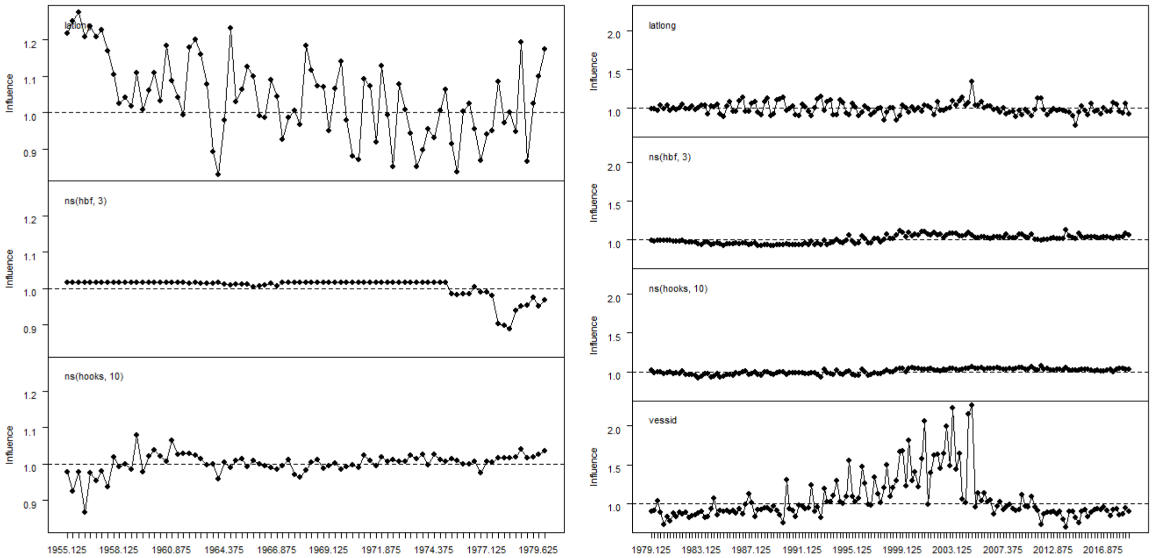

Figure 53: Influence plot for yellowfin region 2N (north-western tropical, regY2_R7) in the periods 1952-1979 (left) and 1979-2018 (right), showing the multiplicative effect (y axis) of each variable on the standardized index.

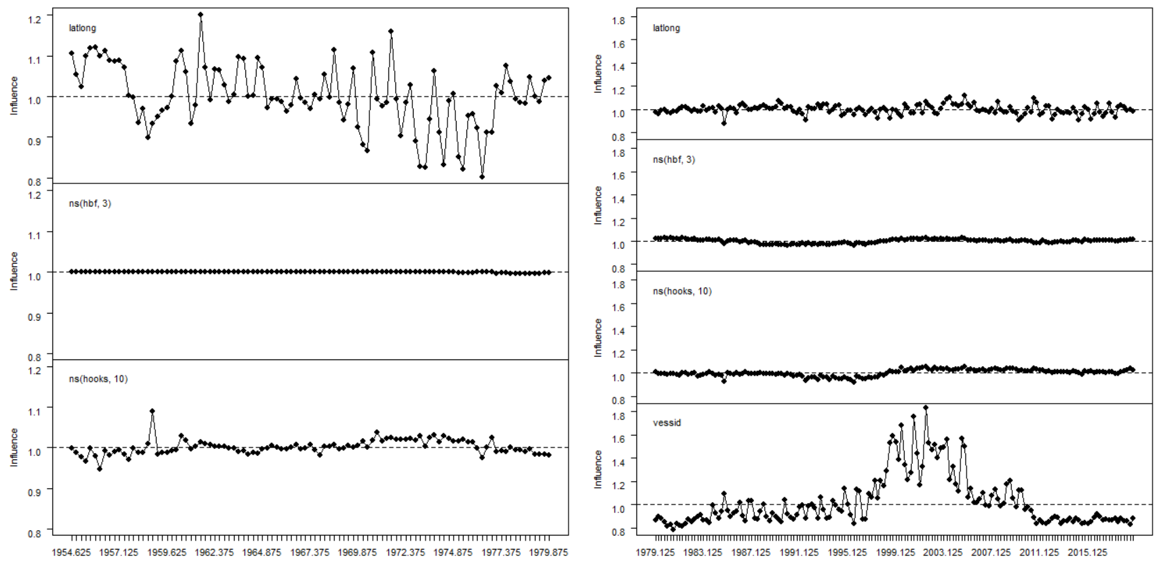

Figure 54: Influence plot for yellowfin region 2 (western tropical, regY_R2) in the periods 1952-1979 (left) and 1979-2018 (right), showing the multiplicative effect (y axis) of each variable on the standardized index.

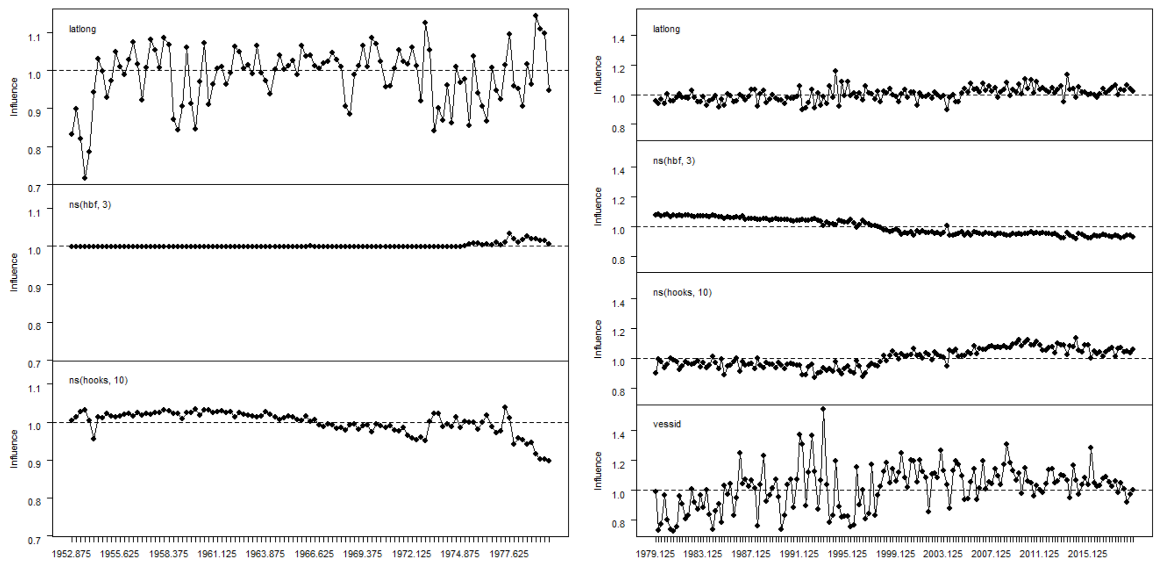

Figure 55: Influence plot for yellowfin region 5 (eastern tropical, regY_R5) in the periods 1952-1979 (left) and 1979-2018 (right), showing the multiplicative effect (y axis) of each variable on the standardized index.

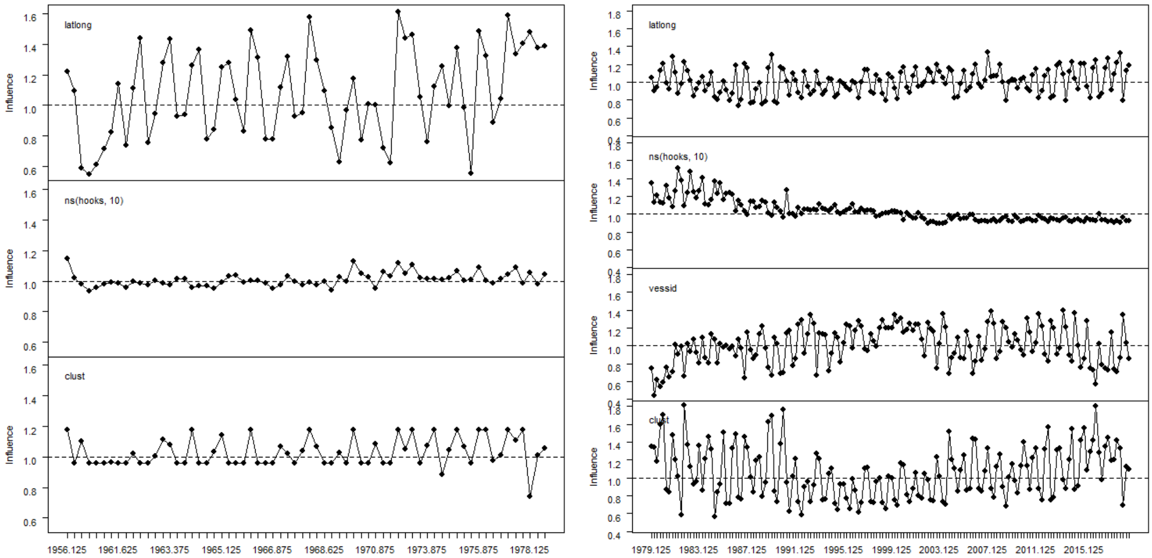

Figure 56: Influence plot for yellowfin region 3 (western temperate, regY_R3) in the periods 1952-1979 (left) and 1979-2018 (right), showing the multiplicative effect (y axis) of each variable on the standardized index.

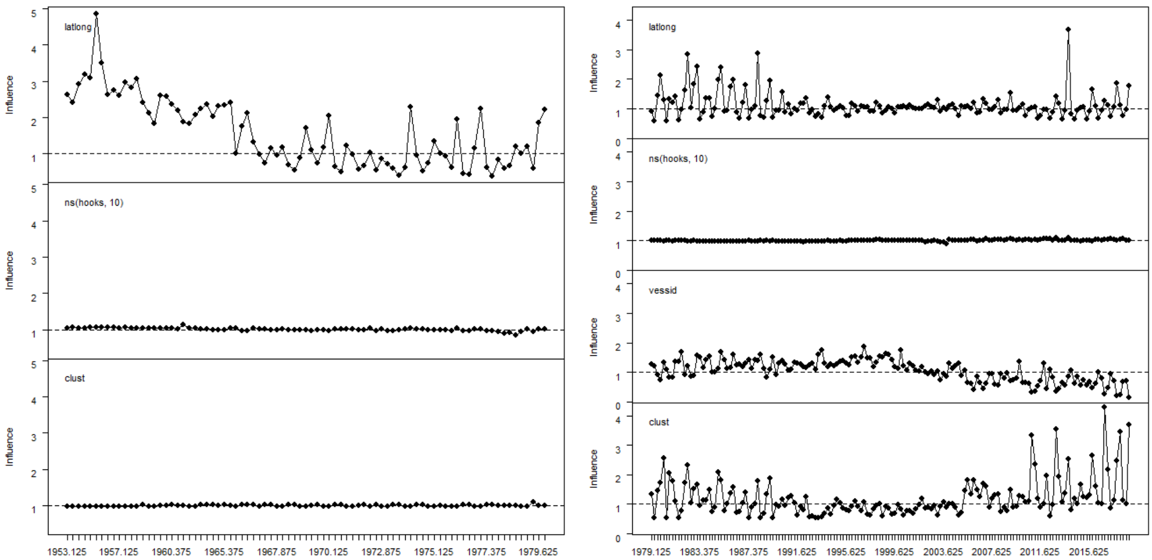

Figure 57: Influence plot for yellowfin region 4 (eastern temperate, regY_R4) in the periods 1952-1979 (left) and 1979-2018 (right), showing the multiplicative effect (y axis) of each variable on the standardized index.

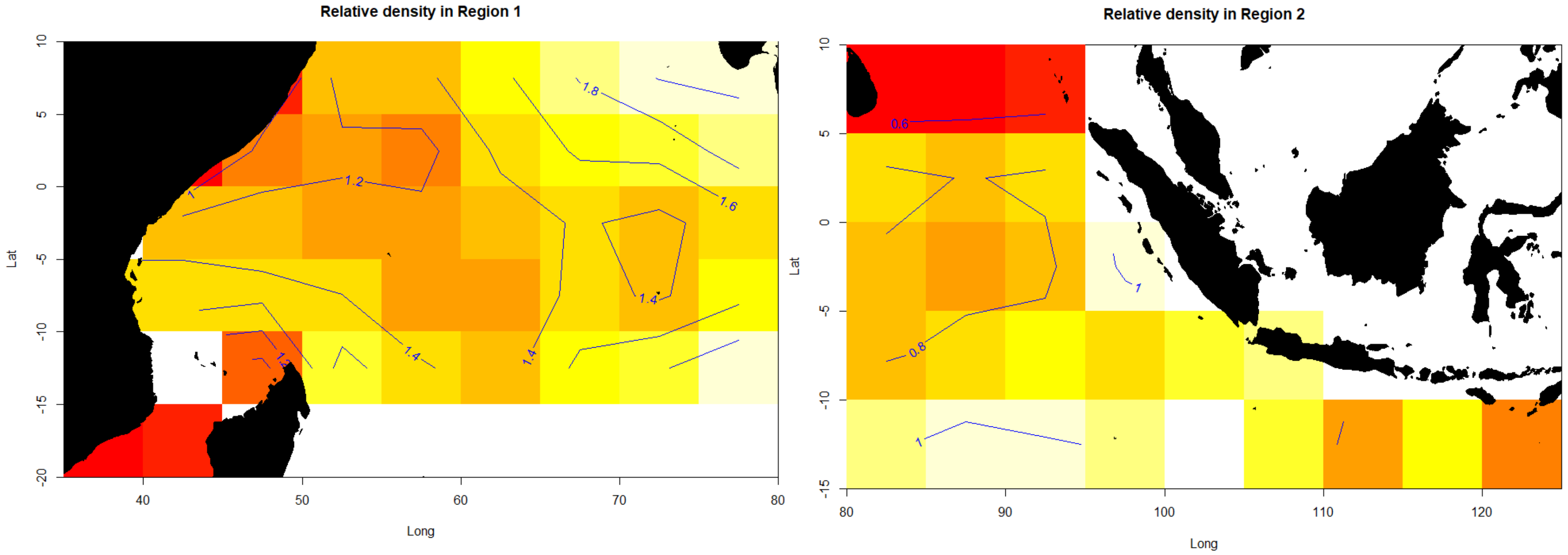

Figure 58: Relative densities by grid cell for tropical bigeye regions 1 (western, regB2_R1) and 2 (eastern, regB2_R2) from the model for 1979 to 2018 with vessel effects. Darker orange and lighter yellow represent lower and higher density respectively. Densities and colours are only comparable within each figure.

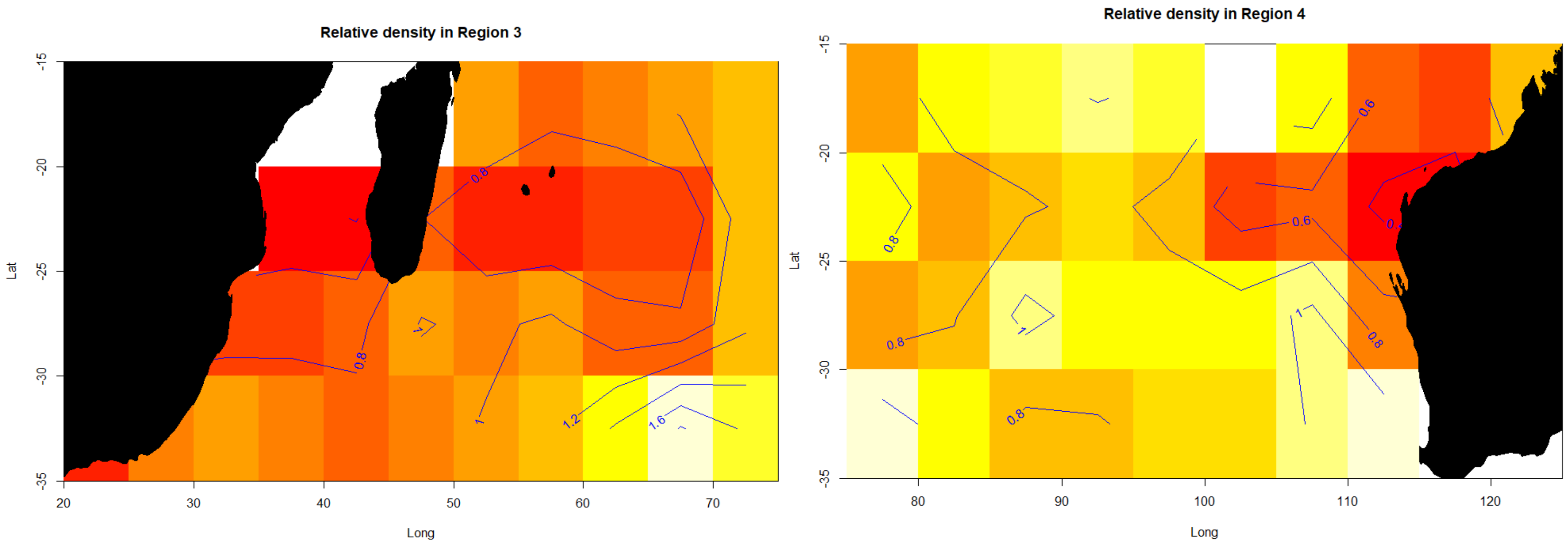

Figure 59: Relative densities by grid cell for temperate bigeye regions 3 (western, regB2_R3) and 4 (eastern, regB2_R4) from the model for 1979 to 2018 with vessel effects. Darker orange and lighter yellow represent lower and higher density respectively. Densities and colours are only comparable within each figure.

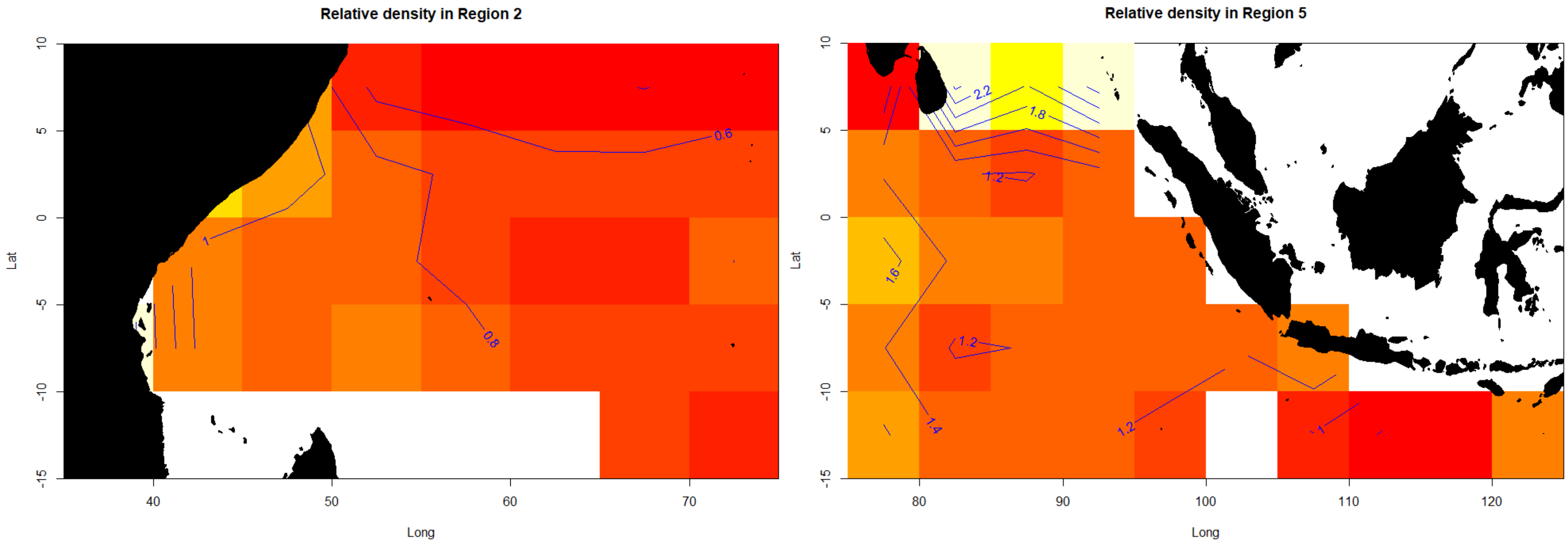

Figure 60: Relative densities by grid cell for tropical yellowfin regions 2 (western, regY_R2) and 5 (eastern, regY_R5) from the model for 1979 to 2018 with vessel effects. Darker orange and lighter yellow represent lower and higher density respectively. Densities and colours are only comparable within each figure.

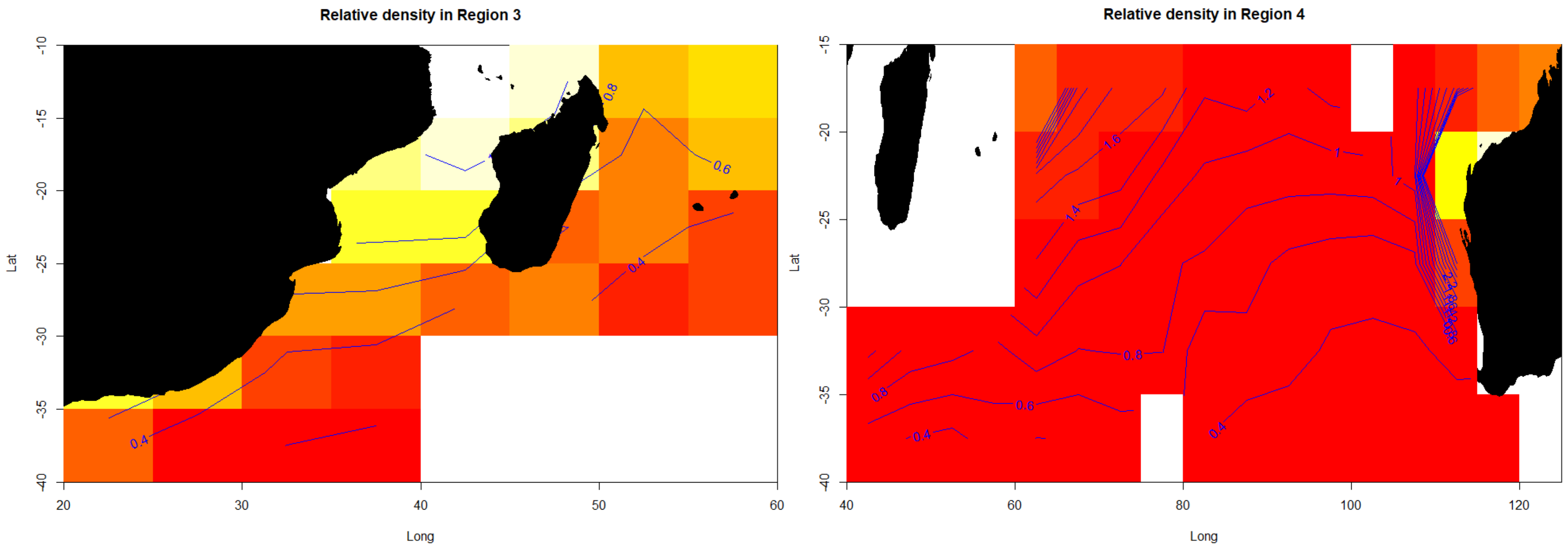

Figure 61: Relative densities by grid cell for temperate yellowfin regions 3 (western, regY_R3) and 4 (eastern, regB2_R4) from the model for 1979 to 2018 with vessel effects. Darker orange and lighter yellow represent lower and higher density respectively. Densities and colours are only comparable within each figure.

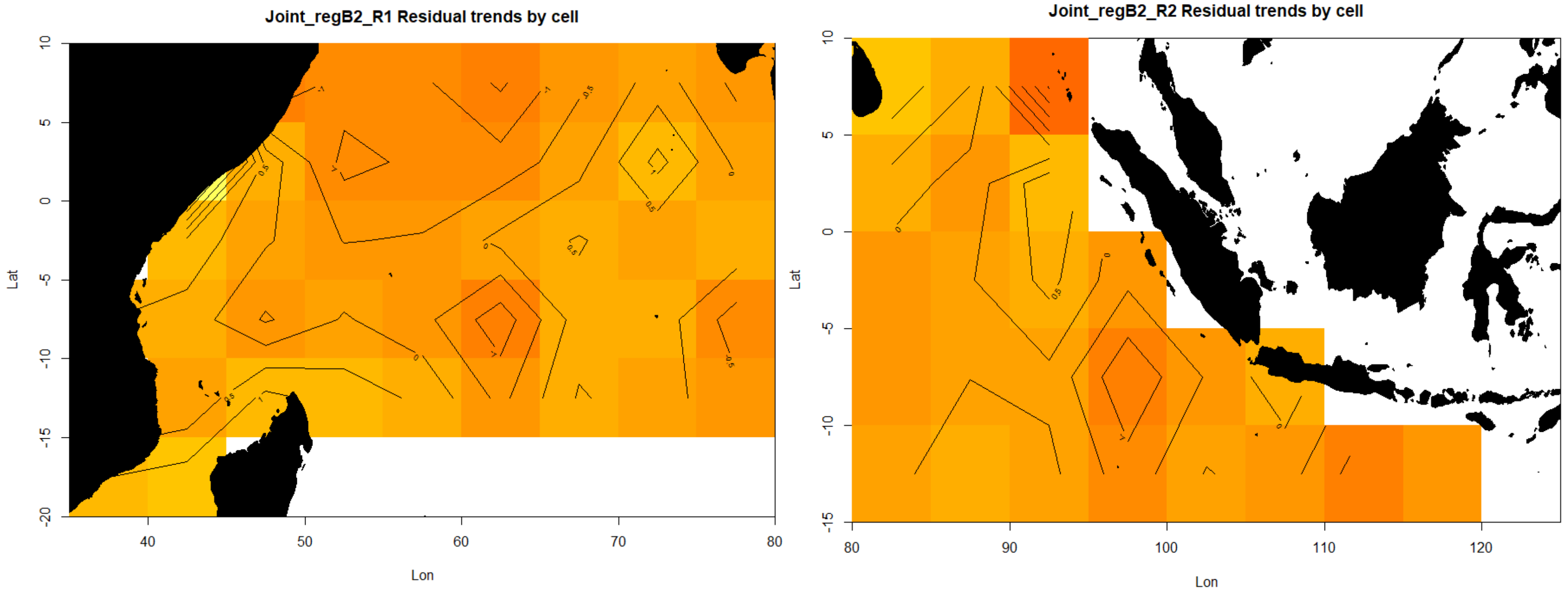

Figure 62: Trends in temporal residuals by grid cell for tropical bigeye regions 1 (western, regB2_R1) and 2 (eastern, regB2_R2) from the model for 1979 to 2018 with vessel effects. The trends in each cell are estimated by regressing the residuals against year-quarter. Darker orange represents decline and lighter yellow represents increase relative to the model average.

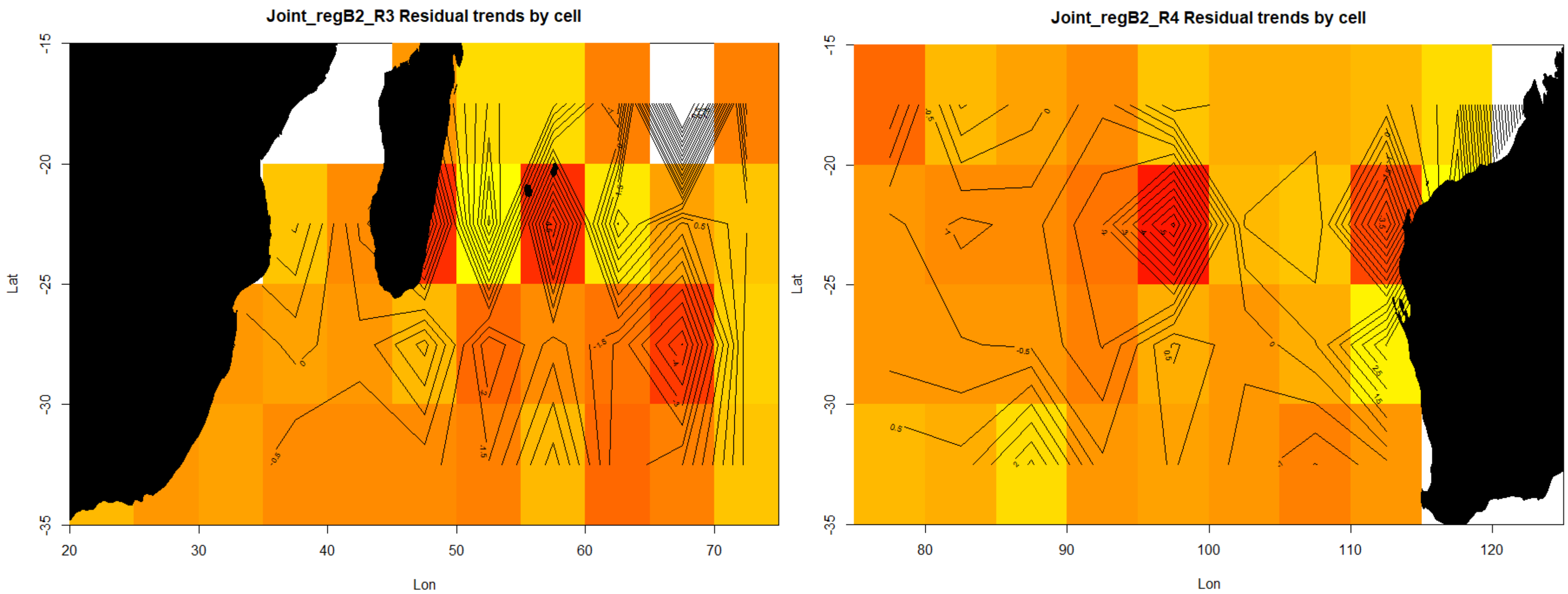

Figure 63: Trends in temporal residuals by grid cell for temperate bigeye regions 3 (western, regB2_R3) and 4 (eastern, regB2_R4) from the model for 1979 to 2018 with vessel effects. The trends in each cell are estimated by regressing the residuals against year-quarter. Darker orange represents decline and lighter yellow represents increase relative to the model average.

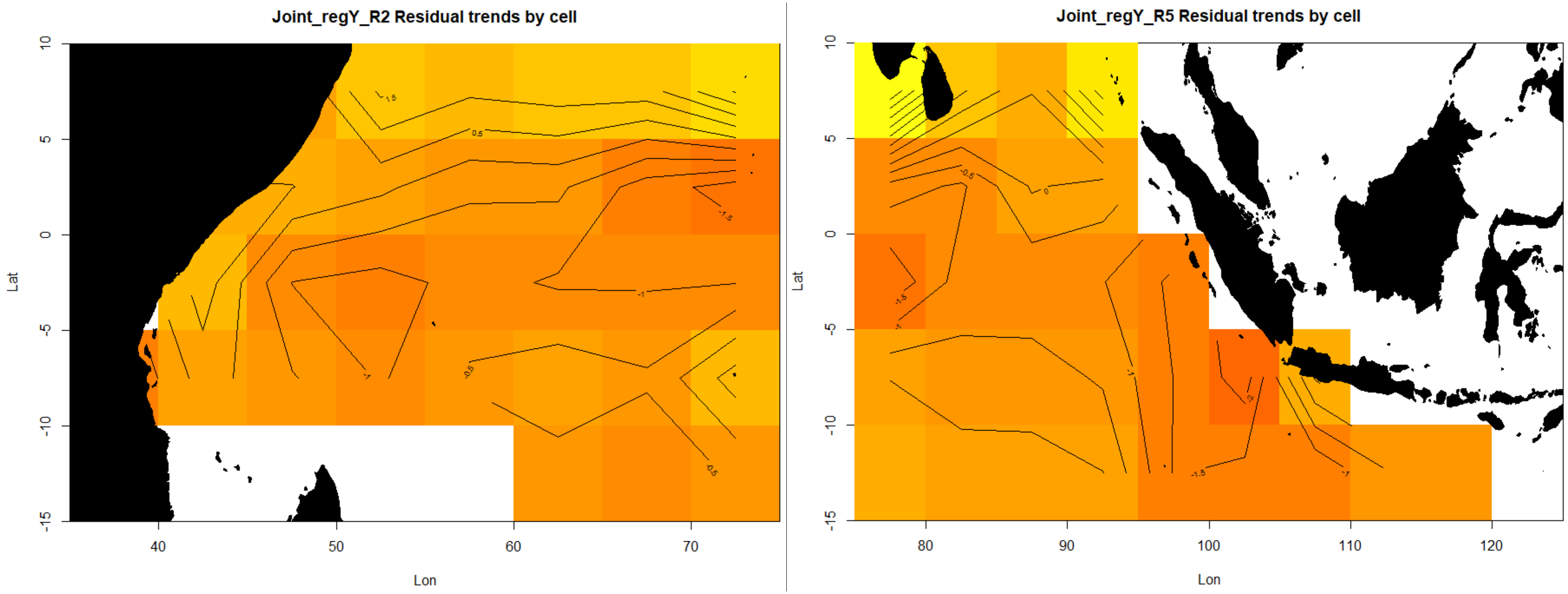

Figure 64: Trends in temporal residuals by grid cell for tropical yellowfin regions 2 (western, regY_R2) and 5 (eastern, regY_R5) from the model for 1979 to 2018 with vessel effects. The trends in each cell are estimated by regressing the residuals against year-quarter. Darker orange represents decline and lighter yellow represents increase relative to the model average.

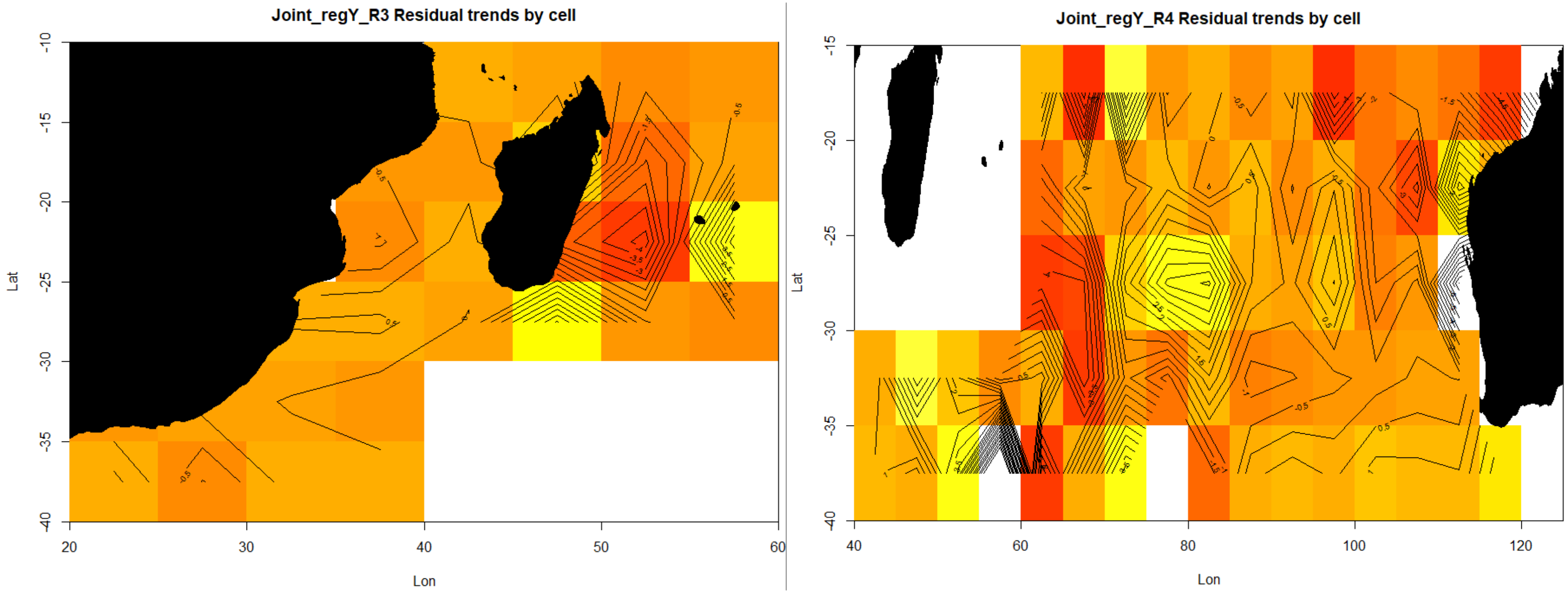

Figure 65: Trends in temporal residuals by grid cell for temperate yellowfin regions 3 (western, regY_R3) and 4 (eastern, regY_R4) from the model for 1979 to 2018 with vessel effects. The trends in each cell are estimated by regressing the residuals against year-quarter. Darker orange represents decline and lighter yellow represents increase relative to the model average.